Self-Consolidating Concrete (SCC) for Infrastructure Elements
Report C – Bond Behavior of Mild Reinforcing Steel

Prepared By:

Missouri University of Science and Technology

Final Report Prepared for Missouri Department of Transportation
2012 August Project TRyy1103 Report cmr 13-003

FINAL Report C

TRyy1103

Project Title: Self-Consolidating Concrete (SCC) for Infrastructure Elements

Report C: Self-Consolidating Concrete (SCC) for Infrastructure Elements: Bond Behavior of Mild Reinforcing Steel in SCC

Prepared for
Missouri Department of Transportation
Construction and Materials

Missouri University of Science and Technology, Rolla, Missouri

July 2012

ABSTRACT

The main objective of this study was to determine the effect on bond performance of mild reinforcing steel in self-consolidating concrete (SCC). The SCC test program consisted of comparing the bond performance of normal and high strength SCC with their respective MoDOT standard mix designs.

Two test methods were used for bond strength comparisons. The first was a direct pull-out test based on the RILEM 7-II-128 "RC6: Bond test for reinforcing steel. 1. Pull-out test" (RILEM, 1994). The direct pull-out tests were performed on specimens with #4 (#13) and #6 (#19) deformed reinforcing bars.

The second test method consisted of a full-scale beam splice test specimen subjected to a four-point loading until failure of the splice. This test method is a non-ASTM test procedure that is generally accepted as the most realistic test method for both development and splice length. The beam splice tests were performed on beams with #6 (#19) reinforcing bars spliced at midspan at a specific length to ensure bond failure occurs prior to shear or flexural failure.

Analysis of the SCC data indicates that using SCC does not result in any increase in the required development length of mild reinforcing.

TABLE OF CONTENTS

Page

APPENDICES

LIST OF ILLUSTRATIONS

Figure Page

LIST OF TABLES

1. INTRODUCTION

1.1. BACKGROUND AND JUSTIFICATION FOR SELF-CONSOLIDATING CONCRETE RESEARCH

1.1.1. General. The key difference between self-consolidating concrete (SCC) and conventional concrete is workability. SCC is characterized by its fluidity and its ability to eliminate the need for mechanical consolidation through the use of vibrators. Typically, three different methods are used for producing an SCC mix design. The first method is by the addition of a viscosity modifying admixture (VMA), along with a water reducer to a conventional concrete mix design. The VMA reduces the likelihood of segregation of the coarse aggregate by increasing the viscosity of the water. The water reducer increases the flowability of the paste. The second method is through increasing the fine-to-coarse aggregate ratio and the addition of a water reducer. The lower coarse aggregate content increases the flowability and lowers the potential for segregation. The third method is essentially a combination of the first two methods.

1.1.2. Benefits of SCC. Because of its unique nature, self-consolidating concrete (SCC) has the potential to significantly reduce costs associated with concrete construction. SCC is a highly flowable, nonsegregating concrete that can be placed without any mechanical consolidation, and thus has the following advantages over conventional concrete:

- decreased labor and equipment costs during concrete placement,
- decreased potential for and costs to repair honeycombing and voids,
- increased production rates of precast and cast-in-place elements, and

- improved finish and appearance of cast and free concrete surfaces (Myers and Volz, 2011).

1.1.3. Concerns with SCC. Concerns exist over the structural implications of SCC in cast-in-place and precast elements. Specifically, higher paste contents, higher fines contents, and the use of smaller, rounded aggregates may significantly alter the bond strength of SCC mixes as compared to traditional concrete mixes with the same compressive strength. These concerns increase for mixtures that use untested aggregate types and various supplementary cementitious materials. Consequently, to achieve the benefits and potential savings with SCC, guidelines are needed for its proper application in bridges, roadways, culverts, retaining walls, and other transportation-related infrastructure components (Myers and Volz, 2011)..

1.2. OBJECTIVES & SCOPE OF WORK

The main objective of this study was to determine the effect on bond performance of SCC. The SCC test program consisted of comparing the bond performance of normal and high strength SCC with their respective MoDOT standard mix designs.

The following scope of work was implemented in an effort to attain these objectives: (1) review applicable literature; (2) develop a research plan; (3) design and construct test fixtures; (4) design and construct test specimens; (5) test specimens to failure and record applicable data; (6) analyze results and conduct comparisons between experimental and control mix designs; (7) develop conclusions and recommendations; (8) prepare this report in order to document the information obtained during this study.

1.3. RESEARCH PLAN

The research plan entailed determining the bond performance of SCC relative to MoDOT standard mix designs. For the SCC test program, two SCC mix designs were determined from a survey of precast suppliers, one normal strength and one high strength, and used for comparison.

Two test methods were used for bond strength comparisons. The first was a direct pull-out test based on the RILEM 7-II-128 "RC6: Bond test for reinforcing steel. 1. Pull-out test" (RILEM, 1994). Although not directly related to the behavior of a reinforced concrete beam in flexure, the test does provide a realistic comparison of bond between types of concrete. A total of 24 direct pull-out test specimens were constructed and tested to bond failure using this test method. The second test method consisted of a full-scale beam splice test specimen subjected to a four-point loading until failure of the splice. This test method is a non-ASTM test procedure that is generally accepted as the most realistic test method for both development and splice length. A total of 12 full-scale beam splice test specimens were constructed and tested to failure.

1.4. OUTLINE

This report consists of six sections and three appendices. Section 1 briefly explains the characteristics, benefits, and concerns of SCC, as well as the study's objective and the manner in which the objective was attained.

Section 2 explains the mechanisms behind bond strength of deformed reinforcing bars embedded in concrete, common methods for testing bond strength, and past bond research conducted on SCC.

Section 3 details the mix designs used in this study and their associated fresh concrete properties as well as the mechanical and strength properties determined at the time of bond testing.

Section 4 details the direct pull-out and beam splice test specimen design, fabrication, and testing setup and procedure.

Sections 5 presents the test result normalization process, the recorded test program results, normalized test results, and the comparisons of SCC results to their control mix designs.

Section 6 restates the findings that were established during the course of this study and presents conclusions and recommendations based on the test results obtained.

2. LITERATURE REVIEW

2.1. BOND CHARACTERISTICS

Due to its very low tensile strength, concrete, by itself, would be a poor structural material to use in members resisting anything but a concentric axial compressive load. The tensile strength of concrete is generally only 10% of its compressive strength. However, the addition of steel reinforcing bars in the areas of the cross section of the member experiencing tensile stresses has proven to be a suitable solution to overcoming the poor tensile strength of concrete. The high tensile strength of steel is able to withstand the tensile stresses upon failure of the concrete. In order to obtain complete composite behavior between the reinforcing steel and the concrete, the tensile stresses must be fully transferred to the steel from the concrete. This transfer of stresses is facilitated by an adequate bond between the steel reinforcing bars and concrete.

The three modes of stress transfer from concrete to deformed steel reinforcement are through chemical adhesion, friction along the steel-concrete interface, and bearing resistance of the ribs on the steel against the surrounding concrete, as shown in **Figure 2.1**. Chemical adhesion refers to the bonding of the steel to the concrete through chemical reactions between the two surfaces. Upon initial loading, the resistance through chemical adhesion is the first stress transfer mechanism to fail. Upon failure of the chemical adhesion, the slipping action of the bar initiates the transfer of stresses from friction and rib anchorage. Frictional forces developed along the smooth faces of the reinforcing bar are relatively small compared to the forces transferred through the ribs. As the bar slip

increases, stress transfer through friction decreases, to a point where most of the tensile stresses are transferred through anchorage of the ribs.

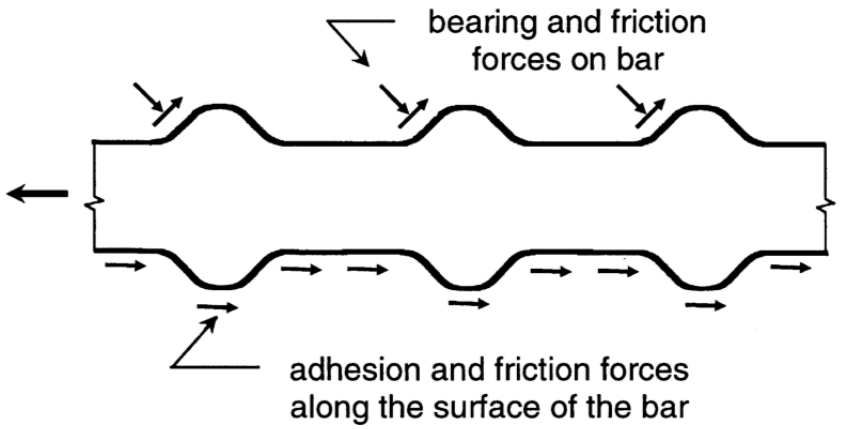

Figure 2.1 – Stress transfer between steel and surrounding concrete (ACI 408R, 2003)

As the load is increased, complete failure of the bond will occur by the concrete crushing against the ribs. One type of bond failure results when the bar is pulled directly out of the concrete, creating a shear plane along the outer edges of the steel ribs. This occurs when there is sufficient concrete cover and clear spacing between the reinforcing bars. Another type of bond failure is a splitting failure of the concrete cover. This occurs when there is insufficient concrete cover or insufficient clear spacing between the reinforcing bars (ACI 408R, 2003).

With adequate bond, tensile stresses can be transferred from the concrete to the reinforcing bar such that the bar will fail through yielding, and eventually fracture. The shortest length required to increase the stress of the bar from zero to the yield stress is called the development length of the bar. The development length of reinforcing steel is

dependent on the bar diameter and yield stress, as well as the coefficient of friction on the steel/concrete interface. The need for reinforcement splices is common in monolithic construction of large members, such as columns extending multiple levels of a structure. The allowable types of tension splices are lapped splices, mechanical splices, and welded splices. Lap slices are the transfer of tensile stresses from one bar to the concrete, then from the concrete to another bar by overlapping the two reinforcing bars. The overlapping distance must be at least the development length of the bar. Mechanical splices are achieved through the use of various steel devices that connect the ends of the two bars being spliced. Welded splices consist of welding the two bars beings spliced together (Wight and MacGregor, 2009).

The factors affecting the bond strength between reinforcing steel bars and concrete are a function of the structural characteristics of the member, as well as characteristics of the bar and concrete. One structural characteristic that plays a large role in affecting the bond strength of steel and concrete is the concrete cover and spacing between bars. As the concrete cover and bar spacing increase, the bond strength will also increase. The increase in bond strength is attributed to the decreasing likelihood of splitting failures with large spacing and cover. Another structural characteristic affecting bond strength is the presence of transverse reinforcement. The presence of transverse reinforcement surrounding the embedded bar slows the progressions of splitting cracks, which effectively increases bond strength. Also, the location of the bar during casting of the member affects the bond strength between the steel and concrete. Bars with a large volume of concrete cast below them have lower bond strengths than bars cast at the

bottom of a member. This lower bond strength is caused by concrete settlement and the presences of excess bleed water around top-cast bars (ACI 408R, 2003).

Reinforcing bar and concrete properties also play a role in affecting the bond strength of steel and concrete. Bar size and geometry can greatly alter bond strength. Larger bars with higher relative rib areas achieve higher total bond forces than small bars. Bar surface condition, such as cleanliness and coating, significantly affect bond strength. While bars with rust and mill scale do not adversely affect bond strength, surface contaminants such as mud, oil, and other nonmetallic coatings will decrease bond strength. Also, epoxy coated bars have a tendency to reduce bond strength. Concrete properties such as compressive and tensile strength, and fracture energy will also affect bond strength. Increasing compressive and tensile strengths, and fracture energy will subsequently increase bond strength. The addition of transverse reinforcement also increases the extent that the concrete compressive strength affects bond strength. Also, increasing the aggregate percentage in a concrete mix, as well as aggregate strength, will increase bond strength (ACI 408R, 2003).

2.2. COMMON BOND TESTS

There have been numerous test methods created to determine the bond strength between concrete and steel reinforcing bars. There are four common methods of bond testing. Two small-scale test methods are the direct pull-out test and the beam-end pullout test. Two large-scale test methods are the beam anchorage test and the beam splice test. The direct pull-out test specimen, shown in **Figure 2.2**, is the most common of the four tests listed above due to the ease of fabricating the test specimens and performing the test.

This test is run by supporting the concrete and applying tension to the reinforcing bar until failure, as shown in **Figure 2.2**. This bond test is the least accurate test for defining the actual bond strength and is best used for comparison purposes only.

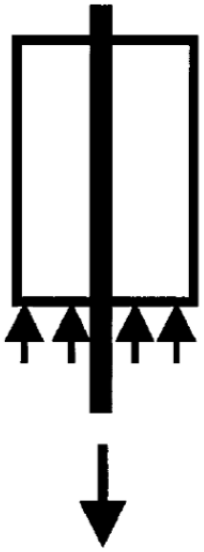

Figure 2.2 – Direct pull-out test specimen (ACI 408R, 2003)

The beam-end pull-out, also called the modified cantilever beam, test specimen is shown in **Figure 2.3**. This test is relatively easy to construct and perform and gives an accurate representation of how embedded reinforcing bars would behave in a full-scale beam. The compressive force applied must be located at least the same distance as the embedded length away from the end of the reinforcing bar. A length of reinforcing bar at the contact surface is left unbounded in order to prevent a conical failure surface from forming.

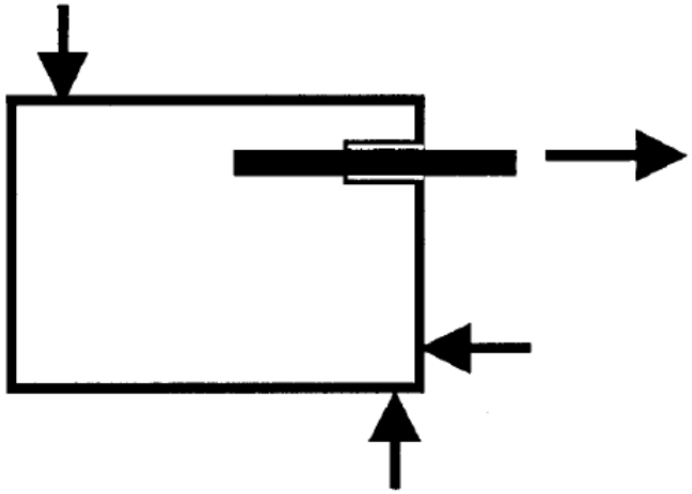

Figure 2.3 – Beam-end pull-out test specimen (ACI 408R, 2003)

The beam anchorage test specimen is shown in **Figure 2.4**. This test specimen is meant to represent a full-scale beam with two cracked sections and a known length of bonded area. This test specimen is designed to measure development length of the reinforcing bar. **Figure 2.5** shows the beam splice test specimen. This test specimen is designed to measure the splice length of the reinforcing bar. The reinforcing bar splice placement and loading configuration is developed to subject the spliced region to a constant moment along the length of the splice. Current ACI 318-08 (ACI 318-08, 2008) design provisions for development length and splice length are based primarily on data from this type of test. Bond strengths determined from both test specimens are generally similar.

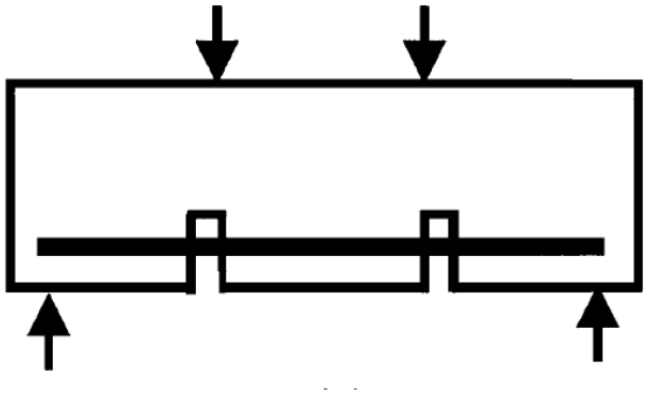

Figure 2.4 – Beam anchorage test specimen (ACI 408R, 2003)

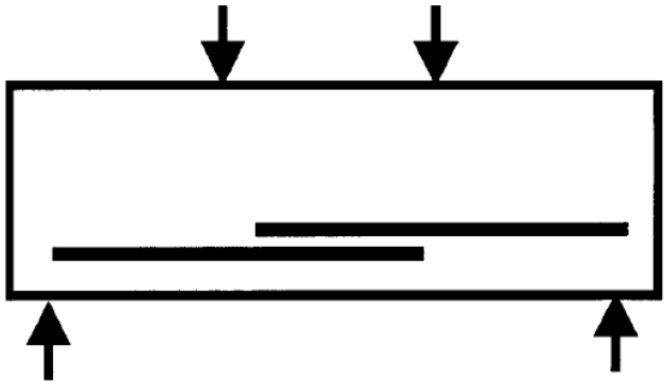

Figure 2.5 – Beam splice test specimen (ACI 408R, 2003)

2.3. SELF-CONSOLIDATING CONCRETE BOND RESEARCH

The key difference between SCC and conventional concrete is workability. SCC is characterized by its fluidity and its ability to eliminate the need for mechanical consolidation via the use of vibrators. Typically, three different methods are used for producing an SCC mix design. The first method is by the addition of a viscosity modifying admixture (VMA), along with a water reducer to a conventional concrete mix design. The VMA reduces the likelihood of segregation of the coarse aggregate by increasing the viscosity of the water. The water reducer increases the flowability of the

paste. The second method is through increasing the fine-to-coarse aggregate ratio and the addition of a water reducer. The lower coarse aggregate content increases the flowability and lowers the potential for segregation. The third method is essentially a combination of the first two methods.

There have been numerous studies conducted to determine the bond performance of SCC relative to conventional concrete. One such study was conducted at Ryerson University entitled "Bond Strength of Deformed Bars in Large Reinforced Concrete Members Cast with Industrial Self-Consolidating Concrete Mixture" (Hassan *et al*, 2009). This study focused on comparing the bond performance of deformed bars embedded in large, heavily reinforced direct pull-out specimens made with conventional and self-consolidating concrete. The pull-out specimens were 13 ft. (4000 mm) long, 4 ft. tall (1200 mm), and 1 ft. wide (300 mm). Thirty #6 (#20) deformed bars were bonded 6 in. (150 mm) and a plastic sleeve was used to debond the other half of the embedded bar. The bars were placed 6, 20, and 34 in. (150, 510, and 870 mm) from the bottom of the specimen in order to examine the effect of the depth of cast concrete beneath the bar (top bar effect). Longitudinal reinforcement of nine #11 (#36) bars at the top, three #8 (#25) bars at the bottom, and eight #5 (#16) bars spaced evenly between the top and bottom bars. Closed stirrups spaced 6.3 in. (160 mm) on center and consisting of #3 (#11) bars were used for transverse reinforcement. The embedded bars were divided into 5 groups that were tested at 1, 3, 7, 14, and 28 days to track bond strength development. All embedded bars were tested to failure. The authors concluded that no significant differences were seen between SCC and conventional concrete in terms of bond strength development. Also, the normalized bond stress at failure was slightly higher for SCC than

conventional concrete for 3, 7, 14, and 28 days (Hassan *et al.*, 2009). However, only pull-out specimens were tested.

Another study focusing on comparing bond strengths of SCC with conventional concrete through direct pull-out specimens was conducted in Iran entitled "Bond Strength of Reinforcing Steel in Self-Compacting Concrete" (Foroughi-Asl *et al.*, 2008). The direct pull-out specimens were based on the RILEM 7-II-128 "RC6: Bond test for reinforcing steel. 1. Pull-out test" (RILEM, 1994). The specimens consisted of embedding #3 (#10), #5 (#16), and #6 (#20) ribbed reinforcing bars in a 6 in. (150 mm) concrete cube. A plastic sleeve was used to debond a 2 in. (50 mm) length of bar at the base of the specimen, leaving 4 in. (100 mm) of bonded length. All direct pull-out specimens were tested to failure. The test results of this study indicate that SCC performs at the same level as conventional concrete in terms of bond strength. However, it was noted that due to the retarding effect of the water reducing admixture used in this study, the bond strength of SCC developed slower than that of conventional concrete (Foroughi-Asl *et al.*, 2008).

Researchers at Université de Toulouse in France conducted a study entitled "Bond and Cracking Properties of Self-Consolidating Concrete" (Castel *et al.*, 2008). The focus of this program was to determine the bond strength and cracking behavior of SCC and conventional concrete by conducting tension member and beam flexure tests. The tension member test was performed on a 19.7-in-long (500 mm) concrete block with a square, 3.94-in.-wide (100 mm) cross section. A length of deformed, #4 (#13) reinforcing bar was embedded in the center of the concrete section. Two tension member tests were performed for each type of concrete. The full-scale beam specimens were 6.6 ft. (2000

mm) long, with a cross section of 6 in. x 7.9 in. (150 mm x 200 mm). The longitudinal reinforcement consisted of two #3 (#10) and two #2 (#6) deformed reinforcing bars on the bottom and top of the cross section, respectively. Transverse reinforcement consisted of #2 (#6) closed stirrups spaced at 7.8 in. (198 mm) on center along the entire length of the beam. Cracks along the beam were evaluated at service and ultimate loads. One beam test was conducted for each concrete type and both beams failed by crushing of the concrete in the compression zone. The tension member test results indicated that there was no difference in transfer length between SCC and conventional concrete. The transfer lengths for each concrete decreased slightly as the concrete compressive strength increased. The beam test results indicated that there was no significant difference in cracking moment between SCC and conventional concrete. The moment capacity and bending stiffness at service level loads were also similar (Castel *et al.***,** 2008).

A study comparing bond strength between SCC and conventional concrete through testing full-scale beam specimens was also conducted in Turkey entitled "Strength of Tension Lap-Splices in Full Scale Self-Compacting Concrete Beams" (Turk *et al.*, 2009). Full-scale beam specimens were constructed with two lap splices of longitudinal bars in the tension region of the beam cross section. The beams were then subjected to a 4-point-loading until failure. Twelve beam specimens were cast in this study; six beams for each mix design. The beams were 6.6 ft. (2000 mm) in length, with a cross section of 7.9 in. x 12 in. (200 mm x 300 mm). Three of the six beams were constructed with #5 (#16) longitudinal reinforcing bars and the other three contained #6 (#20) longitudinal bars. The longitudinal bars were spliced 12.2 in. (310 mm) at midspan of the beam and subjected to a constant moment. The splice length was chosen to ensure

no yielding of the bars occurred. Transverse reinforcement consisted of #3 (#10) bars spaced at 3.1 in. (80 mm) on center along the entire length of the beam, effectively confining the spliced region. The clear cover in each beam was 1.2 in. (30 mm). All beams were loaded to failure. The normalized bond strengths of the SCC beam specimens were 4% higher than the control specimens for both bar diameters. It was also noted that the SCC beam specimens produced longer cracks than the control specimens, giving evidence that the paste in the SCC more thoroughly coated the reinforcing bar (Turk *et al.*, 2009).

Another study was conducted in Spain comparing the bond strength of SCC and conventional concrete entitled "Bond Behaviour of Reinforcement in Self-Compacting Concretes" (Valcuende and Parra, 2008). Comparison of bond strengths was accomplished through the use of direct pull-out tests. The specimens tested in this study included 7.9 in. (200 mm) cube specimens and square cross-section, 4.9-ft.-tall (1500 mm) columns. One length of #5 (#16) diameter reinforcing bars was embedded into each cube specimen, with a bonded length of 3.15 in. (80 mm). Twelve cube specimens were constructed for each mix design. Of the twelve cubes constructed, six specimens were tested at 28 days and the other six specimens were tested at 90 days. Six lengths of #5 (#12) bars were embedded into each column, with a bonded length of 2.36 in. (60 mm). Four columns were constructed for each mix design. At 28 days, six 5.9 in. (150 mm) cube specimens were cut from the column and tested to bond failure. Rubber sleeves were used to ensure the specified length of bar remained undboned from the surrounding concrete. The bars in each column were located 2.95 in. (75 mm), 10.83 in. (275 mm), 18.7 in. (475 mm), 26.57 in. (675 mm), 41.34 in. (1050 mm), and 56.1 in. (1425 mm)

from the bottom of the specimen. The columns were constructed to evaluate top-bar effect. The test results obtained indicate that the SCC specimens exhibited higher bond strength than that of the conventional concrete specimens. The authors noted that SCC behaved more homogeneously than the conventional concrete mixes in the column test specimens. This indicates that top-bar effect is less pronounced in SCC than in conventional concrete (Valcuende and Parra, 2008).

SCC bond strength relative to conventional concrete was also studied and detailed in a report entitled "Effect of Reinforcing Bar Orientation and Location on Bond with Self-Consolidating Concrete" (Castel *et al.*, 2006). Direct pull-out tests were constructed to compare bond strengths. Also, reinforcing bars were cast vertically and horizontally in the concrete to determine the effect of bar orientation on bond strength. The pull-out specimens were 4.73 in. (120 mm) long, with a cross section of 4 in. x 4 in. (100 mm x 100 mm). The reinforcing bars embedded in the concrete were #5 (#12) plain and ribbed bars. The bonded length was 2.36 in. (60 mm) for each specimen. The specimens were cast in 19.7 in. (500 mm) lengths and sawn into three parts at 28 days. Two pull-out specimens were tested for each configuration. The effect of bar location was also tested through the use of large specimens. The same reinforcing bars were used for the large test specimens. The specimens were 59.1 in. (1100 mm) tall and the reinforcing bars were spaced 4 in. (100 mm) apart, evenly along the height of the specimen. At 28 days, the large specimen was cut to create smaller specimens the same size as the small pull-out specimens. The test results indicated that the orientation of the deformed bars had a similar influence on bond strength for both 3,625 psi (25 MPa) SCC and conventional concrete. Bond strengths for the 5,800 psi (40 MPa) concrete mixes were not affected by

bar orientation. Reduction in bond strength was seen for each concrete type as the amount of concrete cast below the bar increased in the large specimen tests. Similar reductions were seen for both SCC and conventional concrete. Overall, SCC exhibited higher bond strength than conventional concrete for both concrete strengths (Castel *et al.*, 2006).

Another study evaluating the bond behavior of SCC was entitled "Self-Compacting Concrete (SCC) Time Development of the Materials and the Bond Behaviour" (Dehn *et al.*, 2000). This study focused on evaluating the bond strength increase over time in SCC by testing direct pull-out specimens at 1, 3, 7, and 28 days. The direct pull-out test specimens consisted of a cylinder of concrete that was 4 in. (100 mm) in diameter and 4 in (100 mm) long. Reinforcing consisted of #3 (#10) bars embedded 2 in. (50 mm) in the concrete, with an unbonded length of 2 in. (50 mm). A plastic sleeve was used to ensure the appropriate length of bar remained unbonded during casting. A total of twelve specimens were cast and three specimens at each specified day to evaluate the bond strength gain over time. The tested specimens were then compared to the bond law of conventional concrete developed by Konig and Tue. The test results indicated that the bond behavior of SCC was superior to that of conventional concrete (Dehn *et al.*, 2000).

Another test comparing bond strengths of SCC and conventional concrete was entitled "Development of Bond Strength of Reinforcement Steel in Self-Consolidating Concrete" (Chan *et al.*, 2003). This study compares bond strengths of SCC and conventional concrete by testing direct pull-out specimens. Full-scale walls were constructed with reinforcing bars embedded parallel to the depth of the wall. The specimen was 47.24 in. x 35.43 in. x 169.29 in. (1200 mm x 900 mm x 4300 mm). Three

rows of deformed reinforcing bars were embedded horizontally at 7.87, 19.7, and 31.5 in. (200, 500, and 800 mm) from the bottom of the specimen. A length of 4 in. (100 mm) was bonded and lengths of polyvinyl chloride (PVC) were used as bond breakers at both ends of the embedded reinforcing bars. The test results collected indicated that the extent of differing bond strengths with respect to elevation at casting was less significant with SCC than with conventional concrete. Also, SCC exhibited significantly higher bond strength and less top-bar effect than the conventional concrete (Chan *et al.*, 2003).

3. MIX DESIGNS AND CONCRETE PROPERTIES

3.1. INTRODUCTION

The following chapter contains the mix designs for both the self-consolidating concrete (SCC) mix designs and their respective controls. Also included in this chapter are the methods and results of the testing done to determine the fresh and hardened properties of each mix.

3.2. CONCRETE PROPERTIES

3.2.1. Fresh Concrete Properties. Various tests were conducted on the fresh concrete prior to casting the test specimens. The type of fresh concrete test was dependent on the type of concrete being tested. A slump test was performed on all the conventional concrete mixes upon arrival of the concrete mixing truck in accordance with ASTM C143/C143M "Standard Test Method for Slump of Hydraulic-Cement Concrete" (ASTM C143/C143M, 2010). A standard mold for the slump test was dampened and placed on a metal slump pan. Then the mold was filled to one-third of its volume with the fresh concrete. The concrete was then rodded 25 times uniformly over the cross section with a standard tamping rod. This process was repeated for the subsequent two layers. Upon finishing the last layer, the top of the concrete was smoothed using the tamping rod and any excess concrete was removed from around the base of the mold. The mold was then lifted vertically slowly in accordance with the ASTM established method noted above. The length that the top of the fresh concrete slumped upon removal of the mold was recorded as the slump of the concrete. The slump test is shown in **Figure 3.1.**

Figure 3.1 – Slump test

Two unique test methods were conducted on the SCC to determine workability. The first was the slump flow test in accordance with ASTM C1611/C1611M "Standard Test Method for Slump Flow of Self-Consolidating Concrete" (ASTM C1611/C1611M, 2009). The same mold used for the slump test was also used for the slump flow test. The inside of the mold was dampened and placed upside down (large opening facing upward) on a metal slump pan. The mold was then filled in a continuous manner until the mold was slightly overfilled above its top. The surface was then leveled with a strike-off bar, and then the mold was raised vertically slowly in accordance with the ASTM. When the concrete had stopped flowing, the diameter of the concrete was measured along perpendicular axes and averaged to determine the slump flow. The slump flow test is shown in **Figure 3.2**.

Figure 3.2 – Slump flow test

The second unique test for SCC was the J-ring test conducted in accordance with ASTM C1621/C1621M "Standard Test Method for Passing Ability of Self-Consolidating Concrete by J-Ring" (ASTM C1621/C1621M, 2009). The procedure for the J-ring test is the same as for the slump flow. However, after dampening the mold, it is placed on the slump pan in the center of a standard J-ring. The same filling, finishing, and mold removal procedures as those used for the slump flow are then conducted for the J-ring test. The diameter of the concrete ring was then measured in two perpendicular locations and averaged. The J-ring test is shown in **Figure 3.3**.

Figure 3.3 – J-ring test

The unit weight and air content were also determined. The unit weight of the fresh concrete was determined in accordance with ASTM C138/C138M "Standard Test Method for Density (Unit Weight), Yield, and Air Content (Gravimetric) of Concrete" (ASTM C138/C138M, 2010). A steel cylindrical container was used as the measure for this test. The inside of the measure was first dampened, and then it was weighed and measured to determine its empty weight and volume, respectively. Then fresh concrete was added to the measure to one-third of its volume. The concrete was then rodded 25 times with a standard tamping rod and the measure was struck with a rubber mallet 15 times around its outside perimeter. This step was repeated for the second and third level of concrete. Upon filling the measure, the concrete was finished with a strike-off plate and any excess concrete was removed from the rim of the measure using a sponge. The measure was then weighed to determine its weight and the weight of the concrete it contained. The weight of the measure was then subtracted from the combined weight of

the measure and the concrete to determine the weight of the concrete. The weight of the concrete was then divided by the volume of the measure to determine the unit weight of the concrete.

The air content of the concrete was determined in accordance with ASTM C231/C231M "Standard Test Method for Air Content of Freshly Mixed Concrete by the Pressure Method" (ASTM C231/C231M, 2010). A standard type-B meter was used for this test. The same steel container and filling procedure used for determining the unit weight were used for the air content test. After completing the filling process, the flange of the cover assembly was thoroughly cleaned and clamped onto the steel container. Both petcocks were opened and water was added to one petcock until the water emerged from the other petcock to remove any excess air in the steel container. The air bleeder valve was then closed and air was pumped into the container until the gauge hand was on the initial pressure line. Both petcocks were then closed and the main air valve was opened while simultaneously tapping the container smartly with a rubber mallet. The air content shown on the gauge was then recorded as the air content of the concrete.

3.2.2. Compressive Strength of Concrete. The concrete compressive strength was determined in accordance with ASTM C39/39M "Standard Test Method for Compressive Strength of Cylindrical Concrete Specimens" (ASTM C39/C39M, 2011). The specimens consisted of 4 in. (102 mm) diameter, 8 in. (203 mm) tall cylinders for each mix design. **Figure 3.4** displays the cylinders being cast. Prior to testing, the cylinders were capped in order to eliminate the effect of point stresses caused by an uneven surface. The capped cylinders were then subjected to a compressive axial load across their entire circular cross section until failure, applied at a rate appropriate for the

testing apparatus and in conformance with ASTM C39/C39M. The test setup is shown in **Figure 3.5**.

Figure 3.4 – Casting compressive strength cylinders

Figure 3.5 – Compressive strength test setup

3.2.3. Modulus of Rupture of Concrete. The modulus of rupture was determined in accordance with ASTM C78/C78M "Standard Test Method for Flexural Strength of Concrete (Using Simple Beam Third-Point Loading) (ASTM C78/C78M, 2010). The test consists of subjecting a 6 in. x 6 in. x 24 in. (152 mm x 152 mm x 610 mm) concrete beam to a four-point load until failure. **Eq. 3.1** was used to determine the modulus of rupture from each beam test result.

$$R = \frac{PL}{bd^2} \tag{3.1}$$

Where R is the modulus of rupture, P is the maximum applied load, L is the span length, b is the average width of the specimens at the fractured surface, and d is the average depth of the specimen at the fractured surface. The test specimens are shown in **Figure 3.6** and the test setup is shown in **Figure 3.7**.

Figure 3.6 – Modulus of rupture test specimens

Figure 3.7 – Modulus of rupture test setup

3.2.4. Splitting Tensile Strength of Concrete. The splitting tensile strength was determined in accordance with ASTM C496/C496M "Standard Test Method for Splitting Tensile Strength of Cylindrical Concrete Specimens" (ASTM C496/C496M, 2011). The specimens consisted of 6 in. (152 mm) diameter, 12 in. (305 mm) tall cylinders for each mix design, which were tested upon reaching the appropriate concrete compressive strength. **Eq. 3.2** was used to determine the splitting tensile strength of each cylinder test result.

$$T = \frac{2P}{\pi l d} \tag{3.2}$$

Where T is the splitting tensile strength, P is the maximum applied load, l is the length of the specimen, and d is the diameter of the specimen. The splitting tensile strength test setup is shown in **Figure 3.8**.

Figure 3.8 – Splitting tensile strength test setup

3.3. SELF-CONSOLIDATING CONCRETE (SCC) MIX DESIGNS

A survey of Missouri precast suppliers was conducted in order to obtain representative SCC mix designs currently in use throughout the state, particularly in large metropolitan areas such as St. Louis and Kansas City. The results of this survey were then used to develop a normal strength and a high strength SCC mix design, with specified compressive strengths of 6,000 psi (41.4 MPa) and 10,000 psi (69 MPa), respectively. The target air content was 6% and the target slump flow was 23 to 28 in. (584 to 711 mm) for both SCC mix designs. Two standard MoDOT mix designs with the same specified compressive strengths as their respective SCC mix designs were chosen as the controls. The target air content was 6% and the target slump was 4 to 5 in. (102 to 127 mm) for both control mix designs. The air entraining admixture MB-AE-90 and the water reducing admixture Glenium 7700 were used to obtain the necessary properties.

3.3.1. Normal Strength Control Mix Design. The normal strength control mix design was designated C6-58L and is shown in **Table 3.1**.

Table 3.1 – C6-58L mix proportions

Ingredient	Weight (lb./yd^3)
w/cm	0.37
Cement (Type 1)	750
Coarse Aggregate	1,611
Fine Aggregate	1,166
MB-AE-90	1.5 oz./cwt.
Glenium 7500	4.7 oz./cwt.

Conversion: 1 lb./ yd^3 = 0.59 kg/m^3
1 oz. = 29.6 ml
1 lb. = 0.45 kg

The slump, air content, and unit weight of the concrete used for the fabrication of test specimens was determined upon arrival of the concrete mixing truck. The slump measured 8 in. (203 mm), the air content measured 9.0%, and the unit weight measured 139.6 lb./ft^3 (2240 kg/m^3).

Test specimens for determining the compressive strength, splitting tensile strength, and modulus of rupture of the concrete were fabricated along with the bond test specimens. The concrete compressive strength test results are shown in **Table 3.2** and plotted in **Figure 3.9**. The splitting tensile strength results are shown in **Table 3.3**. The modulus of rupture test results are shown in **Table 3.4**.

Table 3.2 – Compressive strength data of C6-58L

Day	Average Strength (psi)
1	3,695
3	5,115
7	5,330
14	5,910
16	5,720

Conversion: 1 psi = 6.9 kPa

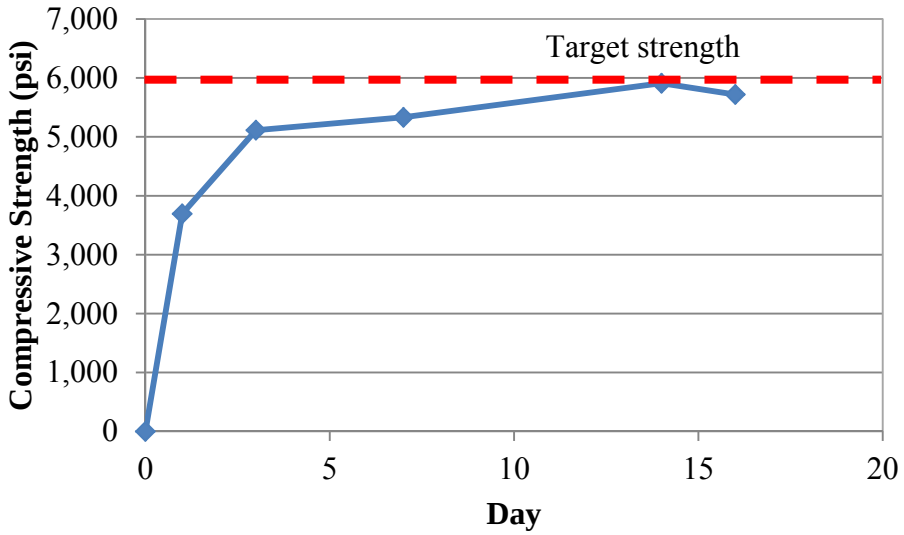

Figure 3.9 – Plot of C6-58L compressive strength
Conversion: 1 psi = 6.9 kPa

Table 3.3 – Splitting tensile strength test results for C6-58L

Specimen	Peak Load (lb.)	Splitting Tensile Strength (psi)
C6-58L-1	43,155	380
C6-58L-2	51,870	460
C6-58L-3	50,250	445
	Average:	430

Conversion: 1 lb. = 4.45 N
1 psi = 6.9 kPa

Table 3.4 – Modulus of rupture test results for C6-58L

Specimen	Peak Load (lb.)	Modulus of Rupture (psi)
C6-58L-1	6,255	520
C6-58L-2	6,310	530
C6-58L-3	5,670	480
C6-58L-4	5,375	440
	Average:	490

Conversion: 1 lb. = 4.45 N
1 psi = 6.9 kPa

3.3.2. SCC Normal Strength Mix Design. The SCC normal strength mix design was designated S6-48L and is shown in **Table 3.5**.

The slump flow, J-ring, air content, and unit weight of the concrete used for the fabrication of test specimens was determined upon arrival of the concrete mixing truck. The slump flow measured 24 in. (610 mm), the J-ring measured 20.75 in. (527 mm), the air content measured 6%, and the unit weight measured 145.7 lb./ft^3 (2330 kg/m^3).

Table 3.5 – S6-48L mix proportions

Ingredient	Weight (lb./yd^3)
w/cm	0.37
Cement (Type 1)	750
Coarse Aggregate	1,333
Fine Aggregate	1,444
MB-AE-90	1.5 oz./cwt.
Glenium 7500	6.2 oz./cwt.

Conversion: 1 lb./ yd^3 = 0.59 kg/m^3
1 oz. = 29.6 ml
1 lb. = 0.45 kg

Test specimens for determining the compressive strength, splitting tensile strength, and modulus of rupture of the concrete were fabricated along with the bond test

specimens. The concrete compressive strength test results are shown in **Table 3.6** and plotted in **Figure 3.10**. The splitting tensile strength results are shown in **Table 3.7**. The modulus of rupture test results are shown in **Table 3.8**.

Table 3.6 – Compressive strength data of S6-48L

Day	Average Strength (psi)
1	5,320
3	6,990
5	6,840

Conversion: 1 psi = 6.9 kPa

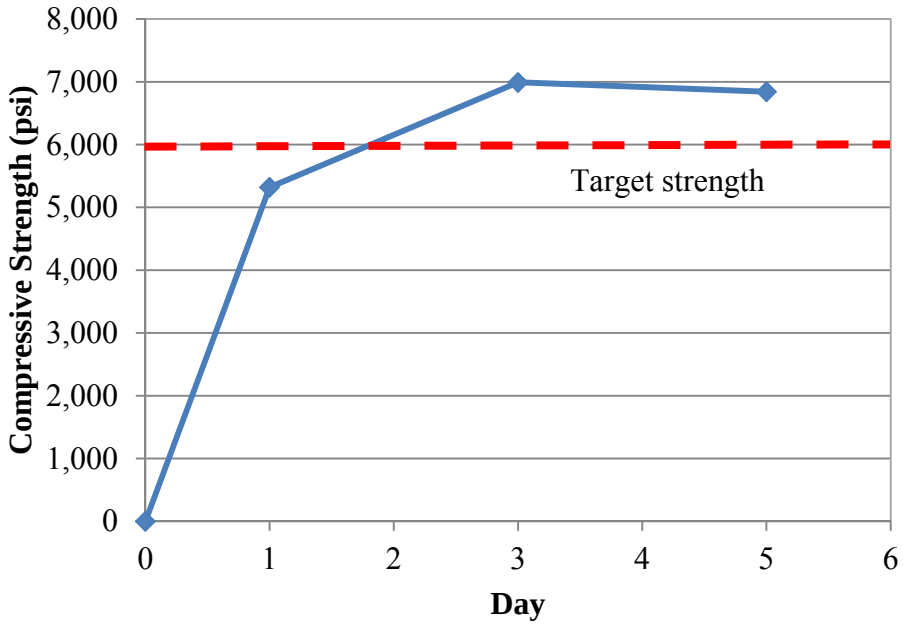

Figure 3.10 – Plot of S6-48L compressive strength
Conversion: 1 psi = 6.9 kPa

Table 3.7 – Splitting tensile strength test results for S6-48L

Specimen	Peak Load (lb.)	Splitting Tensile Strength (psi)
S6-48L-1	53,760	475
S6-48L-2	62,580	555
S6-48L-3	62,790	555
	Average:	530

Conversion: 1 lb. = 4.45 N
1 psi = 6.9 kPa

Table 3.8 – Modulus of rupture test results for S6-48L

Specimen	Peak Load (lb.)	Modulus of Rupture (psi)
S6-48L-1	5,155	430
S6-48L-2	5,680	470
S6-48L-3	6,980	570
S6-48L-4	6,210	520
	Average:	495

Conversion: 1 lb. = 4.45 N
1 psi = 6.9 kPa

3.3.3. High Strength Control Mix Design. The high strength control mix design was designated C10-58L and is shown in **Table 3.9**.

Table 3.9 – C10-58L mix proportions

Ingredient	Weight (lb./yd^3)
w/cm	0.30
Cement (Type 1)	840
Fly Ash (Class C)	210
Coarse Aggregate	1,440
Fine Aggregate	1,043
MB-AE-90	1.3 oz./cwt.
Glenium 7500	5 oz./cwt.

Conversion: 1 lb./ yd^3 = 0.59 kg/m^3
1 oz. = 29.6 ml
1 lb. = 0.45 kg

The slump, air content, and unit weight of the concrete used for the fabrication of test specimens was determined upon arrival of the concrete mixing truck. The slump measured 2 in. (51 mm), the air content measured 2.5%, and the unit weight measured 152.2 lb./ft^3 (2440 kg/m^3).

Test specimens for determining the compressive strength, splitting tensile strength, and modulus of rupture of the concrete were fabricated along with the bond test specimens. The concrete compressive strength test results are shown in **Table 3.10** and plotted in **Figure 3.11**. The splitting tensile strength results are shown in **Table 3.11**. The modulus of rupture test results are shown in **Table 3.12**.

Table 3.10 – Compressive strength data of C10-58L

Day	Average Strength (psi)
1	6,715
3	8,000
7	8,995
14	9,265
17	9,625

Conversion: 1 psi = 6.9 kPa

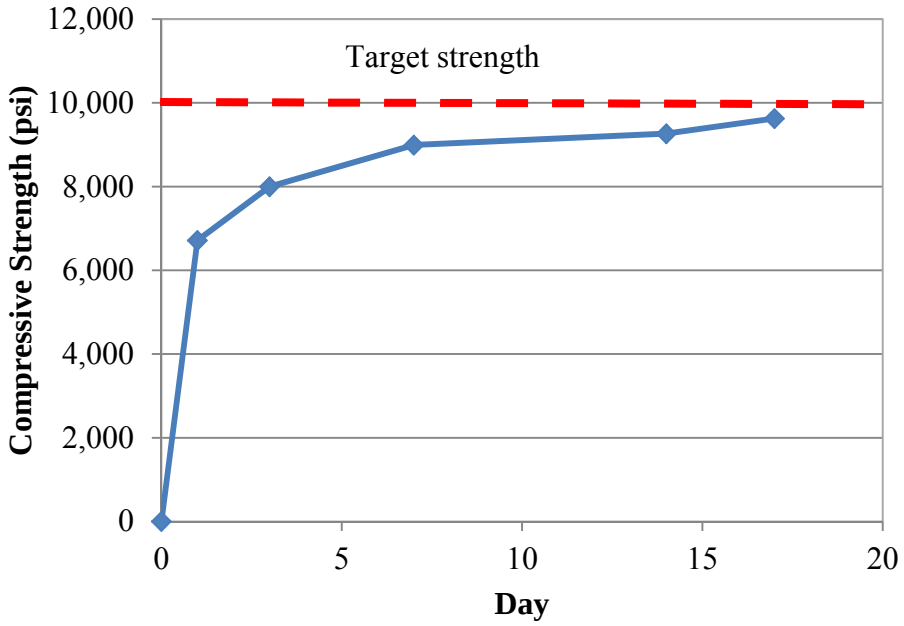

Figure 3.11 – Plot of C10-58L compressive strength

Conversion: 1 psi = 6.9 kPa

Table 3.11 – Splitting tensile strength test results for C10-58L

Specimen	Peak Load (lb.)	Splitting Tensile Strength (psi)
C10-58L-1	67,380	600
C10-58L-2	62,595	555
C10-58L-3	62,685	555
	Average:	570

Conversion: 1 lb. = 4.45 N
1 psi = 6.9 kPa

Table 3.12 – Modulus of rupture test results for C10-58L

Specimen	Peak Load (lb.)	Modulus of Rupture (psi)
C10-58L-1	8,585	705
C10-58L-2	7,925	645
C10-58L-3	8,345	680
C10-58L-4	9,220	730
	Average:	690

Conversion: 1 lb. = 4.45 N
1 psi = 6.9 kPa

3.3.4. SCC High Strength Mix Design. The SCC high strength mix design was designated S10-48L and is shown in **Table 3.13**.

Table 3.13 – S10-48L mix proportions

Ingredient	Weight (lb./yd^3)
w/cm	0.30
Cement (Type 1)	840
Fly Ash (Class C)	210
Coarse Aggregate	1,192
Fine Aggregate	1,291
MB-AE-90	1 oz./cwt.
Glenium 7500	7.2 oz./cwt.

Conversion: 1 lb./ yd^3 = 0.59 kg/m^3
1 oz. = 29.6 ml
1 lb. = 0.45 kg

The slump flow, J-ring, air content, and unit weight of the concrete used for the fabrication of test specimens was determined upon arrival of the concrete mixing truck. The slump flow measured 23.5 in. (597 mm), the J-ring measured 21.5 in. (546 mm), the air content measured 3.0%, and the unit weight measured 149.4 lb./ft^3 (2400 kg/m^3).

Test specimens for determining the compressive strength, splitting tensile strength, and modulus of rupture of the concrete were fabricated along with the bond test specimens. The concrete compressive strength test results are shown in **Table 3.14** and plotted in **Figure 3.12**. The splitting tensile strength results are shown in **Table 3.15**. The modulus of rupture test results are shown in **Table 3.16**.

Table 3.14 – Compressive strength data of S10-48L

Day	Average Strength (psi)
1	6,640
3	8,255
7	9,055
14	9,880
16	9,755

Conversion: 1 psi = 6.9 kPa

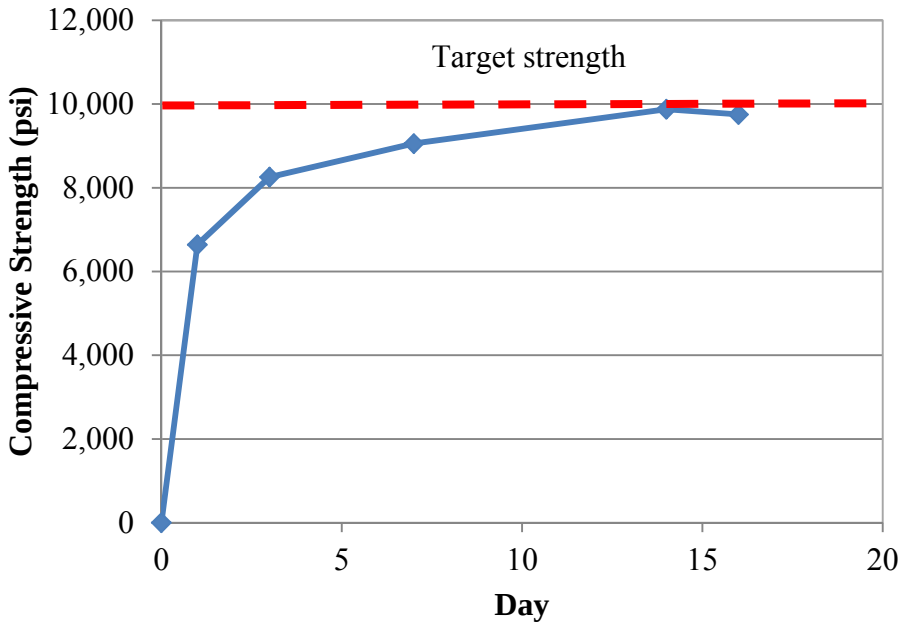

Figure 3.12 – Plot of S10-48L compressive strength
Conversion: 1 psi = 6.9 kPa

Table 3.15 – Splitting tensile strength test results for S10-48L

Specimen	Peak Load (lb.)	Splitting Tensile Strength (psi)
S10-48L-1	70,770	625
S10-48L-2	59,925	530
S10-48L-3	61,215	540
	Average:	565

Conversion: 1 lb. = 4.45 N
1 psi = 6.9 kPa

Table 3.16 – Modulus of rupture test results for S10-48L

Specimen	Peak Load (lb.)	Modulus of Rupture (psi)
S10-48L-1	5,925	480
S10-48L-2	7,400	605
S10-48L-3	6,670	550
S10-48L-4	6,465	535
	Average:	540

Conversion: 1 lb. = 4.45 N
1 psi = 6.9 kPa

4. EXPERIMENTAL PROGRAM

4.1. INTRODUCTION

The experimental program included both direct pull-out tests, as well as full-scale beam splice specimen tests. The direct pull-out specimens were based on RILEM 7-II-128 “RC6: Bond test for reinforcing steel. 1. Pull-out test” (RILEM, 1994). The beam splice specimen tests were based on recommendations in ACI 408R-03 “Bond and Development of Straight Reinforcing Bars in Tension” (ACI 408R-03, 2003). The following is a discussion of the design, setup, instrumentation, and procedures for both testing methods.

4.2. DIRECT PULL-OUT TEST

4.2.1. Direct Pull-out Specimen Design. The direct pull-out specimen tests were based on the RILEM 7-II-128 “RC6: Bond test for reinforcing steel. 1. Pull-out test” (RILEM, 1994). Several changes were made to the recommended test specimen based on results from previous research (Wolfe, 2011). The test involves casting a length of reinforcing bar within a concrete cylinder and applying a direct tension force on the bar until the bonded length fails. Although not directly related to the behavior of a reinforced concrete beam in flexure, the test does provide a realistic comparison of bond between types of concrete.

The RILEM standard states that the reinforcing bar will be embedded in the concrete a total length of 15 times the bar diameter to be tested. A bond breaker a length of 7.5 times the bar diameter is to be placed so that the bar is unbonded from the bottom

surface to halfway in the concrete, leaving a bonded length of 7.5 times the bar diameter. The unbounded length at the bottom of the concrete segment is to reduce restraint stresses caused by friction with the loading head. Previous testing showed this bonded length to be too long and yielding of the bar occurred prior to failure in some instances (Wolfe, 2011). To ensure the bond failed before the bar yielded, the total concrete depth was reduced to 10 times the bar diameter with a bonded length of 5 times the bar diameter.

The RILEM standard specifies a square concrete cross section with sides having a length of 8.75 in. (222 mm). For this test program, a circular concrete cross section with a diameter of 12 in. (305 mm) was used instead. This change eliminated the potential for a splitting failure (side cover failure) and also maintained a constant cover for the reinforcing bar.

The protocol for the direct pull-out tests included two bar sizes – #4 (#13) and #6 (#19) – in order to evaluate the bond performance over a range of reinforcing sizes. The total length of each bar was 40 in (1016 mm). A length of 3/8 in. (10 mm) was left exposed at the top of the specimen to measure bar slip using a Linear Voltage Differential Transformer (LVDT). **Figures 4.1** and **4.2** are schematic diagrams of the specimen dimensions for the #4 (#13) and #6 (#19) bars, respectively.

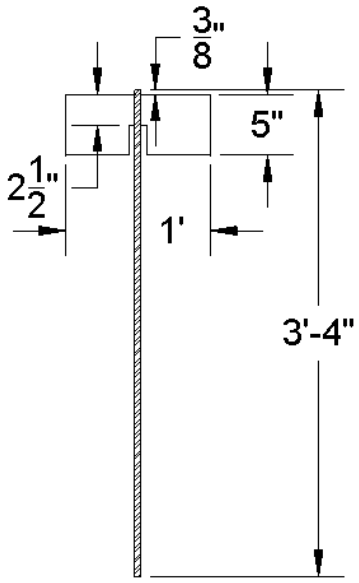

Figure 4.1 – Pull-out specimen with dimensions for #4 (#13) reinforcing bars
Conversion: 1 in. = 25.4 mm

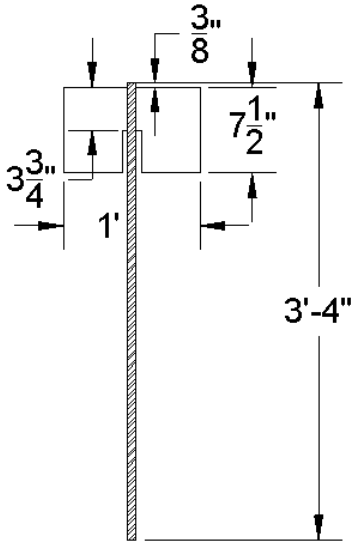

Figure 4.2 – Pull-out specimen with dimensions for #6 (#19) reinforcing bars
Conversion: 1 in. = 25.4 mm

4.2.2. Direct Pull-out Specimen Fabrication. The formwork base for the direct pull-out test specimen was constructed with a 14-in.-square (356 mm), 3/8-in.-thick (10 mm) section of plywood. A hole that was 1/16 in. (0.16 mm) larger than the bar diameter being tested was drilled through the center of the plywood squares. Cardboard tubing (Quick-Tube) was then cut to the required length, depending on the bar size being tested. Waterproof silicone adhesive caulk was then used to bind the cardboard tubing to the plywood squares.

The reinforcing bar for each specimen was sectioned into 40 in. (1016 mm) lengths. Polyvinyl chloride (PVC) tubing was used to form the bond breaker. For the #4 (#13) bar, the PVC had an inside diameter of 3/4 in. (19 mm) and was sectioned into lengths of 2.5 in. (64 mm). For the #6 (#19) bar, the PVC had an inside diameter of 1 in. (25 mm) and was sectioned into 3.75 in. (95 mm) lengths. A mark was made on each bar to facilitate the placement of the PVC bond breaker. The PVC was slid onto the reinforcing bar and shims of cardboard were used to center the bar in the PVC. The PVC was then adhered to the reinforcing bar using waterproof silicone adhesive caulk and was carefully finished to ensure there were no gaps in the caulk for the concrete paste to get between the bar and the PVC.

The top of the formwork was also a 14-in.-square (356 mm) of 3/8-in.-thick (10 mm) plywood with a hole drilled through its center. To ensure that the bars were plumb within the concrete encasement, prior to constructing the specimens, the reinforcing bars were placed in the completed forms and leveled. Upon leveling the bars, an outline of the cylindrical form was drawn on the underside of the top plywood square. Wood spacers were then screwed into the plywood square along the outline of the cardboard tubing.

The specimens were cast by first placing the reinforcing bar through the hole in the base of the formwork. Concrete was then placed in the cylindrical formwork and consolidated as necessary. After proper placement of the concrete, the exposed surface was finished. The top of the formwork was then carefully slid down the reinforcing bar and the wood spacers were fit snugly over the cylindrical forms. The reinforcing bar was checked to ensure it was plumb and then the sides of the cylindrical forms were lightly vibrated. The pull-out and companion material property specimens were allowed to cure until the concrete reached its specified strength prior to testing. The cardboard tubing was removed on the day of testing. Construction of the pull-out specimens is shown in **Figure 4.3**, with complete specimens shown in **Figure 4.4**.

Figure 4.3 – Pull-out specimen construction

Figure 4.4 – Completed specimens

4.2.3. Direct Pull-out Test Setup. Testing of the direct pull-out specimens was completed using a 200,000-lb-capacity (890 kN) testing machine manufactured by Tinius Olson. The test setup is shown in **Figures 4.5** and **4.6**. The cylindrical forms were removed immediately prior to testing. A neoprene pad with a hole in its center was placed on the top platform of the test machine to ensure uniform bearing of the concrete. The specimens were flipped upside down and the reinforcing bar was then threaded through the hole in the neoprene pad on the top platform and placed between the grips installed on the middle platform. An LVDT was then clamped to a stand, and the stand was placed on top of the concrete section of the specimen. The needle of the LVDT was placed on top of the 3/8 in. (10 mm) length of exposed reinforcing bar to measure slip.

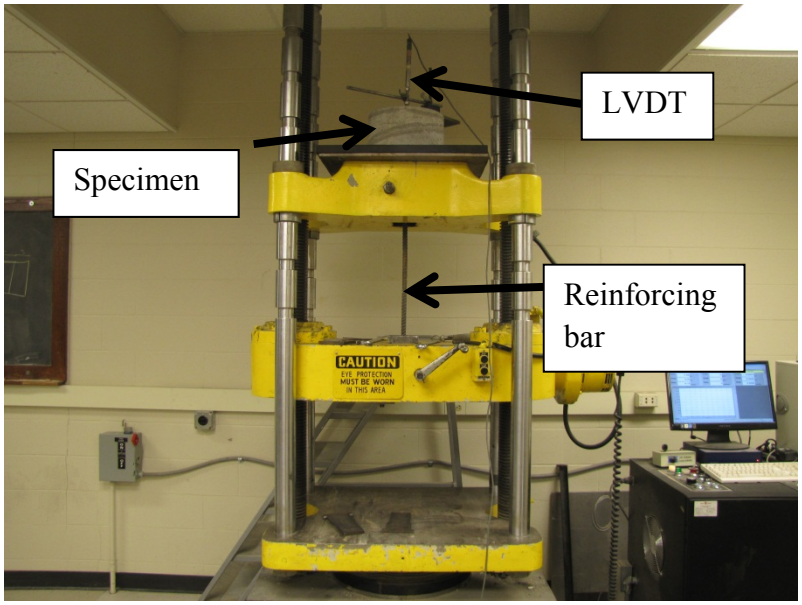

Figure 4.5 – Direct pull-out test setup

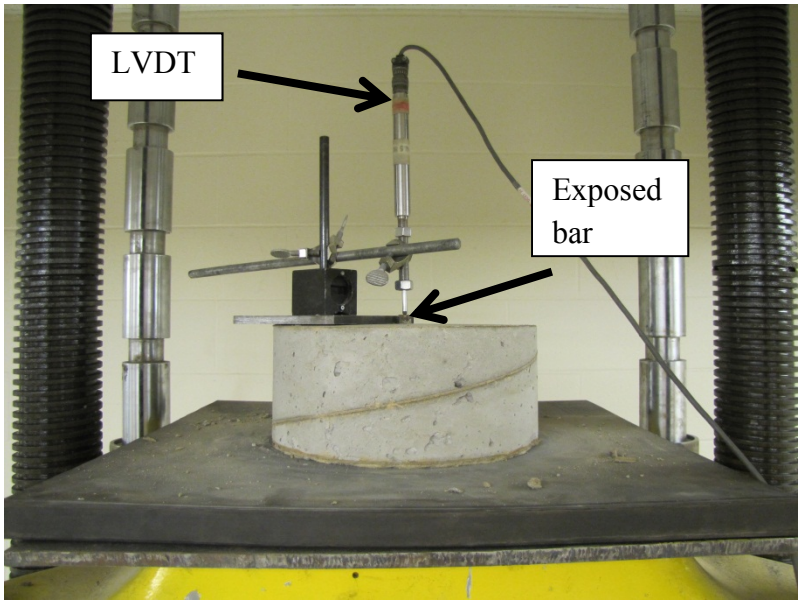

Figure 4.6 – LVDT installation to measure bar slip

4.2.4. Direct Pull-out Test Procedure. The middle platform was manually positioned to allow for the reinforcing bar to be clamped. The equipment controlling the

Tinius Olson was programed to apply a displacement controlled load rate of 0.1 in. (3 mm) per minute. Upon initiating a new test, the LVDT data collection platform was started and the clamps were closed around the reinforcing bar while the middle platform was simultaneously lowered. This step was done to seat the test specimen and apply an initial load sufficient to maintain a proper grip on the reinforcing bar during testing. The test program was then initiated and allowed to run until a distinct peak was observed in the applied load vs. bar slip plot. This step was done to ensure there was no residual load carrying capacity in the bonded region and that the proper failure load was determined. At that point, the test program and LVDT data collection platform were both stopped and the test specimen was removed.

4.3. BEAM SPLICE TEST

4.3.1. Beam Splice Specimen Design. The beam splice test specimens were designed following a non-ASTM test procedure that is generally accepted as the most realistic test method for both development and splice length. This test consists of applying a full-scale beam specimen to a four-point loading until failure of the splice occurs. The splice is located in the region of the beam subjected to a constant moment, and thus constant stress. The realistic stress-state in the area of the reinforcing bars makes for an accurate representation of the bond strength of the tested member (ACI 408R-03, 2003).

Details of the beam splice specimens used in this current study are shown in **Figures 4.7** and **4.8**. The beams measured 10 ft. (3050 mm) in length, with a cross section of 12 in. x 18 in. (305 mm x 457 mm) and contained a splice centered at midspan.

Transverse steel consisting of #3 (#10), ASTM A615-09, Grade 60, U-shaped stirrups were used for shear reinforcement. A stirrup spacing less than the ACI 318-08 maximum stirrup spacing was used to ensure that bond failure occurred prior to shear failure. The stirrups were terminated at approximately 5 in. (127 mm) from each end of the splice to eliminate the effects of confinement within the splice region. The longitudinal reinforcement consisted of three, ASTM A615-09, Grade 60, #6 (#19) bars spliced at midspan of the beam. The splice length was based on a percentage of the development length of the longitudinal reinforcing bars calculated in accordance with ACI 318-08 "Building Code Requirements for Structural Concrete" (ACI 318-08, 2008) (**Eq. 4.1**).

$$l_d = \left(\frac{3}{40} \frac{f_y}{\lambda \sqrt{f_c'}} \frac{\Psi_t \Psi_e \Psi_s}{\left(\frac{c_b + K_{tr}}{d_b} \right)} \right) d_b \qquad (4.1)$$

Where l_d is the development length, f_y is the specified yield strength of reinforcement, λ is the lightweight concrete modification factor, f'_c is the specified compressive strength of concrete, Ψ_t is the reinforcement location modification factor, Ψ_e is the reinforcement coating modification factor, Ψ_s is the reinforcement size modification factor, c_b is the smaller of the distance from center of a bar to nearest concrete surface and one-half the center-to-center spacing of bars being developed, K_{tr} is the transverse reinforcement index, and d_b is the nominal diameter of the reinforcing bar.

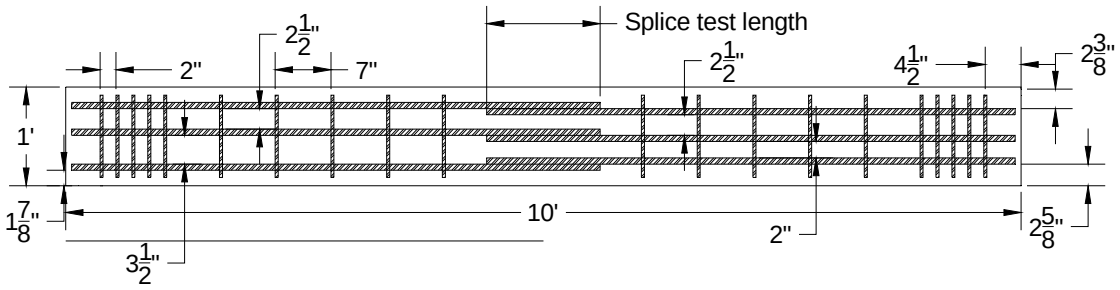

Figure 4.7 – Beam splice specimen reinforcing layout
Conversion: 1 in. = 25.4 mm

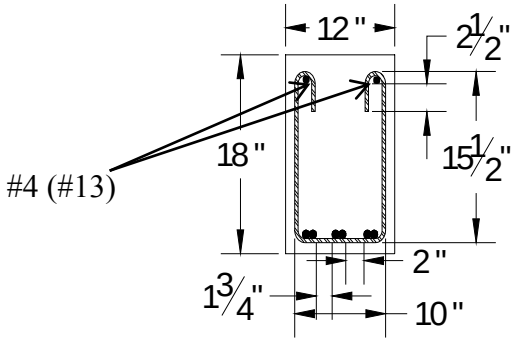

Figure 4.8 – Beam splice specimen cross section
Conversion: 1 in. = 25.4 mm

To ensure bond failure before yielding of the reinforcing bar, a splice length less than the code required development length was used in the test specimen. Prior researchers used one-half of a Class B splice as the lap length (Wolfe, 2011). However, several test specimens in that study exhibited signs of yielding in the reinforcement prior to bond failure. Therefore, for this current study, the splice length was limited to 70% of the development length.

4.3.2. Beam Splice Specimen Fabrication. The concrete formwork consisted of five removable and reusable pieces constructed from steel and wood. The pieces were connected through the use of steel keys and wire ties were used to hold the keys in place. The original beam forms were 14 ft. (4267 mm) in length. Consequently, 4 ft. (1219 mm)

wooden bulkheads were constructed to reduce the length of the beam forms to 10 ft. (3048 mm).

The #3 (#10) reinforcing bars were then sectioned to the appropriate length and bent to form the U-stirrups. The longitudinal reinforcement was sectioned to the appropriate length to obtain the proper splice length, as well as create a standard hook at the opposite end for proper development. All rust and mill scale was removed from the spliced region of each bar using a wire brush cup attached to an electric grinder. This step was done to ensure the bond strength was not affected in any way by the existence of rust and mill scale, thus maintaining conformity between the splice in each specimen. The longitudinal bars were then placed on saw-horses, aligned to obtain the appropriate splice length, and the stirrups were secured to the longitudinal bars using steel wire tires. A strain gauge was attached to the longitudinal bars at one end of each splice to monitor the strain during testing. Then, to ensure the stirrups stayed aligned vertically within the forms, two #4 (#13) bars were tied to the top bend of the stirrups and the end stirrups were tied to the hooked ends of the longitudinal bars. A finished reinforcing bar cage is shown in **Figure 4.9**.

Figure 4.9 – Finished reinforcing bar cage

Two of the cages were then lowered into the beam forms using 1 in. (25 mm) steel chairs on the bottom and sides to maintain 1 in. (25 mm) of clear cover to the outside edge of the stirrups. The third cage was turned upside down and 1.5 in. (38 mm) chairs were attached to the bottom of the cage to maintain clear cover to the splice at the top of the beam. Then, 1 in. (25 mm) chairs were also attached to the side of the stirrups to maintain 1 in. (25 mm) clear cover to the stirrups. Steel crossties were attached to the tops of the beam forms to maintain the proper beam width along the depth of the beam. Hooks were then tied to the crossties to facilitate transportation of the specimen after curing. **Figure 4.10** shows a picture of the spliced region in the beam forms, and **Figure 4.11** displays the three cages in their respective forms.

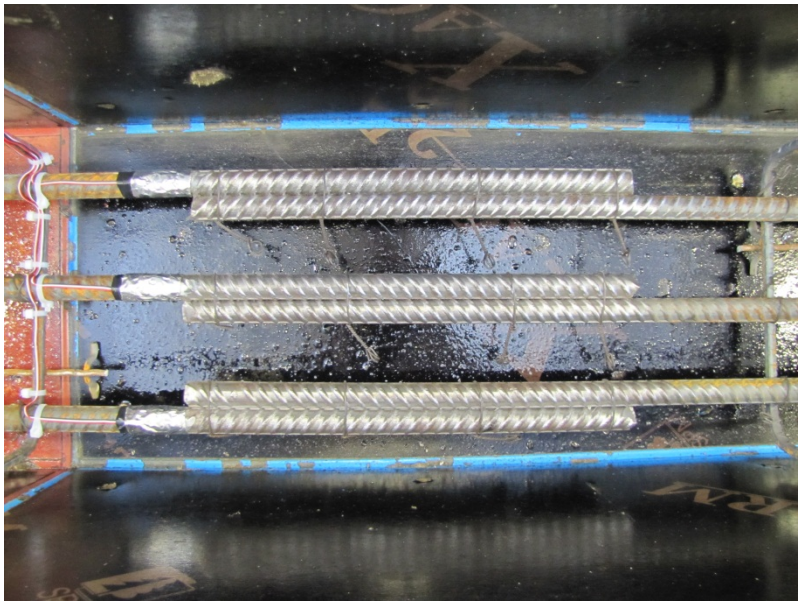

Figure 4.10 – Spliced longitudinal bars for normal strength concrete

Figure 4.11 – Reinforcing bar cages in beam forms

The concrete used to construct the specimens was delivered from a local ready-mix facility, Rolla Ready Mix (RRM). The mix design was supplied to RRM although

some of the water was held in abeyance in order to adjust the water content at the lab. Once the concrete truck arrived at the lab, the slump was measured and the reserve water was added as necessary to arrive at the required water-to-cementitious material ratio. At that point, all necessary activators and admixtures were added to the concrete truck, which was then mixed at high speed for 10 minutes to obtain the final material. At this point, the fresh concrete was loaded into a concrete bucket as shown in **Figure 4.12**. The bucket was then positioned with the overhead crane to facilitate placement of the concrete into the formwork as shown in **Figure 4.13**. The concrete was then consolidated as required for the particular concrete mix. This process was repeated until the beam forms were filled. The tops of the beams were then finished using trowels as shown in **Figure 4.14**.

Figure 4.12 – Concrete bucket being filled with fresh concrete

Figure 4.13 – Placement of concrete into beam forms

Figure 4.14 – Finished beams in forms

Once the concrete reached initial set, the beam specimens and companion material property specimens were covered with wet burlap and plastic. The specimens were

allowed to cure until the concrete compressive strength reached a minimum of 1500 psi (10.3 MPa), at which point they were removed from the forms and remained within the temperature-controlled High Bay Lab. The beams were then tested upon reaching their respective design compressive strengths.

4.3.3. Beam Splice Specimen Test Setup. A schematic and photograph of the test setup are shown in **Figures 4.15** and **4.16**, respectively. The test consists of subjecting the beam splice specimen to four-point loading, ensuring that the region containing the splice is located in a constant moment region. The beam was then placed onto the supports. Two steel rollers were placed on the top surface of the beam specimen and steel spreader beams were used to transfer the applied load from two 140-kip-capacity (623 kN) hydraulic actuators.

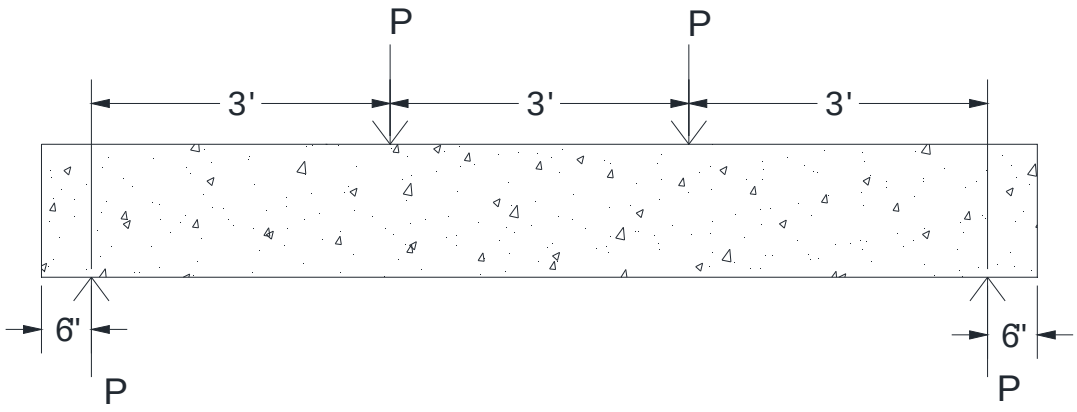

Figure 4.15 – Beam loading schematic
Conversion: 1 in. = 25.4 mm

The process of installing the beams into the test setup started with marking the center point, load points, and spreader beam outline onto each specimen. The strain gauge wires were then attached to a strain gauge converter box for subsequent attachment to the data acquisition system. At this point, the overhead crane was used to transport the beams

to a location adjacent to the test setup. The beams were then lowered onto steel rollers to facilitate placement into the test setup. The beam was then rolled into a position where the center point mark was directly below the center web stiffener on the spreader beam. One end was lined up with the spreader beam, lifted off of the steel roller with a hydraulic jack, and then lowered onto the support. This process was then repeated for the other support to line the beam up properly in the test frame. Once the beam was positioned within the test frame, metal plates were installed at the load point marks and the transfer beam was lowered into place. **Figure 4.16** shows the beam in the load frame located at the Missouri S&T High-Bay Structures Laboratory. A segment of aluminum angle was attached to the midpoint of the beam and an LVDT was placed on the aluminum to measure the deflection at midspan during testing as shown in **Figure 4.17**. The strain gauge wire converter box was then attached to the data acquisition system.

Figure 4.16 – Beam positioned within load frame

Figure 4.17 – LVDT installation

4.3.4. Beam Splice Test Procedure. Prior to beginning the test, the data acquisition system was initiated to record applied load, LVDT data, and strain gauge data. The load was then applied by the two 140-kip-capacity (623 kN) hydraulic actuators acting through the spreader beams. Each test was performed under displacement control, and the load was applied in a series of loading steps of 0.02 in. (0.5 mm), which corresponded to a load of approximately 3 kips (13 kN), until failure. Electronic measurements of strain and deformation were recorded throughout the entire loading history of the specimens. The crack patterns in the concrete were marked at every other load step to track propagation as the load was increased. Loading of the beams continued until a very prominent failure occurred, which was usually signaled both audibly and by a significant drop in the load-deflection behavior of the specimen.

5. SCC TEST RESULTS AND EVALUATION

5.1. DIRECT PULL-OUT TEST RESULTS

The direct pull-out specimens were constructed to evaluate the bond performance of SCC. The MoDOT standard mix design was used as a baseline for test result comparisons. A total of 24 direct pull-out test specimens were constructed for the SCC test program. There were six test specimens constructed for each of the four mix designs, which consisted of two SCC mixes and two control mixes. Of the six specimens constructed for each mix design, three specimens contained a #4 (#13) reinforcing bar and three specimens contained a #6 (#19) reinforcing bar. The test matrix for the SCC direct pull-out test program is shown in **Table 5.1**.

Table 5.1 – SCC direct pull-out test matrix

Mix I.D.	Bar Size	No. of Specimens
C6-58L	#4 (#13)	3
	#6 (#19)	3
S6-48L	#4 (#13)	3
	#6 (#19)	3
C10-58L	#4 (#13)	3
	#6 (#19)	3
S10-48L	#4 (#13)	3
	#6 (#19)	3

The applied load and corresponding slip of each reinforcing bar through the surrounding concrete were recorded for each test. Once compiled, the maximum applied load (peak load) for each test specimen was determined and used for bond strength comparison. **Table 5.2** displays the peak load for each of the test specimens in the SCC

test program, as well as average and coefficient of variation (COV) for each group of data. The first number in the specimen name represents the bar size, the following PO designates that specimen as a pull-out specimen, and the final number is the number of the specimen. Plots of the peak load for the C6-58L, S6-48L, C10-58L, and S10-48L specimens are shown in **Figures 5.1**, **5.2**, **5.3**, and **5.4**, respectively. The plots indicate that results from tests having the same parameters are relatively similar. This fact is also demonstrated by the relatively small COV within a group of test specimens, with the highest being 5%. The consistent results between tests with the same parameters lend confidence in the ability of this test to accurately compare the bond strength between mix designs.

The load and slip data were also plotted for comparison of test results. An example of a load vs. slip plot is shown in **Figure 5.5**. All other load vs. slip plots have a similar shape and only differ in the magnitude of the values plotted. The mode of failure of all the pull-out test specimens consisted of the reinforcing bar slipping through the concrete section. Appendix E contains the load vs. slip plots for all 24 pull-out specimens.

Table 5.2 – SCC pull-out test results

Mix	Bar Size	Specimen	Max Applied Load (lb.)	Average Applied Load (lb.)	COV (%)
C6-58L	#4 (#13)	4PO1	12,320	12,109	3.6
		4PO2	12,394		
		4PO3	11,612		
	#6 (#19)	6PO1	29,997	29,665	1.1
		6PO2	29,659		
		6PO3	29,340		
S6-48L	#4 (#13)	4PO1	15,395	15,214	1.8
		4PO2	14,893		
		4PO3	15,354		
	#6 (#19)	6PO1	36,129	36,022	2.9
		6PO2	34,941		
		6PO3	36,996		
C10-58L	#4 (#13)	4PO1	18,527	18,926	5.2
		4PO2	18,210		
		4PO3	20,042		
	#6 (#19)	6PO1	43,347	43,682	0.8
		6PO2	43,997		
		6PO3	43,701		
S10-48L	#4 (#13)	4PO1	17,713	17,948	1.3
		4PO2	17,939		
		4PO3	18,191		
	#6 (#19)	6PO1	40,805	40,154	1.6
		6PO2	40,114		
		6PO3	39,542		

Conversion: 1 in. = 25.4 mm
1 lb. = 4.45 N

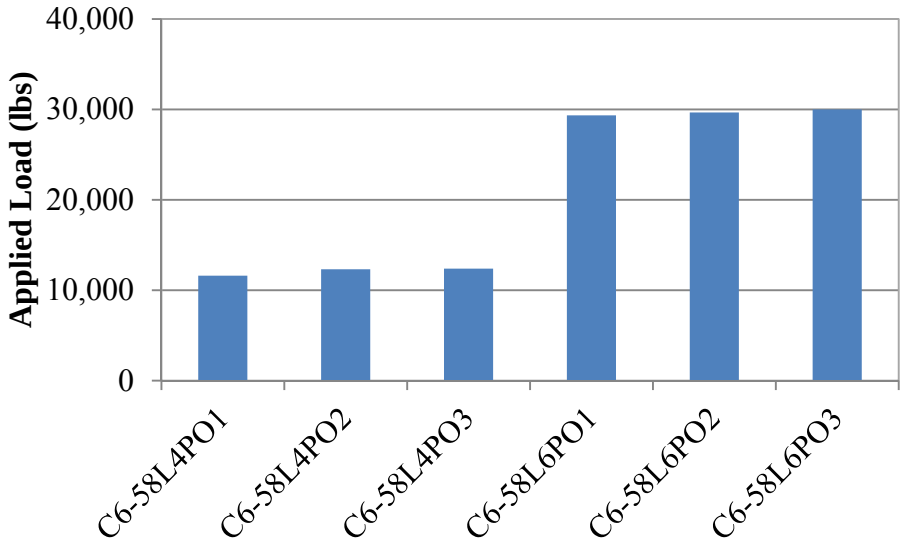

Figure 5.1 –C6-58L pull-out test results
Conversion: 1 lb. = 4.45 N

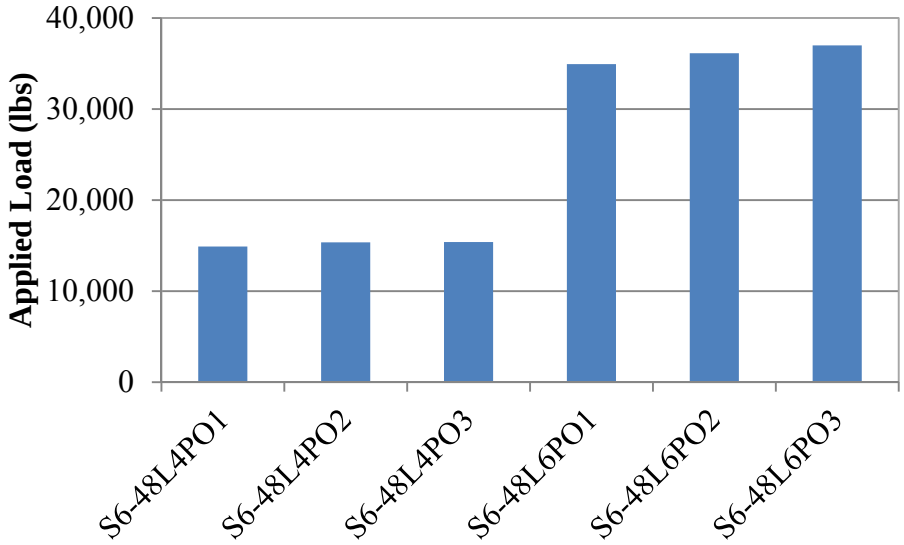

Figure 5.2 – S6-48L pull-out test results
Conversion: 1 lb. = 4.45 N

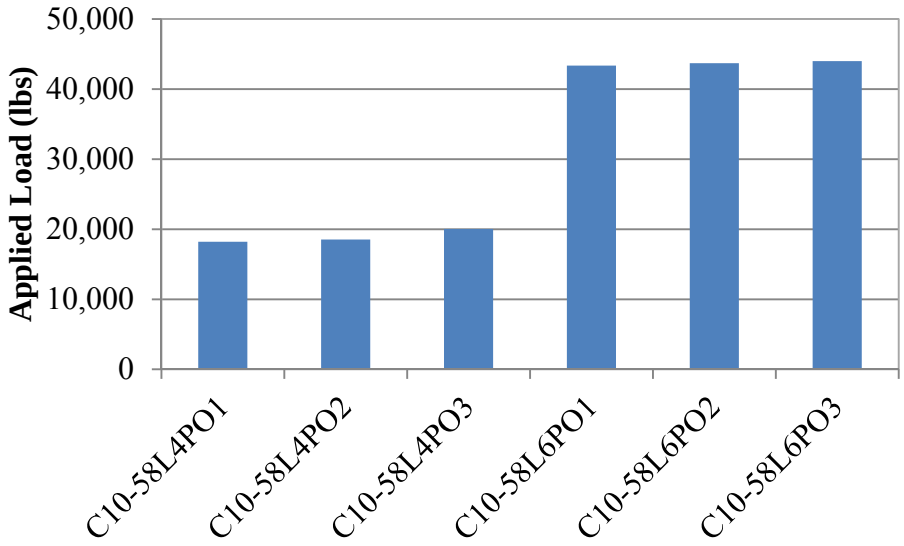

Figure 5.3 – C10-58L pull-out test results
Conversion: 1 lb. = 4.45 N

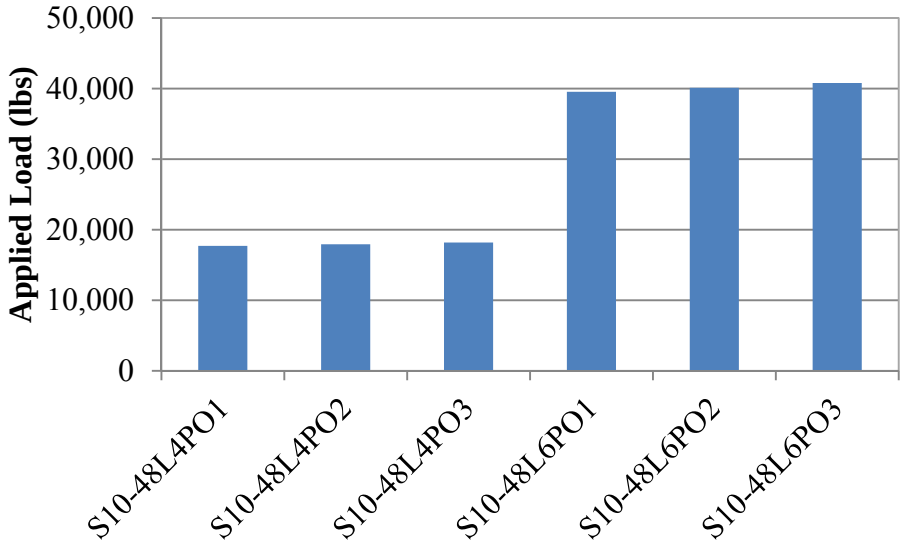

Figure 5.4 – S10-48L pull-out test results
Conversion: 1 lb. = 4.45 N

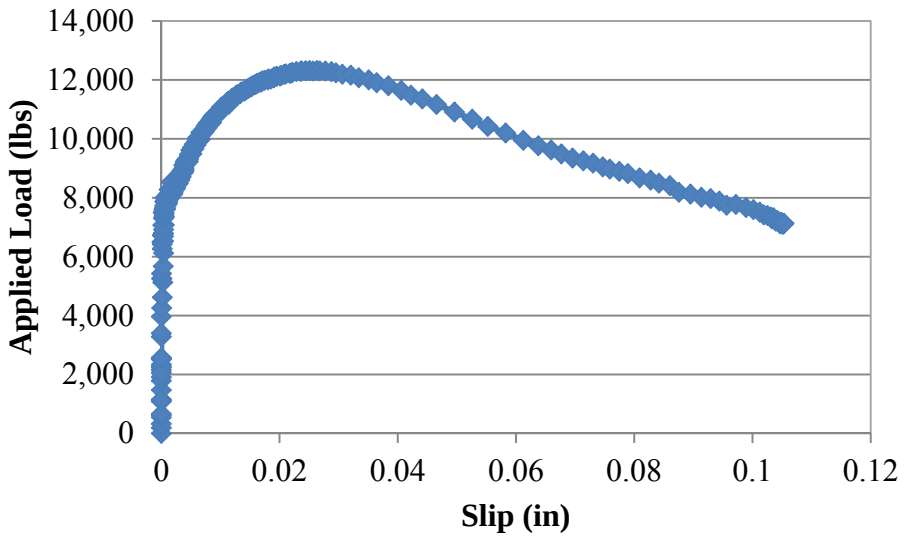

Figure 5.5 – Example SCC applied load vs. slip plot
Conversion: 1 lb. = 4.45 N
1 in. = 25.4 mm

5.2. BEAM SPLICE TEST RESULTS

The beam splice test specimens were constructed to evaluate the bond performance of SCC under more realistic loading conditions. The MoDOT standard mix design was used as a baseline for test result comparisons. A total of 12 test specimens with 3#6 (#19) longitudinal reinforcing bars spliced at midspan were constructed for the SCC test program. There were three specimens constructed for each of the four concrete mix designs to be evaluated. Of the three test specimens, two specimens were constructed with the spliced reinforcing bars located at the bottom of the beam cross section and one specimen was constructed with the splice at the top of the beam cross section to evaluate top-bar effect. The test matrix for the SCC beam splice test program is shown in **Table 5.3**. A splice length of 11.71 in. (297 mm) with three splices was used for each normal strength test specimen and 14.18 in. (360 mm) with four splices was used for each high strength test specimen. An extra splice was added to the high strength test specimens

because 70% of the calculated development length for the high strength mix design with three splices was relatively small (much less than the ACI 318-08 minimum). To obtain a higher splice length, four splices were used in the high strength mix design specimens. By decreasing the clear spacing between the bars being developed, the calculated development length was increased.

Table 5.3 – SCC beam splice test matrix

Mix I.D.	Bar Size	Splice Location	No. of Specimens
C6-58L	#6 (#19)	Bottom	2
		Top	1
S6-48L	#6 (#19)	Bottom	2
		Top	1
C6-58L	#6 (#19)	Bottom	2
		Top	1
S6-48L	#6 (#19)	Bottom	2
		Top	1

The applied load, corresponding midspan deflection, and corresponding strain at the end of each bar splice was recorded for each test. The peak load and peak stress were collected for each test specimen and are shown in **Table 5.4**. The bottom splice specimens are denoted with the abbreviation BB and the top splice specimens are denoted with the abbreviation TB. Steel stress recorded at failure of the specimen was determined by averaging the strain readings from each strain gage in a member and finding the peak strain that occurred during loading. This peak strain was then multiplied by the modulus of elasticity of the steel determined from the tension test to determine peak stress. The peak loads for the C6-58L, S6-48L, C10-58L, and S10-48L specimens are plotted in **Figures 5.6**, **5.7**, **5.8**, and **5.9**, respectively.

Table 5.4 – Peak load and reinforcing bar stress

Mix	Specimen	Steel Stress Recorded at Failure (ksi)	Peak Load (kips)
C6-58L	**BB1**	49.5	47.8
	BB2	50.8	55.4
	TB	54.7	47.3
S6-48L	**BB1**	63.2	60.8
	BB2	59.7	58.2
	TB	50.6	53.4
C10-58L	**BB1**	62.0	85.4
	BB2	57.9	76.1
	TB	73.8	87.7
S10-48L	**BB1**	54.9	78.3
	BB2	65.5	83.3
	TB	79.2	96.9

Conversion: 1 ksi = 6.9 MPa

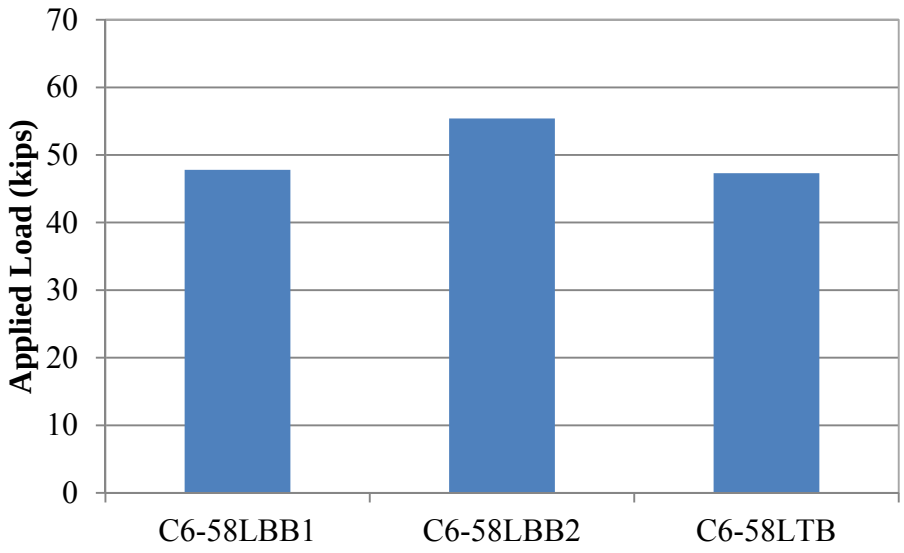

Figure 5.6 – C6-58L peak load data plot

Conversion: 1 kip = 4.45 kN

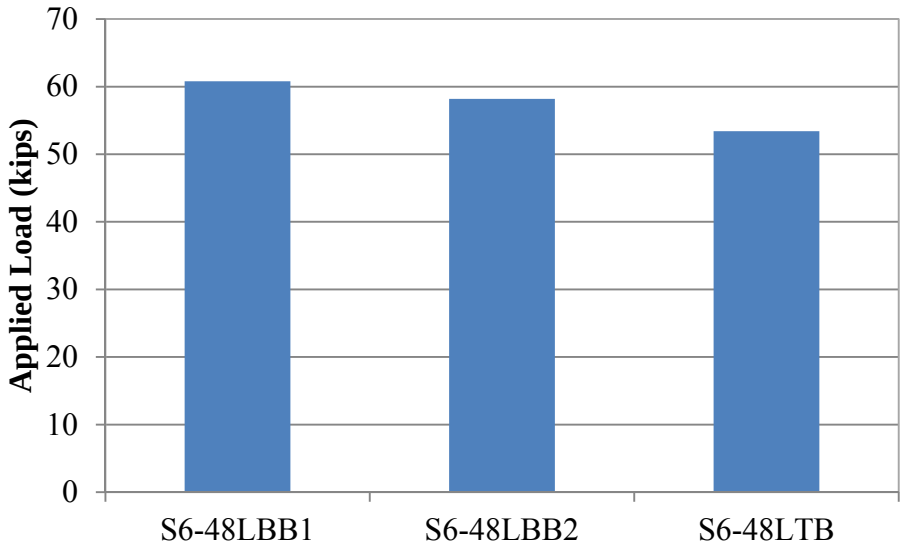

Figure 5.7 – S6-48L peak load data plot
Conversion: 1 kip = 4.45 kN

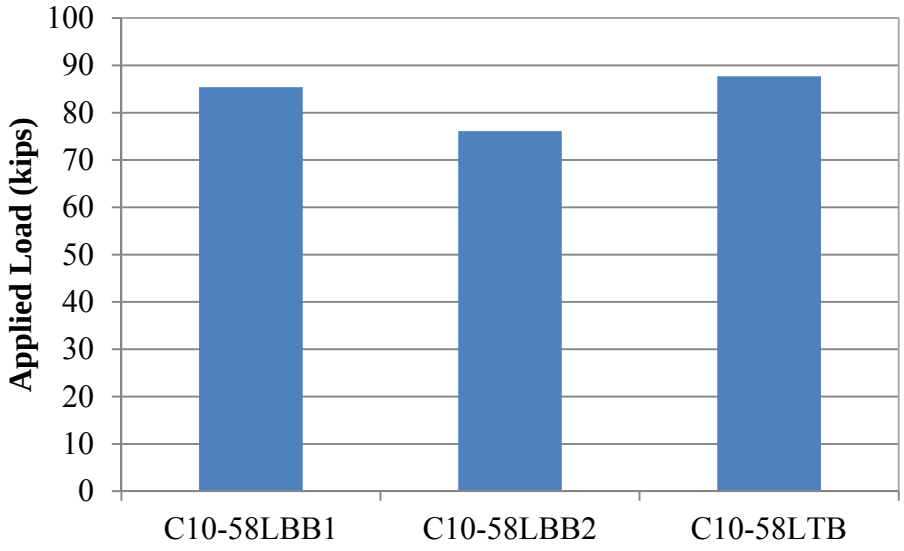

Figure 5.8 – C10-58L peak load data plot
Conversion: 1 kip = 4.45 kN

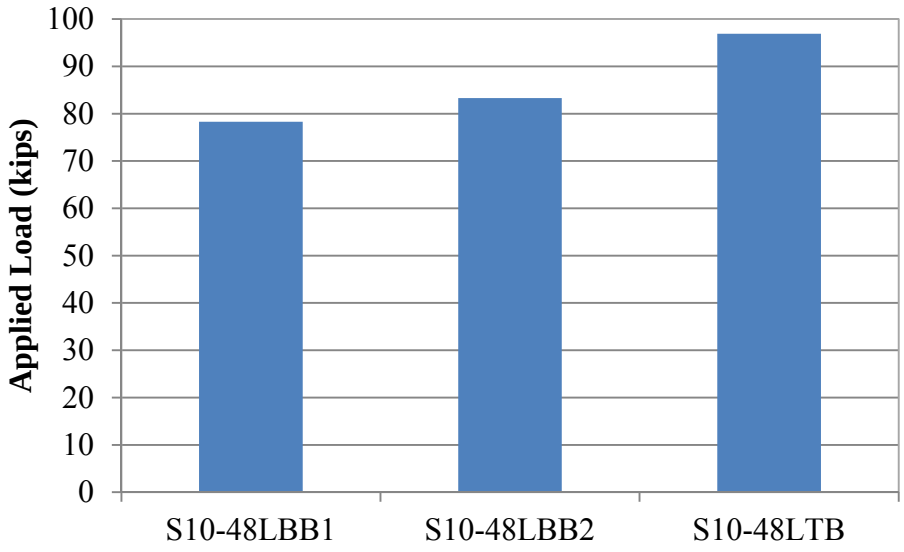

Figure 5.9 – S10-48L peak load data plot
Conversion: 1 kip = 4.45 kN

The deflection and strain data were also plotted with the load data to observe the response of the specimens during testing. A typical load vs. displacement at midspan plot is shown in **Figure 5.10**. A typical load vs. strain plot is shown in **Figure 5.11**. The plots shown are from the S10-48LBB1 specimen. Both plots show that the beam began to develop flexural crack at a load of approximately 20 kips (89 kN). At the failure load, all specimens exhibited visible and audible signs of complete bond failure, having never yielded the reinforcing bars. Evidence of this is shown in the linear behavior indicated in both the load vs. deflection plot and the load vs. strain plot. Appendix E contains the load vs. slip plots for all 12 beam splice specimens.

The cracking patterns in the beam splice specimens also revealed a bond failure. For example, **Figures 5.12** and **5.13** display the failed beam specimen designated C6-58LBB1. Both figures display longitudinal cracking along the bars within the splice zone, which is indicative of a bond-splitting failure. **Figure 5.14** displays a splice revealed due

to spalling of the concrete along the entire splice region. Appendix D contains photographs of the 12 beam splice specimens after failure.

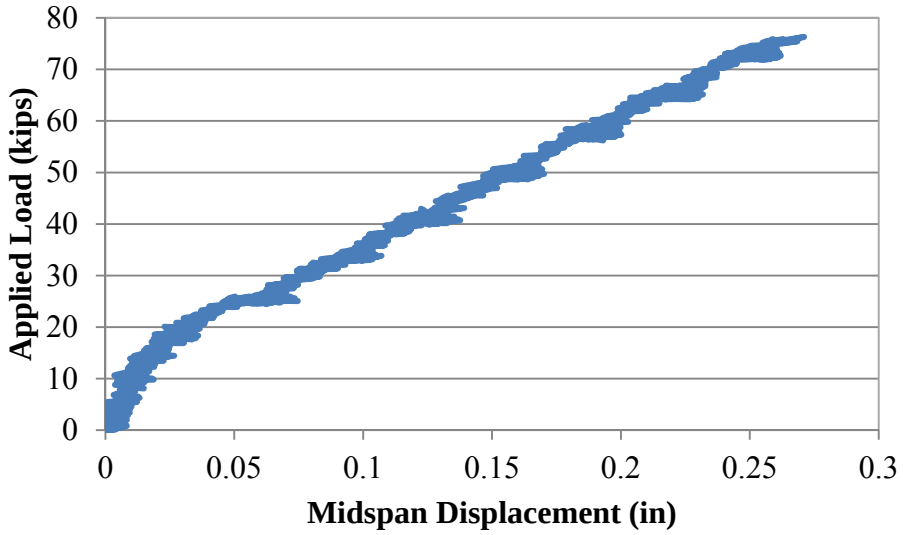

Figure 5.10 – Typical load vs. displacement plot
Conversion: 1 in. = 25.4 mm
1 kip = 4.45 kN

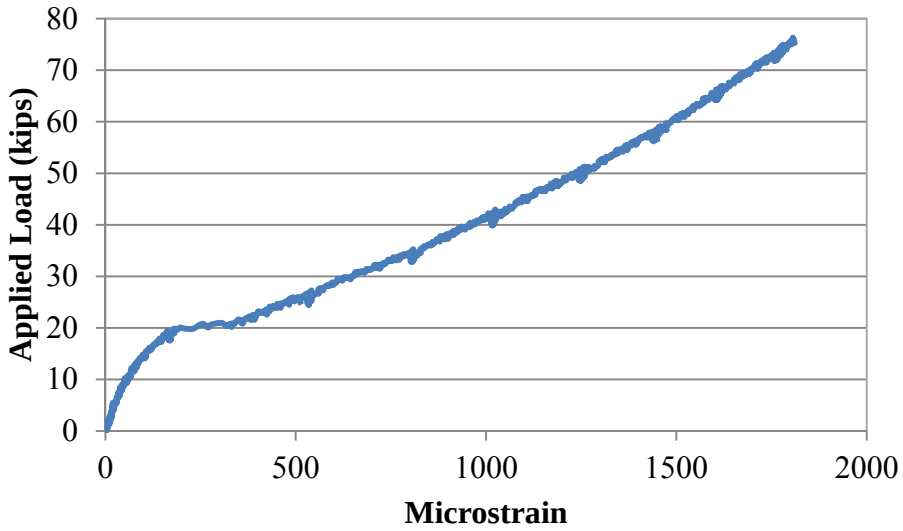

Figure 5.11 – Typical load vs. strain plot
Conversion: 1 kip = 4.45 kN

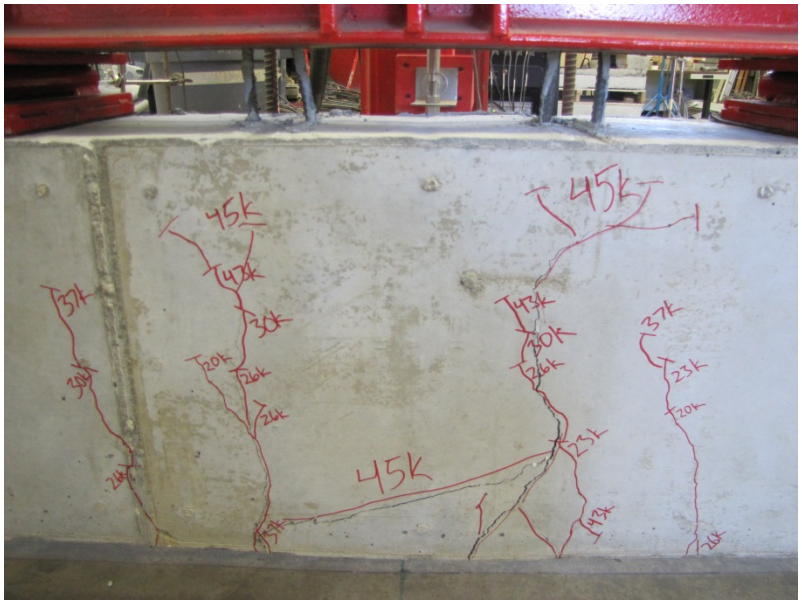

Figure 5.12 – Failed splice region of C6-58LBB1

Figure 5.13 – Bottom of splice region of C6-58LBB1

Figure 5.14 – Bottom of splice region of C10-58LTB with splice revealed

5.3. REINFORCING BAR TENSION TEST

A tension test was performed on the #6 (#19) longitudinal reinforcing bars used in each beam specimen following ASTM E8-09, "Standard Test Methods for Tension Testing of Metallic Materials" (ASTM E9-09). Three 30 in. (762 mm) lengths of reinforcing bar were clamped at each end in a 200,000 pound (890 kN) Tinius Olson testing machine and load was applied until the bar fractured. The strain and applied load were recorded during testing. The strain with a 0.5% offset was recorded and used to determine the yield strength of each bar. The modulus of elasticity was also determined for each bar. The average yield stress of the test was used as a comparison tool to check that the reinforcing bars within the splice region in each beam specimen did not reach yield. **Table 5.5** displays the results of the tension test performed.

Table 5.5 – #6 (#19) reinforcing bar tension test results

Specimen	Yield Stress (ksi)	Average Yield Stress (ksi)	Initial Tangent Modulus (ksi)	Average Modulus (ksi)
1	81.1	81.1	33,130	30,310
2	81.3		26,510	
3	81		31,295	

Conversion: 1 ksi = 6.9 MPa

5.4. ANALYSIS OF RESULTS

5.4.1. Methodology. Direct comparison between test results is not possible due to the fact that the test day concrete strength varies for each mix. Therefore, normalization of the value of interest was completed to facilitate direct comparison of test results. Two separate normalization formulas were used in this study. The first normalization formula is based on the development length equations in ACI 318-08 (ACI 318-08, 2008) and AASHTO LRFD-07 (AASHTO, 2007), shown as **Eqs. 5.1** and **5.2**, respectively. Both equations express the development length of a reinforcing bar in tension as a function of the inverse square root of the compressive strength. Therefore, the first normalization of the test results was based on multiplying values by the square root of the ratio of the specified design strength and the test day compressive strength, shown in **Eq. 5.3**.

$$l_d = \left(\frac{3}{40} \frac{f_y}{\lambda \sqrt{f_c'}} \frac{\Psi_t \Psi_e \Psi_s}{\left(\frac{c_b + K_{tr}}{d_b} \right)} \right) d_b \qquad (5.1)$$

Where l_d is the development length, f_y is the specified yield strength of reinforcement, λ is the lightweight concrete modification factor, f'_c is the specified compressive strength

of concrete, Ψ_t is the reinforcement location modification factor, Ψ_e is the reinforcement coating modification factor, Ψ_s is the reinforcement size modification factor, c_b is the smaller of the distance from center of a bar to nearest concrete surface or one-half the center-to-center spacing of bars being developed, K_{tr} is the transverse reinforcement index, and d_b is the nominal diameter of reinforcing bar.

$$l_{db} = \frac{1.25\ A_b\ f_y}{\sqrt{f_c'}} \geq 0.4\ d_b\ f_y \tag{5.2}$$

Where l_{db} is the tension development length, f_y is the specified yield strength of reinforcement, A_b is the area of reinforcing bar, f'_c is the specified compressive strength of concrete, and d_b is the reinforcing bar diameter.

$$Normalized\ Load = Failure\ load \sqrt{\frac{Design\ strength}{Strength\ at\ testing}} \tag{5.3}$$

The second normalization formula is based on the development length equation in ACI 408R-03 (2003), as shown in **Eq. 5.4**. The development length of a reinforcing bar in tension in this equation is a function of the inverse fourth root of the compressive strength. Therefore, the normalization of the test results was based on the fourth root of the ratio of the specified design strength and the test day compressive strength, as shown in **Eq. 5.5**.

$$l_d = \left(\frac{\left(\frac{f_y}{f_c'^{1/4}} - 1970\,\omega \right) \alpha\,\beta\,\lambda}{62\left(\frac{c\,\omega + K_{tr}}{d_b} \right)} \right) d_b \qquad (5.4)$$

Where l_d is the development length, f_y is the specified yield strength of reinforcement, λ is the lightweight concrete modification factor, f'_c is the specified compressive strength of concrete, α is the reinforcement location modification factor, β is the reinforcement coating modification factor, ω is equal to 0.1 (c_{max}/c_{min}) + 0.9 ≤ 1.25, c is the spacing or cover dimension, d_b is the nominal diameter of reinforcing bar, and K_{tr} is the transverse reinforcement index.

$$Normalized\ Load = Failure\ load \left(\frac{Design\ strength}{Strength\ at\ testing} \right)^{1/4} \qquad (5.5)$$

The design strength for the normal and high strength mix design were 6,000 psi (41.4 MPa) and 10,000 psi (69 MPa), respectively. The strengths at testing for each mix design can be seen in **Table 5.6**.

Table 5.6 - Test day compressive strengths for test specimens

	Test Day Strength (psi)				
	Cylinder 1	**Cylinder 2**	**Cylinder 3**	**Average**	**COV (%)**
C6-58L	5794	5557	5806	5719	2.5
S6-48L	6805	6703	7015	6841	2.3
C10-58L	9403	9832	9639	9625	2.2
S10-48L	9589	9951	9720	9753	1.9

Note: 1 psi = 6.9 kPa

5.4.2. Analysis and Interpretation – Direct Pull-out Test Results. Table 5.7 contains the peak load, concrete strength at time of testing, and normalized peak load for each normal strength test specimen. **Table 5.8** contains the same results for the high strength specimens. **Figure 5.15** is a plot of the average square root normalized peak load for each normal strength mix design and bar size. **Figure 5.16** displays the plot of the average square root normalized peak load for each high strength mix design and bar size. The error bars indicate the range of test data collected. The SCC specimens exhibited similar bond strength relative to the control mix design for both bar sizes. The average of the #4 (#13) S6-48L specimens failed at a load 1,870 lb. (8.3 kN) higher than the control, and the average of the #6 (#19) S6-48L specimens failed at a load 3,416 lb. (15.2 kN) higher than the control, which represents differences of 15.2 and 11.3%, respectively. The average of the #4 (#13) S10-48L specimens failed at a load 1,176 lb. (5.2 kN) lower than the control, and the average of the #6 (#19) S10-48L specimens failed at a load 3,994 lb. (17.8 kN) lower than the control, which represents differences of 6.1 and 9.0%, respectively. However, paired t-tests indicate that there is no statistically significant difference between the results for each mix design, indicating that the SCC has essentially the same bond strength as conventional concrete.

Table 5.7 – SCC normal strength normalized pull-out test results

Mix	Bar Size	Specimen	Peak Load (lb.)	Concrete Compressive Strength (psi)	Normalized Load (lb.)				COV (%)
					Square Root Adjustment	Fourth Root Adjustment	Average of Square Root Adjustment	Average of Fourth Root Adjustment	
C6-58L	#4 (#13)	4PO1	12,320	5,814	12,516	12,417	12,301	12,204	3.6
		4PO2	12,394		12,591	12,492			
		4PO3	11,612		11,796	11,704			
	#6 (#19)	6PO1	29,997		30,473	30,234	30,136	29,900	1.1
		6PO2	29,659		30,130	29,893			
		6PO3	29,340		29,806	29,572			
S6-48L	#4 (#13)	4PO1	15,395	6,916	14,339	14,858	14,171	14,683	1.8
		4PO2	14,893		13,872	14,373			
		4PO3	15,354		14,301	14,818			
	#6 (#19)	6PO1	36,129		33,651	34,868	33,552	34,765	2.9
		6PO2	34,941		32,545	33,722			
		6PO3	36,996		34,459	35,705			

Conversion: 1 lb. = 4.45 N
1 psi = 6.9 kPa

Table 5.8 – SCC high strength normalized pull-out test results

Mix	Bar Size	Specimen	Peak Load (lb.)	Concrete Compressive Strength (psi)	Normalized Load (lb.)				COV (%)
					Square Root Adjustment	Fourth Root Adjustment	Average of Square Root Adjustment	Average of Fourth Root Adjustment	
C10-58L	#4 (#13)	4PO1	18,527	9,625	18,884	18,705	19,292	19,108	5.2
		4PO2	18,210		18,561	18,385			
		4PO3	20,042		20,429	20,234			
	#6 (#19)	6PO1	43,347		44,183	43,763	44,524	44,101	0.8
		6PO2	43,997		44,846	44,419			
		6PO3	43,701		44,544	44,121			
S10-48L	#4 (#13)	4PO1	17,713	9,815	17,879	17,796	18,116	18,032	1.3
		4PO2	17,939		18,107	18,023			
		4PO3	18,191		18,362	18,276			
	#6 (#19)	6PO1	40,805		41,188	40,996	40,530	40,342	1.6
		6PO2	40,114		40,490	40,302			
		6PO3	39,542		39,913	39,727			

Conversion: 1 lb. = 4.45 N
1 psi = 6.9 kPa

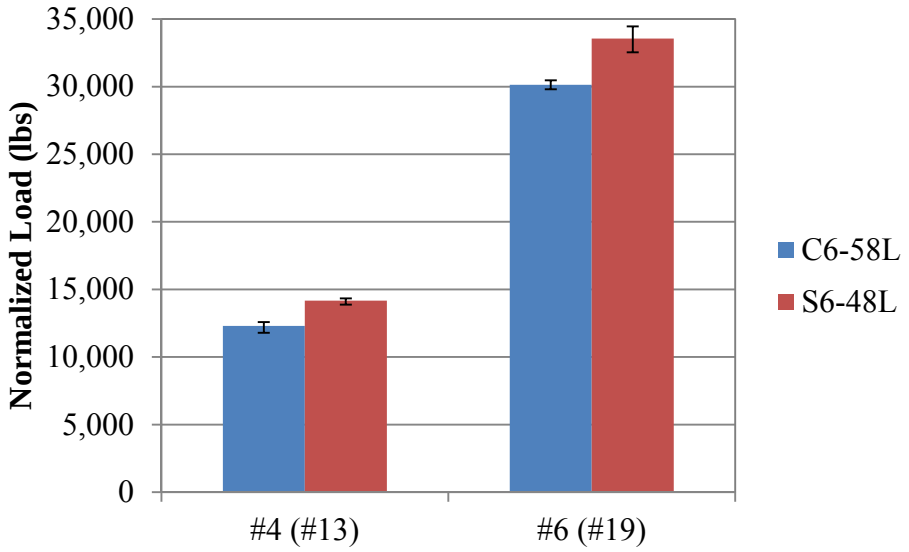

Figure 5.15 – Plot of peak load for each normal strength mix design
Conversion: 1 lb. = 4.45 N

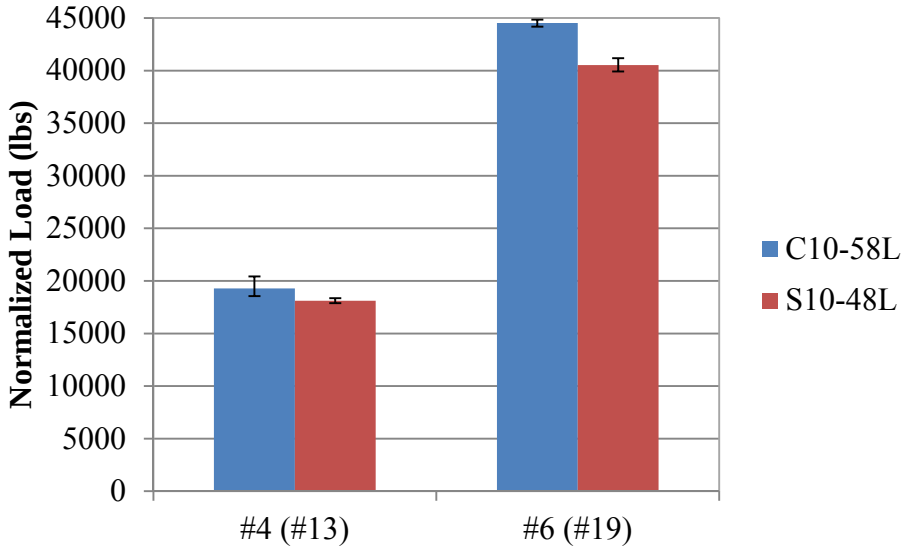

Figure 5.16 – Plot of peak load for each high strength mix design
Conversion:
1 lb. = 4.45 N

Figures 5.17 and **5.18** display a typical plot of the normalized load vs. slip of the #4 (#13) and #6 (#19) pull-out specimens for the normal strength mix designs,

respectively. **Figures 5.19** and **5.20** displays a typical normalized load vs. slip of the #4 (#13) and #6 (#19) pull-out specimens for the high strength mix designs, respectively. The plots indicate that bar slip occurred around the same load for each normal strength test specimen and #4 (#13) high strength specimens. However, bar slip in the #6 (#19) high strength SCC test specimens occurred at a lower load than that of the control specimens. More importantly, the overall behavior was very similar between all four mix designs. This behavior, combined with a forensic investigation of the failed specimens, indicates that the concrete surrounding the bar crushed around the same load for all the normal strength specimens and the #4 (#13) high strength specimens, but at a lower load for the #6 (#19) high strength SCC specimens than that of the control specimens.

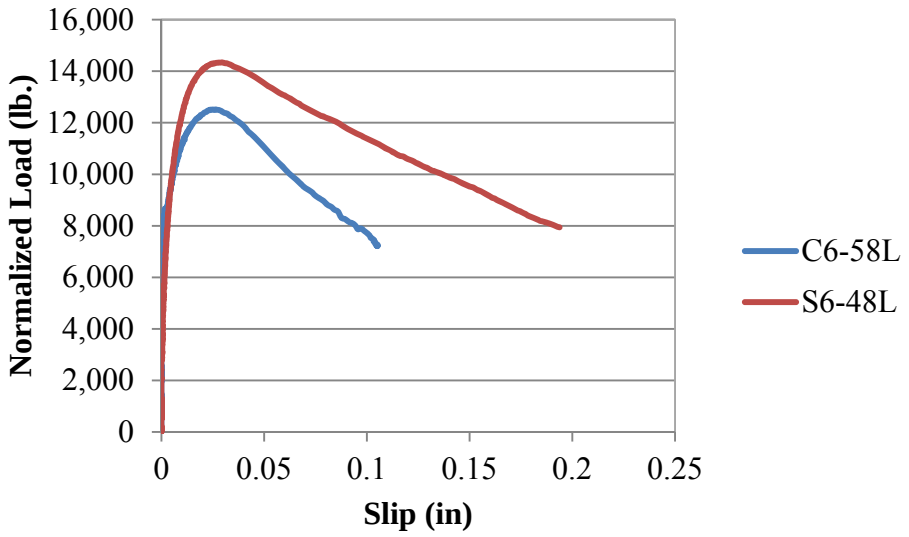

Figure 5.17 – Normal strength normalized load vs. slip plot for #4 (#13) bars
Conversion: 1 in. = 25.4 mm
1 lb. = 4.45 N

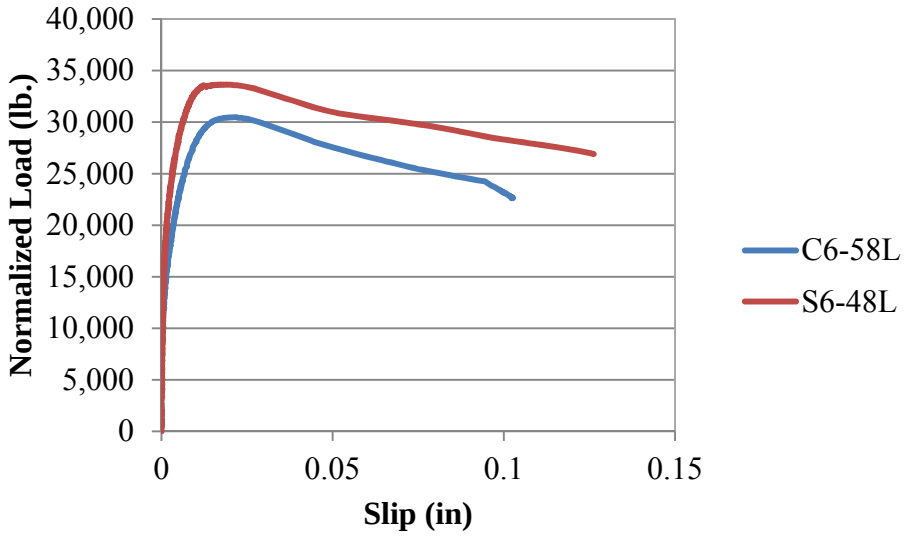

Figure 5.18 – Normal strength normalized load vs. slip plot for #6 (#19) bars
Conversion: 1 in. = 25.4 mm
1 lb. = 4.45 N

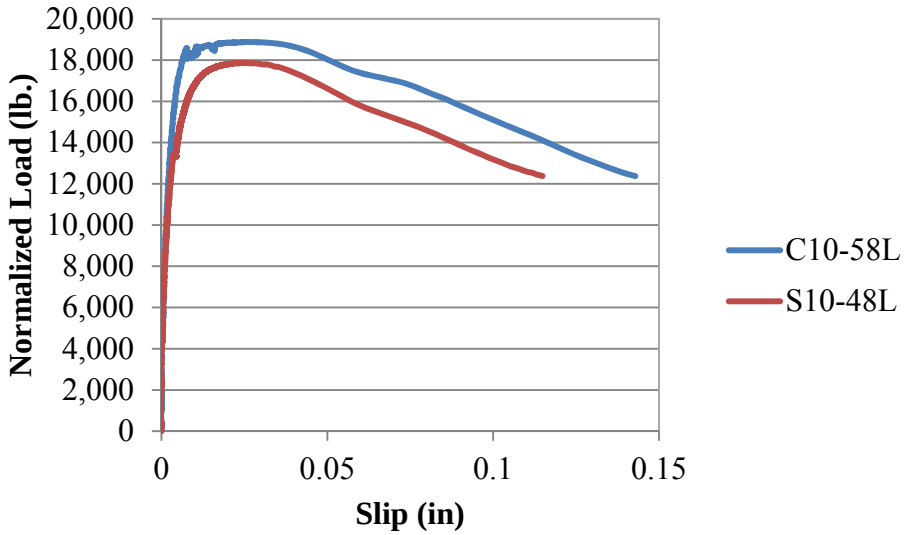

Figure 5.19 – High strength normalized load vs. slip plot for #4 (#13) bars
Conversion: 1 in. = 25.4 mm
1 lb. = 4.45 N

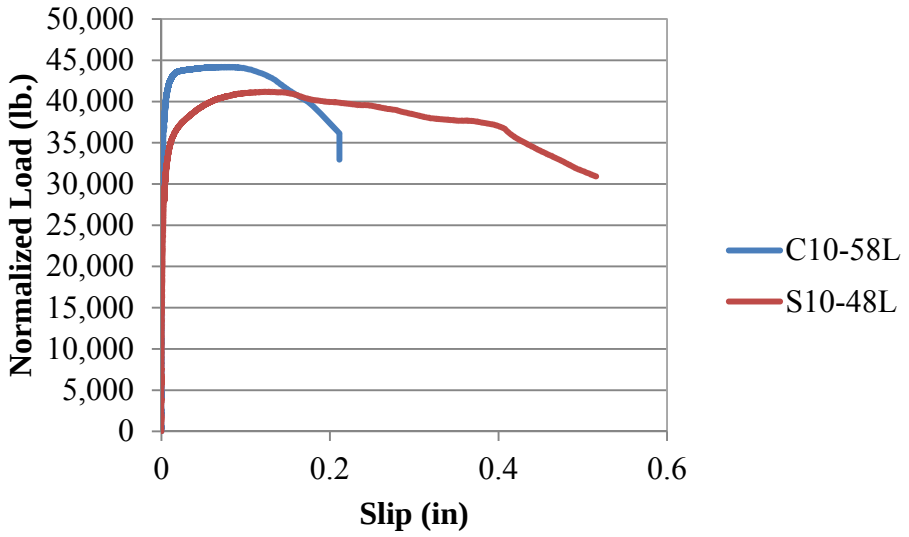

Figure 5.20 – High strength normalized load vs. slip plot for #6 (#19) bars
Conversion: 1 in. = 25.4 mm
1 lb. = 4.45 N

5.4.3. Analysis and Interpretation – Beam Splice Test Results. Table 5.9 contains the peak load, concrete strength at time of testing, and normalized peak load of each specimen tested. The square root normalized peak loads are plotted in **Figures 5.21** and **5.22** for the normal strength and high strength mix designs, respectively. **Table 5.10** contains the measured steel stress at failure, concrete strength at time of testing, and normalized measured steel stress at failure. The square root normalized steel stresses are shown plotted in **Figures 5.23** and **5.24** for the normal strength and high strength mix designs, respectively. The error bars indicate the range of test data collected. The normalized steel stresses were compared to the theoretical stress calculated using the moment-curvature program Response-2000 (Bentz, 2000) and are shown in **Table 5.11**. The moment at midspan of the specimen used when calculating the theoretical stress was a combination of both applied load moment and dead load moment. The applied load moment includes the weight of the spreader beams used to distribute the load from the

actuators. The design concrete strengths of 6,000 psi (41.4 MPa) and 10,000 psi (69 MPa) were used when calculating the theoretical steel stress for the normal and high strength mix designs, respectively.

The average longitudinal bar stress for the S6-48L bottom splice specimens was 6.3 ksi (43.4 MPa) higher than that of the control bottom splice specimens, which represents a difference of 12.4%. The average peak stress for the S10-48L bottom splice specimens was 0.3 ksi (2.1 MPa) higher than that of the control bottom splice specimens, which represents a difference of 0.5%. The peak stress for the S6-48L mix design top splice specimen mix design was 4.4 ksi (30.3 MPa) lower than that of the control specimen, which represents a difference of 7.9%. The peak stress for the S10-48L top splice specimen was 4.7 ksi (32.4 MPa) higher than that of the control specimen, which represents a difference of 6.2%. This data indicates that with the bottom splice specimens, the SCC mix designs performed at the same level as the control mix design. The opposite trend was seen for the normal strength top bar splice specimen. This could be attributed to an issue with segregation in SCC mix designs, as well as the existence of excess bleed water. The coarse aggregate was not evenly distributed along the depth of the member. The loss of coarse aggregate at the top of the member caused the S6-48LTB specimen to fail at a lower stress. The peak stress for the S10-48LTB specimen was higher than that of the control specimen. This indicates segregation was not as much of an issue with the high strength SCC mix design. However, the differences were not statistically significant to justify any definitive conclusions of the top-bar effect for SCC.

Table 5.9 – Normalized peak loads for each specimen

Mix	Specimen	Max Applied Load (kips)	Concrete Compressive Strength (psi)	Normalized Load (kips)			
				Square Root Adjustment	Fourth Root Adjustment	Average of Square Root Adjustment	Average of Fourth Root Adjustment
C6-58L	**BB1**	47.8	5814	48.6	48.2	52.4	52.0
	BB2	55.4		56.3	55.8		
	TB	47.3		48.1	47.7	N/A	N/A
S6-48L	**BB1**	60.8	6916	56.6	58.7	55.4	57.4
	BB2	58.2		54.2	56.2		
	TB	53.4		49.7	51.5	N/A	N/A
C10-58L	**BB1**	85.4	9625	87.0	86.2	82.3	81.5
	BB2	76.1		77.6	76.8		
	TB	87.7		89.4	88.5	N/A	N/A
S10-48L	**BB1**	78.3	9815	79.0	78.7	81.6	81.2
	BB2	83.3		84.1	83.7		
	TB	96.9		97.8	97.4	N/A	N/A

Conversion: 1 ksi = 6.9 MPa

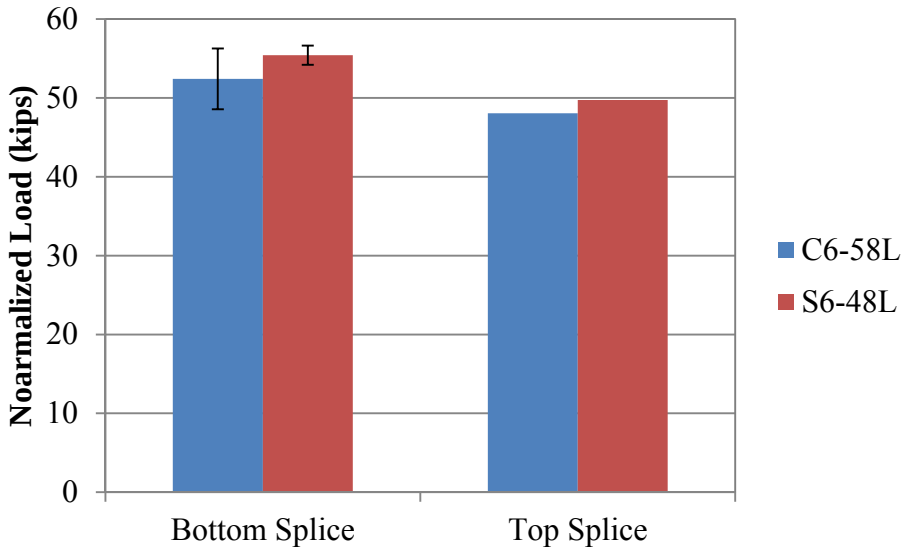

Figure 5.21 – Normalized peak load plot for the normal strength mix design
Conversion: 1 kip = 4.45 kN

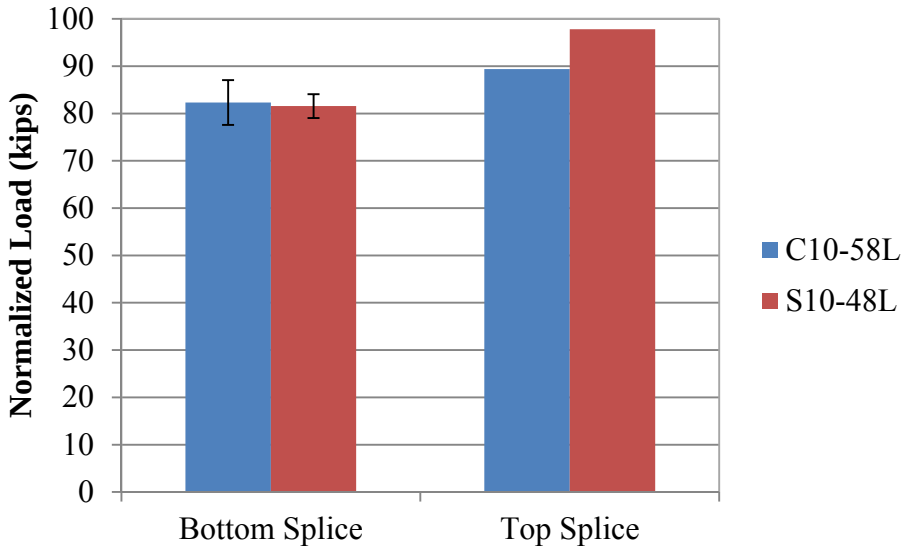

Figure 5.22 – Normalized peak load plot for the high strength mix design
Conversion: 1 kip = 4.45 kN

Table 5.10 – Normalized steel stress at failure for each specimen

Mix	Specimen	Steel Stress Recorded at Failure (ksi)	Concrete Compressive Strength (psi)	Normalized Steel Stress (ksi)	
				Square Root Adjustment	Fourth Root Adjustment
C6-58L	BB1	49.5	5814	50.3	49.9
	BB2	50.8		51.6	51.2
	TB	54.7		55.6	55.2
S6-48L	BB1	63.2	6916	58.9	61.0
	BB2	59.7		55.6	57.6
	TB	50.6		47.2	48.9
C10-58L	BB1	62.0	9625	63.2	62.6
	BB2	57.9		59.0	58.5
	TB	73.8		75.3	74.5
S10-48L	BB1	54.9	9815	55.4	55.2
	BB2	65.5		66.1	65.8
	TB	79.2		80.0	79.6

Conversion: 1 kip = 4.45 kN

Table 5.11 – Normalized steel stress compared to theoretical steel stress at failure

Mix	Specimen	Normalized Steel Stress (ksi)		Calculated Stress at Failure Load (ksi)	Measured/Calculated Stress	
		Square Root Adjustment	Fourth Root Adjustment		Square Root Adjustment	Fourth Root Adjustment
C6-58L	BB1	50.3	49.9	45.5	0.90	1.10
	BB2	51.6	51.2	52.5	1.02	0.97
	TB	55.6	55.2	45.0	0.81	1.23
S6-48L	BB1	58.9	61.0	57.5	0.98	1.06
	BB2	55.6	57.6	55.1	0.99	1.05
	TB	47.2	48.9	50.6	1.07	0.97
C10-58L	BB1	63.2	62.6	79.5	1.26	0.79
	BB2	59.0	58.5	71.0	1.20	0.82
	TB	75.3	74.5	81.6	1.08	0.91
S10-48L	BB1	55.4	55.2	73.0	1.32	0.76
	BB2	66.1	65.8	77.6	1.17	0.85
	TB	80.0	79.6	90.0	1.13	0.88

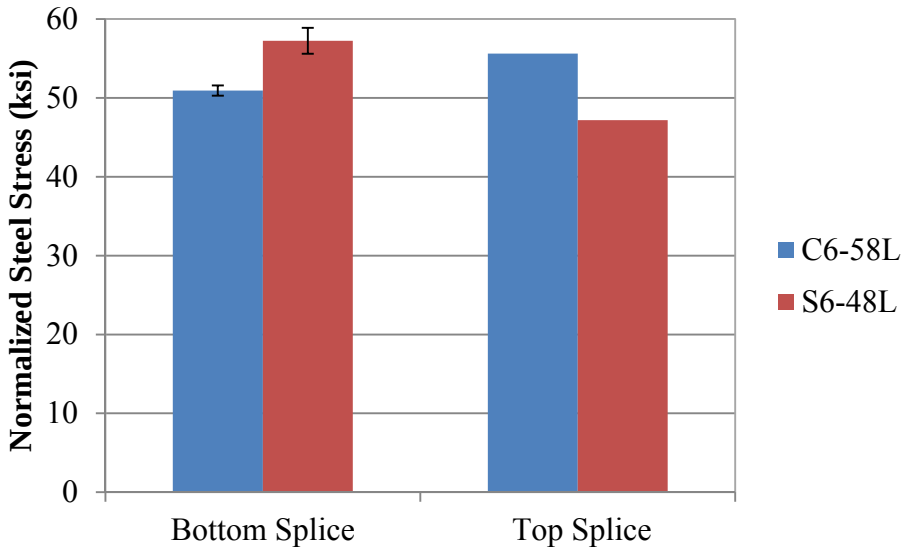

Figure 5.23 – Normalized steel stress at failure load for normal strength mix designs
Conversion: 1 ksi = 6.9 MPa

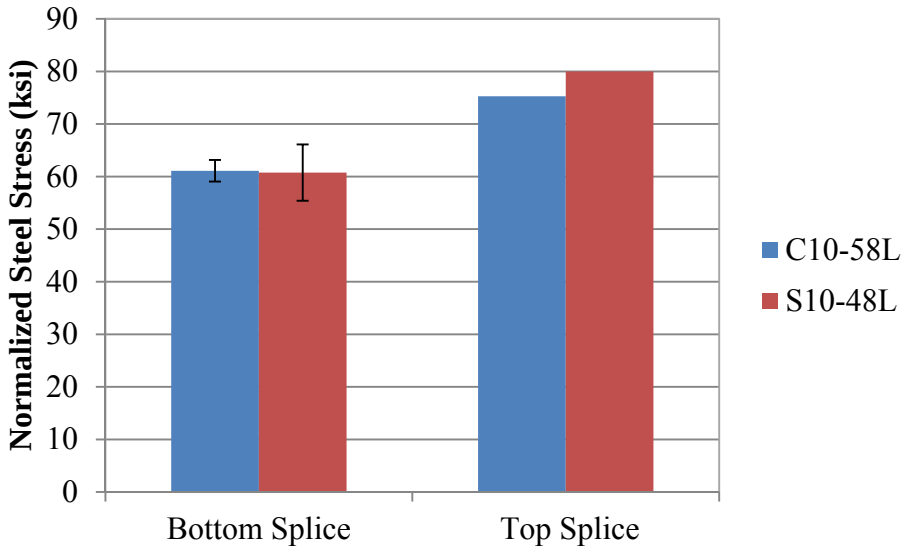

Figure 5.24 – Normalized steel stress at failure load for normal strength mix designs
Conversion: 1 ksi = 6.9 MPa

Normalized load vs. strain of the longitudinal reinforcing bar was also plotted for comparison. A typical plot of the average bottom splice strain for a specimen of each mix

design is shown in **Figures 5.25** and **5.26**. As seen in the plots, all four specimens have two distinct linear sections. The first represents pre-flexural cracking behavior and the second represents post-flexural cracking behavior. Both plots show that, regardless of strength, the SCC mix designs cracked at a higher load than the control mix designs. Most importantly, all load-strain plots indicated linear behavior up to failure. In other words, the reinforcing bars failed in bond, having never reached yield.

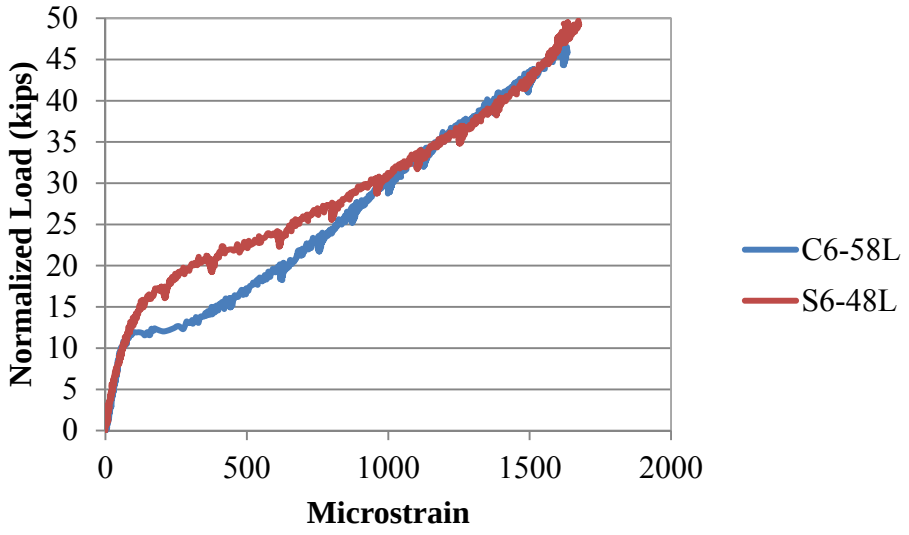

Figure 5.25 – Typical normalized load vs. strain plot for the normal strength specimens
Conversion: 1 kip = 4.45 kN

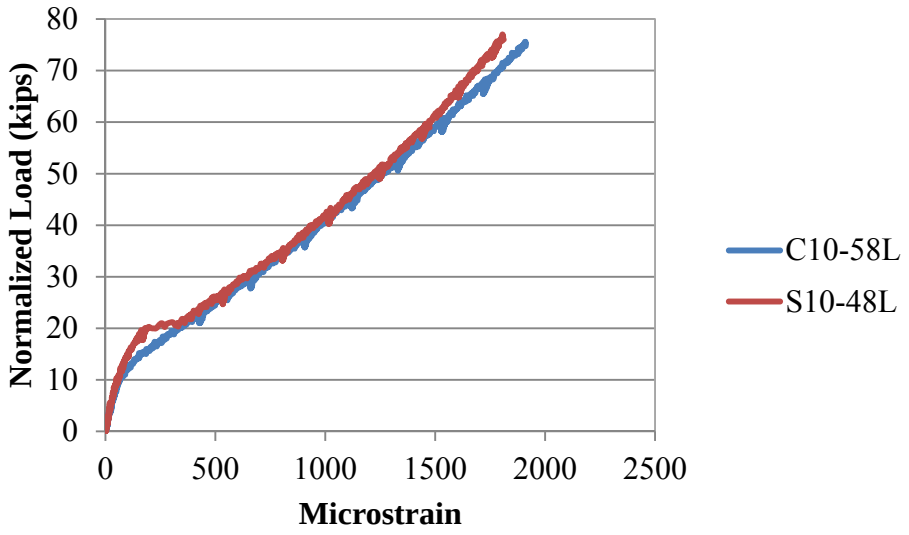

Figure 5.26 – Typical normalized load vs. strain plot for the high strength specimens
Conversion: 1 kip = 4.45 kN

5.5. FINDINGS AND CONCLUSIONS

Based on analysis of the test results, the following conclusions are presented:

1. The average peak load for the #4 (#13), S6-48L and S10-48L pull-out specimens was 15.2% higher and 6.1% lower than that of the control, respectively. The average peak load for the #6 (#19), S6-48L and S10-48L pull-out specimens was 11.3% higher and 9.0% lower than that of the control, respectively. This data indicates that the normal strength SCC mix design has higher bond strength and the high strength SCC has lower bond strength than their respective control mix designs with both bar sizes. Statistical analysis indicates that only the #6 (#19) reinforcing bar, high strength SCC mix design specimens did not perform equally with the control.
2. The average peak bar stress for the S6-48L and S10-48L bottom splice beam specimens was 12.4% higher and 0.5% lower than that of the control

specimens, respectively. The peak bar stress for the S6-48L and S10-48L top splice beam specimens was 7.4% lower and 6.2% higher than that of the control specimens, respectively. This data indicates that both SCC mix designs exhibited improved bond performance under realistic stress states relative to their respective control mix designs when the splice was cast at the bottom of the specimen. Only the high strength SCC mix design exhibited improved bond performance when the splice was cast at the top of the specimen. However, statistical analysis indicates that all four mix designs performed comparably.

6. FINDINGS, CONCLUSIONS, AND RECOMMENDATIONS

The main objective of this study was to determine the effect on bond performance of self-consolidating concrete (SCC). The SCC test program consisted of comparing the bond performance of normal and high strength SCC with their respective MoDOT standard mix designs.

Two test methods were used for bond strength comparisons. The first was a direct pull-out test based on the RILEM 7-II-128 "RC6: Bond test for reinforcing steel. 1. Pull-out test" (RILEM, 1994). Although not directly related to the behavior of a reinforced concrete beam in flexure, the test does provide a realistic comparison of bond between types of concrete. The second test method consisted of a full-scale beam splice test specimen subjected to a four-point loading until failure of the splice. This test method is a non-ASTM test procedure that is generally accepted as the most realistic test method for both development and splice length.

This section contains the findings of the test program, as well as conclusions based on these findings and recommendations for future research.

6.1. FINDINGS

6.1.1. Direct Pull-out Testing. A total of 24 direct pull-out test specimens were constructed for the SCC test program. There were six test specimens constructed for each of the four mix designs, which consisted of two SCC mixes and two control mixes. Of the six specimens constructed for each mix design, three specimens contained a #4 (#13) reinforcing bar and three specimens contained a #6 (#19) reinforcing bar. Each specimen

was tested to failure. The average peak load for the #4 (#13), S6-48L and S10-48L pull-out specimens was 15.2% higher and 6.1% lower than that of the control, respectively. The average peak load for the #6 (#19), S6-48L and S10-48L pull-out specimens was 11.3% higher and 9.0% lower than that of the control, respectively.

6.1.2. Beam Splice Testing. A total of 12 test specimens were constructed with 3#6 (#19) longitudinal reinforcing bars spliced at midspan for the SCC test program. There were three specimens constructed for each of the four concrete mix designs to be evaluated. Of the three test specimens, two specimens were constructed with the spliced reinforcing bars located at the bottom of the beam cross section and one specimen was constructed with the splice at the top of the beam cross section to evaluate top-bar effect. Each specimen was tested to bond failure. The average peak bar stress for the S6-48L and S10-48L bottom splice beam specimens was 12.4% and 0.5% higher than that of the control specimens, respectively. The peak bar stress for the S6-48L and S10-48L top splice beam specimens was 7.4% lower and 6.2% higher than that of the control specimens, respectively.

6.2. CONCLUSIONS

6.2.1. Direct Pull-out Testing. Analysis of the test data indicates that the normal strength SCC mix design has higher bond strength and the high strength SCC mix design has lower bond strength than their respective control mix designs for both bar sizes. Statistical analysis indicates that only the #6 (#19) reinforcing bar, high strength SCC mix design specimens did not perform comparbly with the control.

6.2.2. Beam Splice Testing. Analysis of the test data indicates that both SCC mix designs exhibited improved bond performance under realistic stress states relative to their respective control mix designs when the splice was cast at the bottom of the specimen. Only the high strength SCC mix design exhibited improved bond performance when the splice was cast at the top of the specimen. However, statistical analysis indicates that all four mix designs performed comparably. These findings, along with the findings from the direct pull-out tests, indicate that using SCC is feasible in terms of bond and development of reinforcing steel.

6.3. RECOMMENDATIONS

There have been numerous studies conducted to determine the bond performance of SCC. However, additional studies are needed to establish a database of results that can eventually be used for comparison as well as for future ACI design code changes. Also important for design would be to explore whether or not certain ACI code distinctions, such as confinement, bar size, or bar coating factors, used for conventional concrete designs also apply to SCC, or if they need to be developed specifically for SCC. Below is a list of recommendations for testable variables related to SCC concrete bond behavior:

- Perform tests with a larger variation in bar sizes based on ACI 318 code distinctions for bar size effect on development length,
- Conduct tests determining the effect of different admixtures on the bond performance of SCC,
- Conduct tests determining the effect of various aggregate percentages and types on the bond performance of SCC,

- Perform tests with aggregates from different sources, and
- Perform bond tests on more specimen types mentioned in ACI 408.

APPENDIX A

SCC TEST PROGRAM BEAM SPLICE FAILURE PHOTOGRAPHS

(a) Bottom View

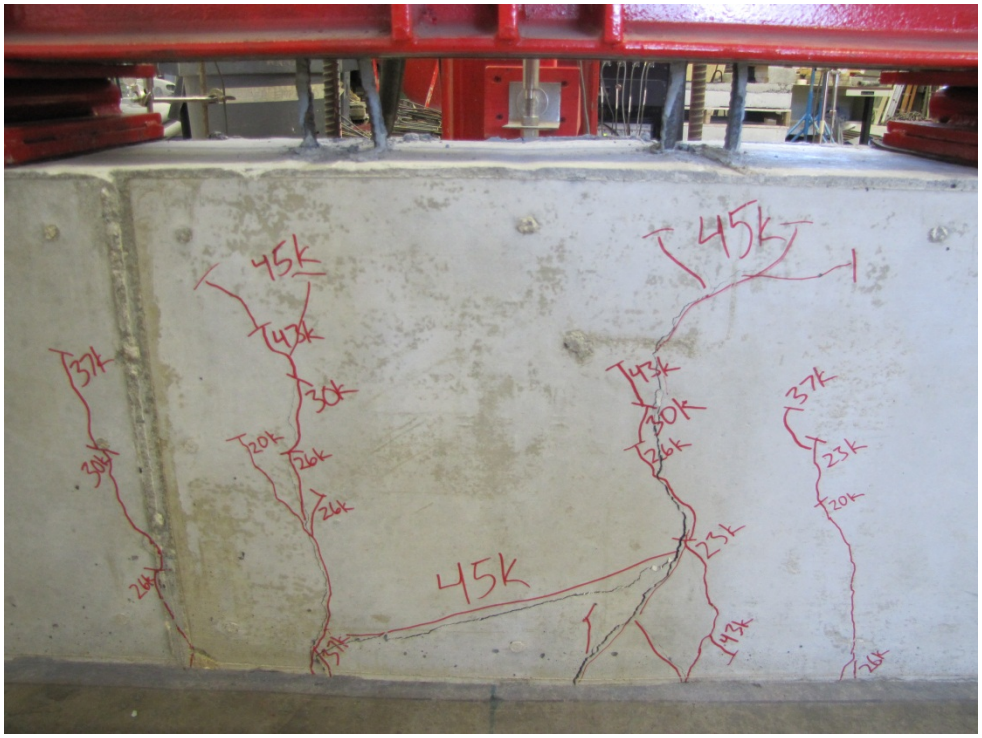

(b) Side View

Figure A.1 – C6-58LBB1

(a) Bottom View

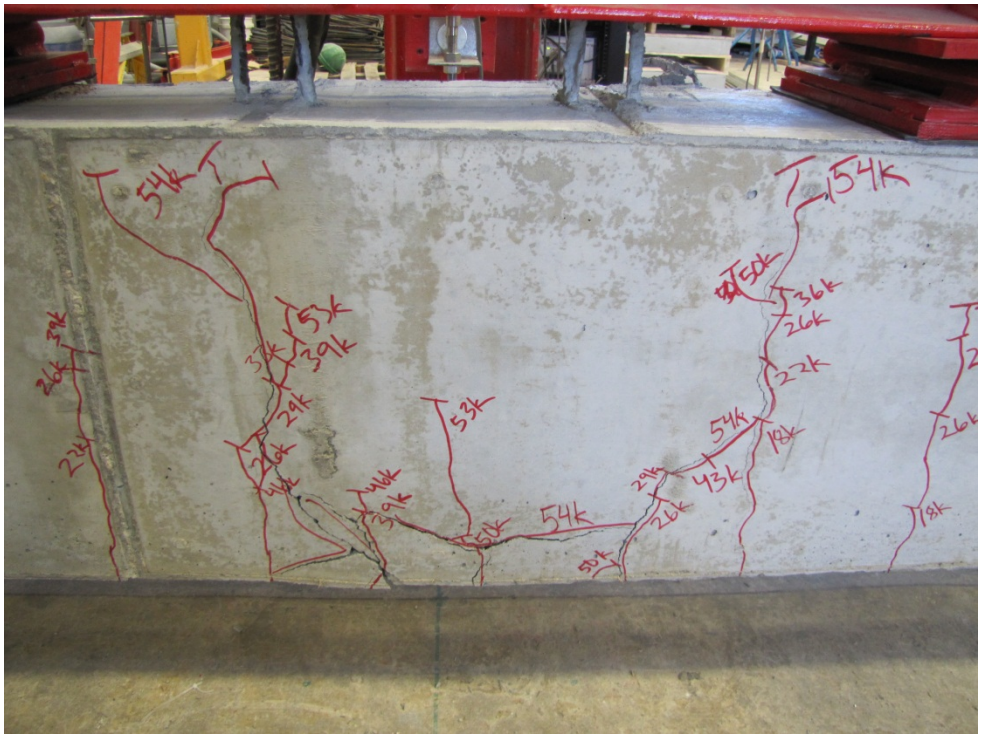

(b) Side View

Figure A.2 – C6-58LBB2

(a) Bottom View

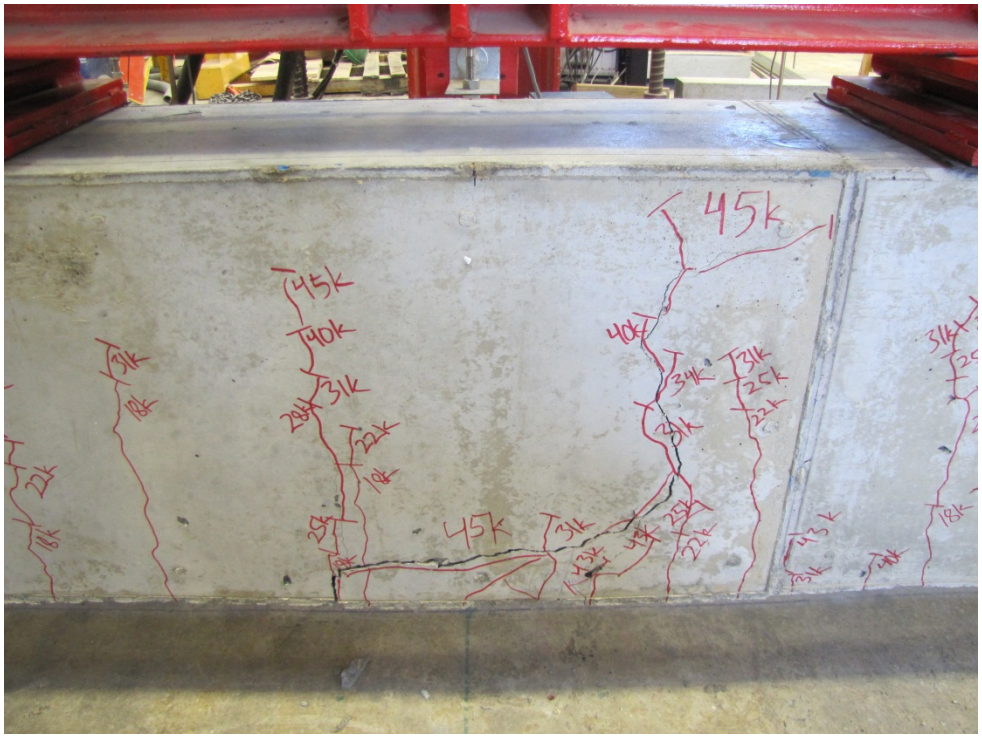

(b) Side View

Figure A.3 – C6-58LTB

(a) Bottom View

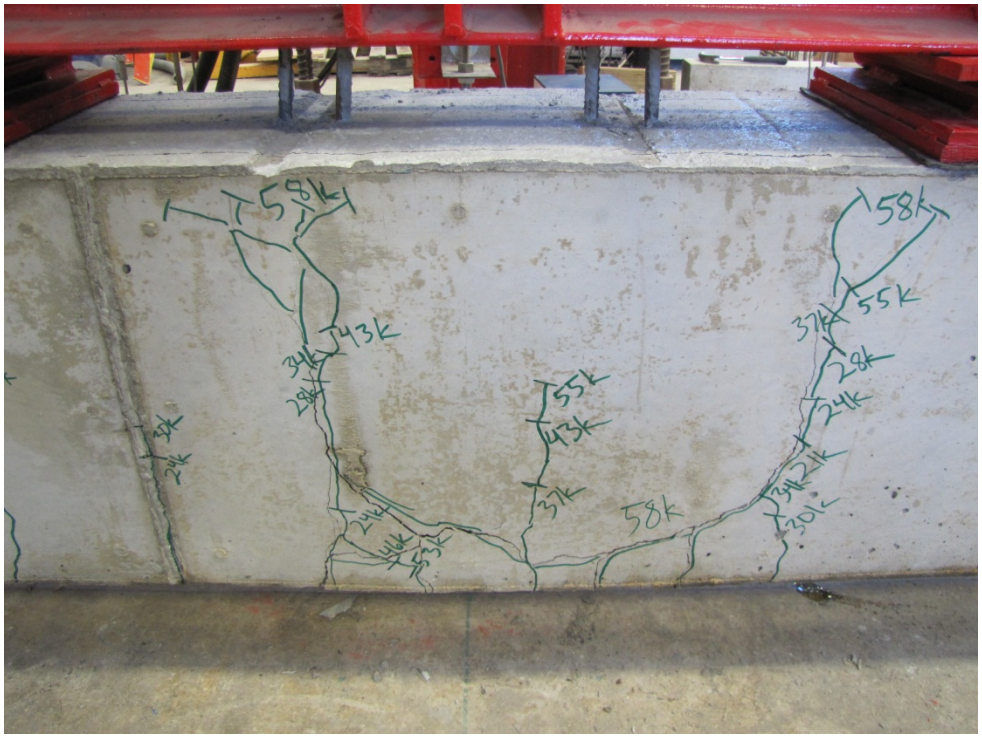

(b) Side View

Figure A.4 – S6-48LBB1

(a) Bottom View

(b) Side View

Figure A.5 – S6-48LBB2

(a) Full crack pattern

(b) Side View

Figure A.6 – S6-48LTB side view

(a) Bottom View

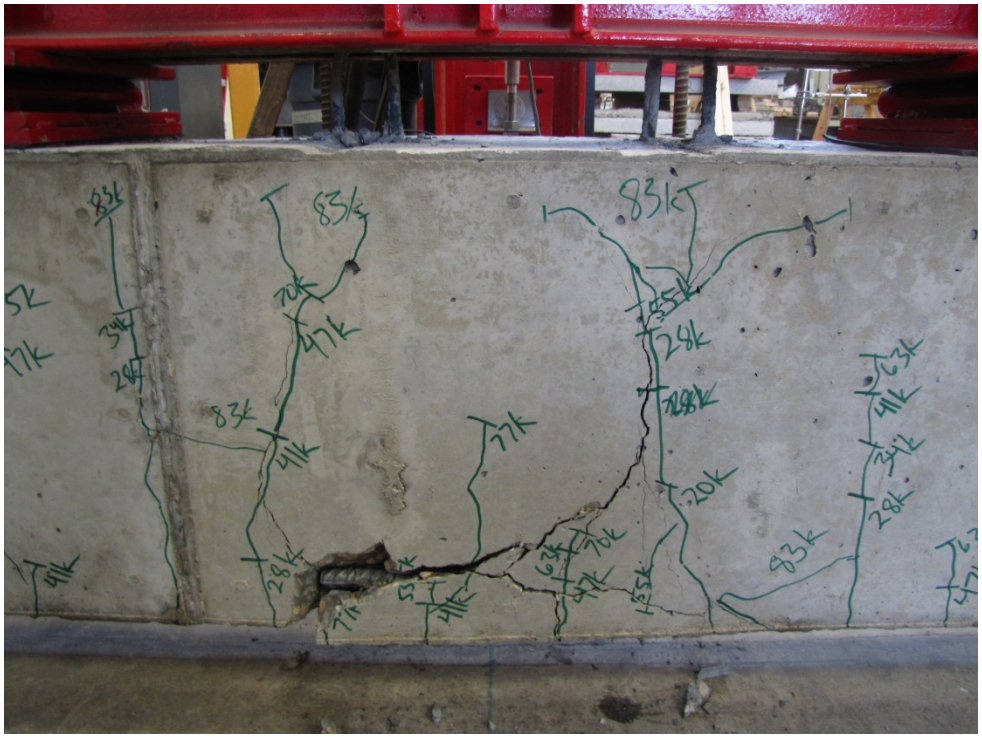

(b) Side View

Figure A.7 – C10-58LBB1

(a) Bottom View

(b) Side View

Figure A.8 – C10-58LBB2

(a) Bottom View

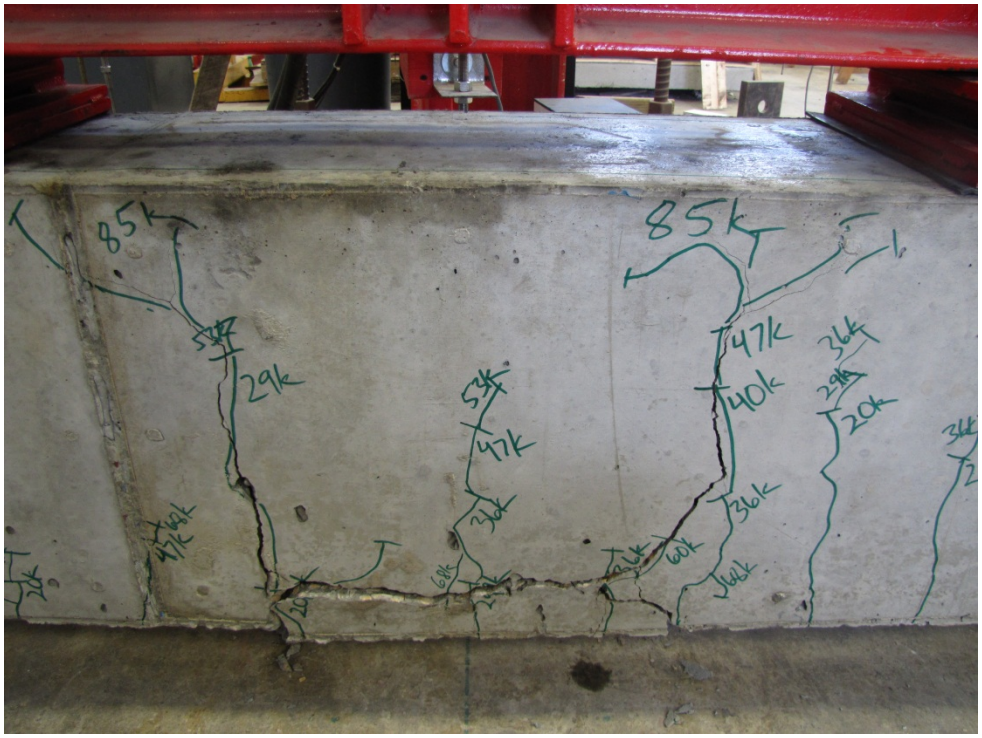

(b) Side View

Figure A.9 – C10-58LTB

(a) Bottom View

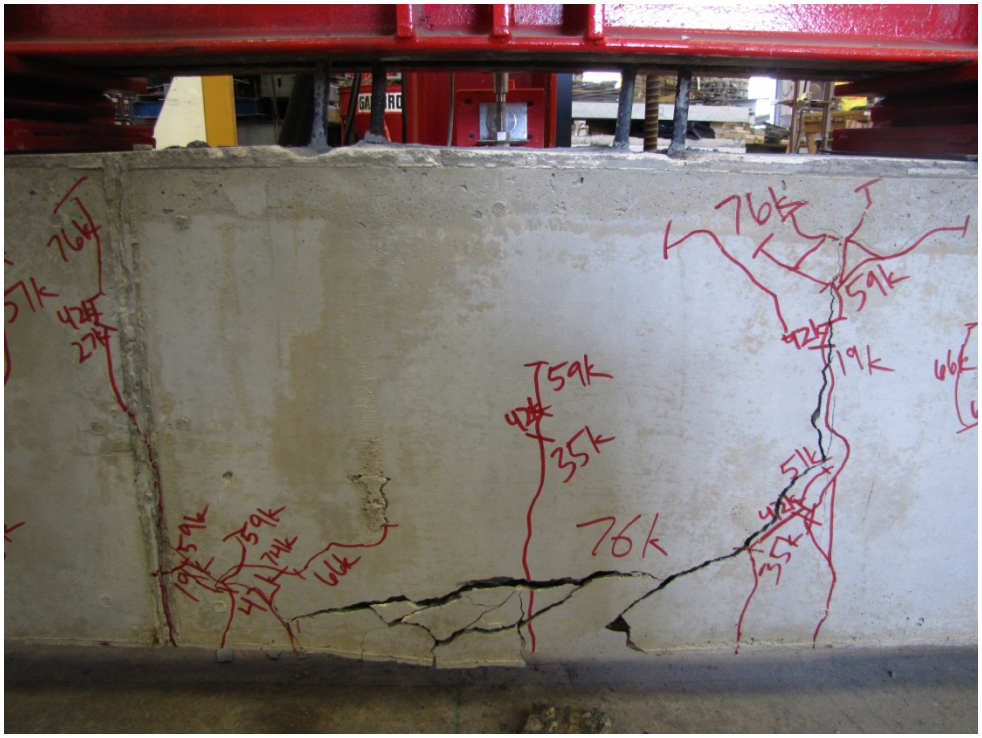

(b) Side View

Figure A.10 – S10-48LBB1

(a) Bottom View

(b) Side View

Figure A.11 – S10-48LBB2

(a) Bottom View

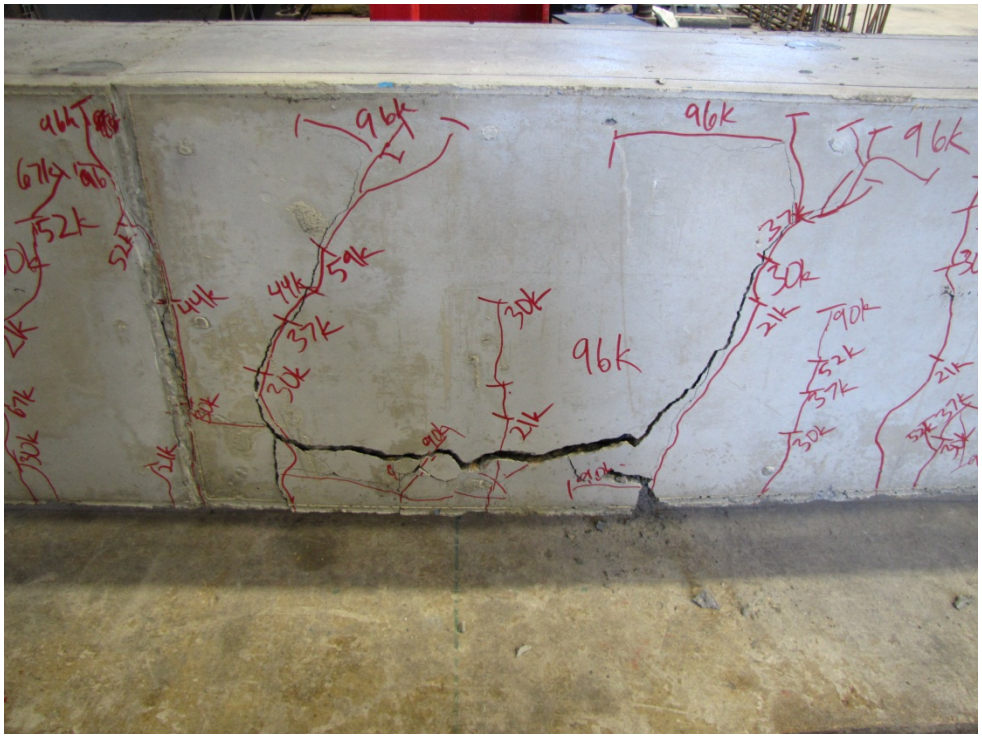

(b) Side View

Figure A.12 – S10-48LTB

APPENDIX B

SCC TEST PROGRAM TEST DATA PLOTS

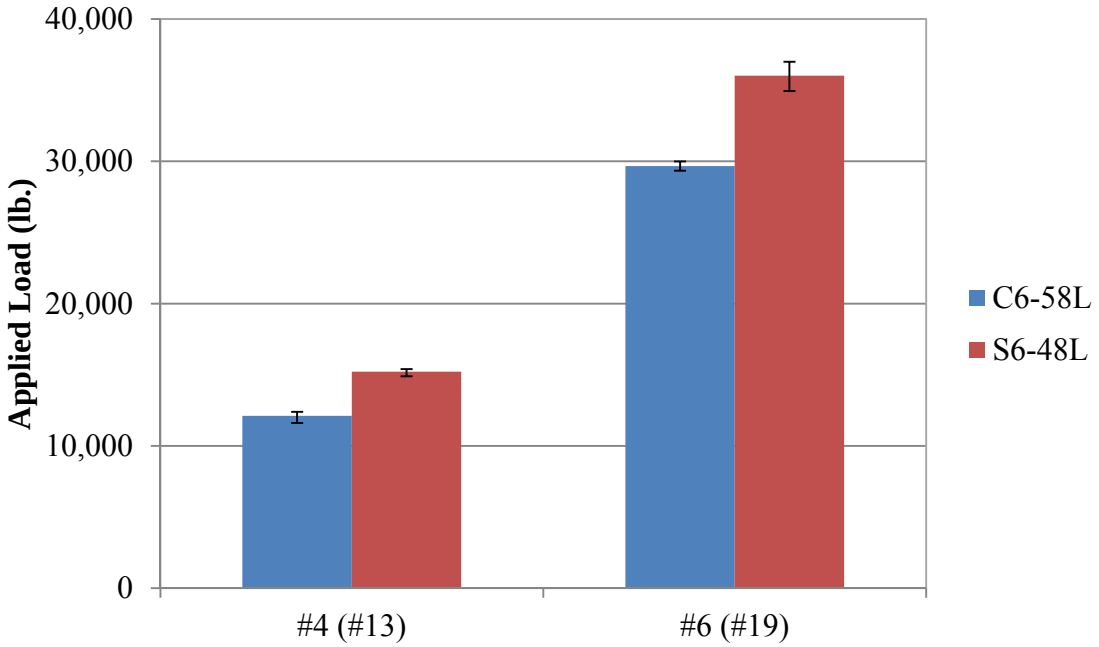

Figure B.1 – Normal strength direct pull-out applied load comparisons
Conversion: 1 lb. = 4.45 N

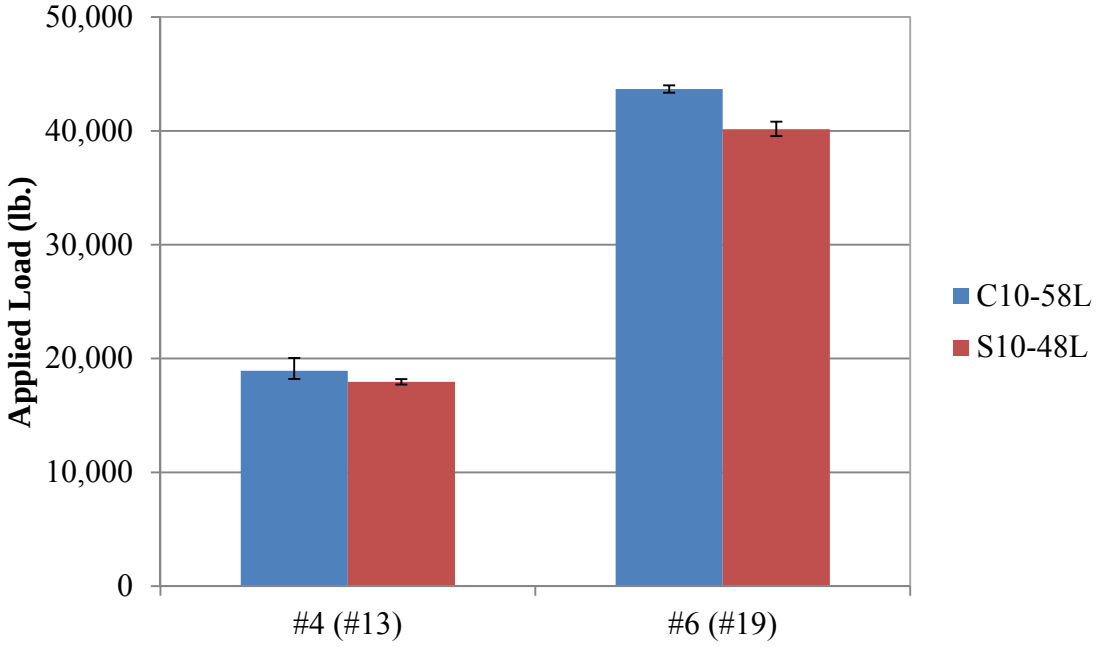

Figure B.2 – High strength direct pull-out applied load comparisons
Conversion: 1 lb. = 4.45 N

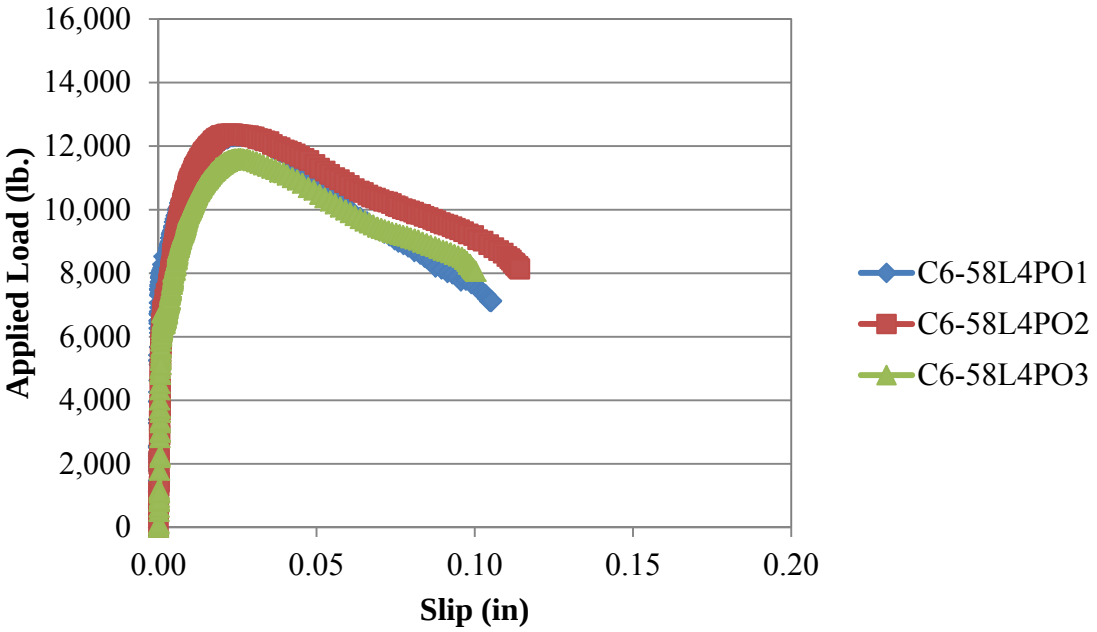

Figure B.3 – Applied load vs. slip plot for #4 (#13) C6-58L
Conversion: 1 in. = 25.4 mm
1 lb. = 4.45 N

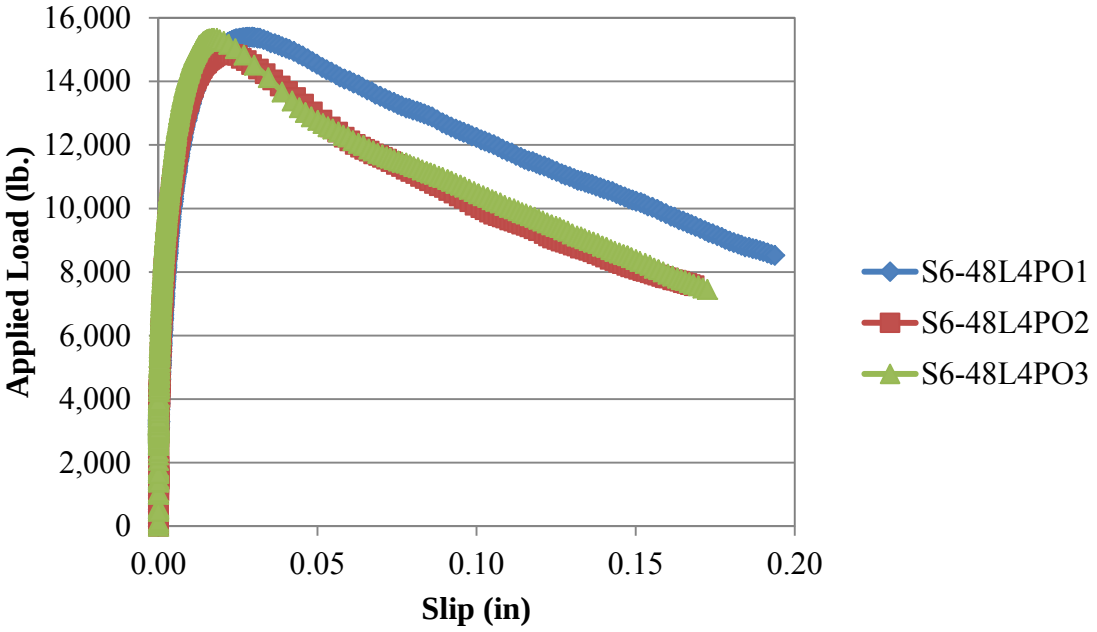

Figure B.4 – Applied load vs. slip plot for #4 (#13) S6-48L
Conversion: 1 in. = 25.4 mm
1 lb. = 4.45 N

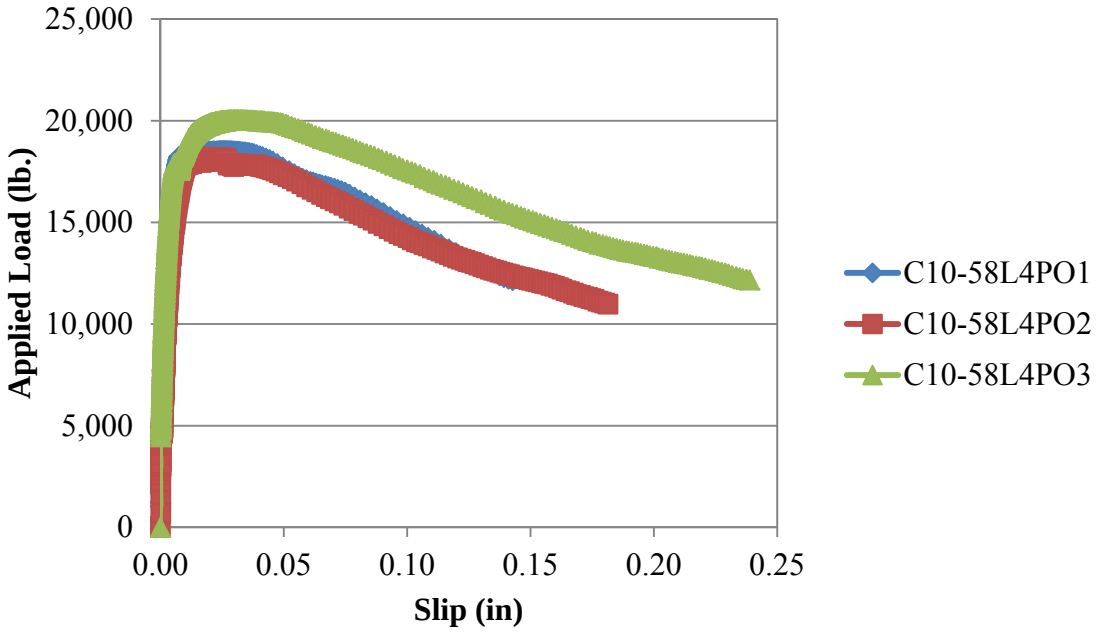

Figure B.5 – Applied load vs. slip plot for #4 (#13) C10-58L
Conversion: 1 in. = 25.4 mm
1 lb. = 4.45 N

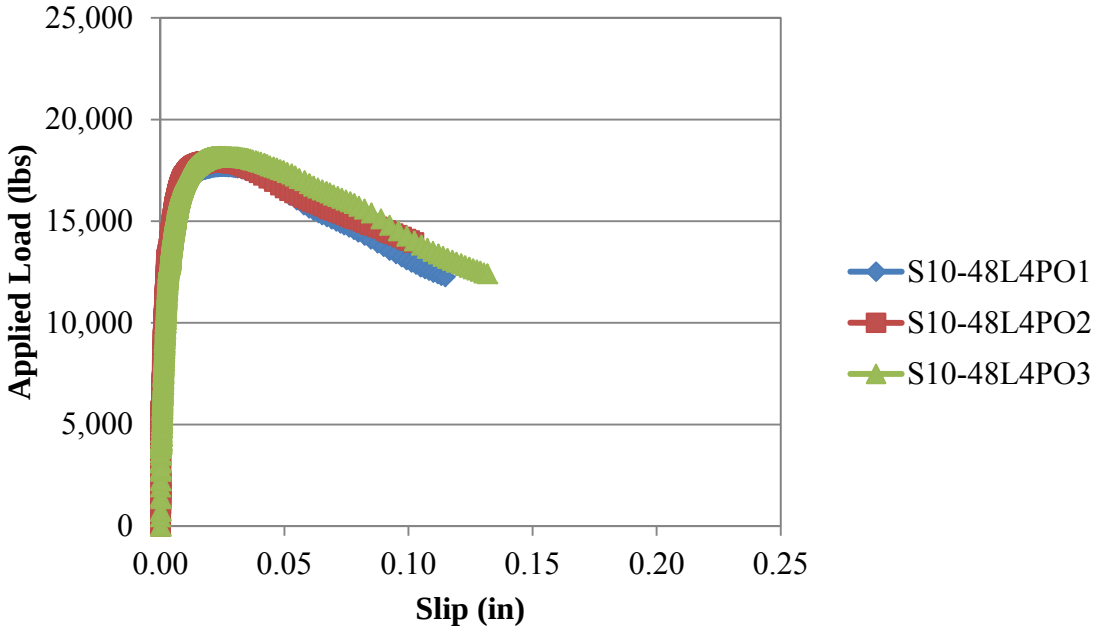

Figure B.6 – Applied load vs. slip plot for #4 (#13) S10-48L
Conversion: 1 in. = 25.4 mm
1 lb. = 4.45 N

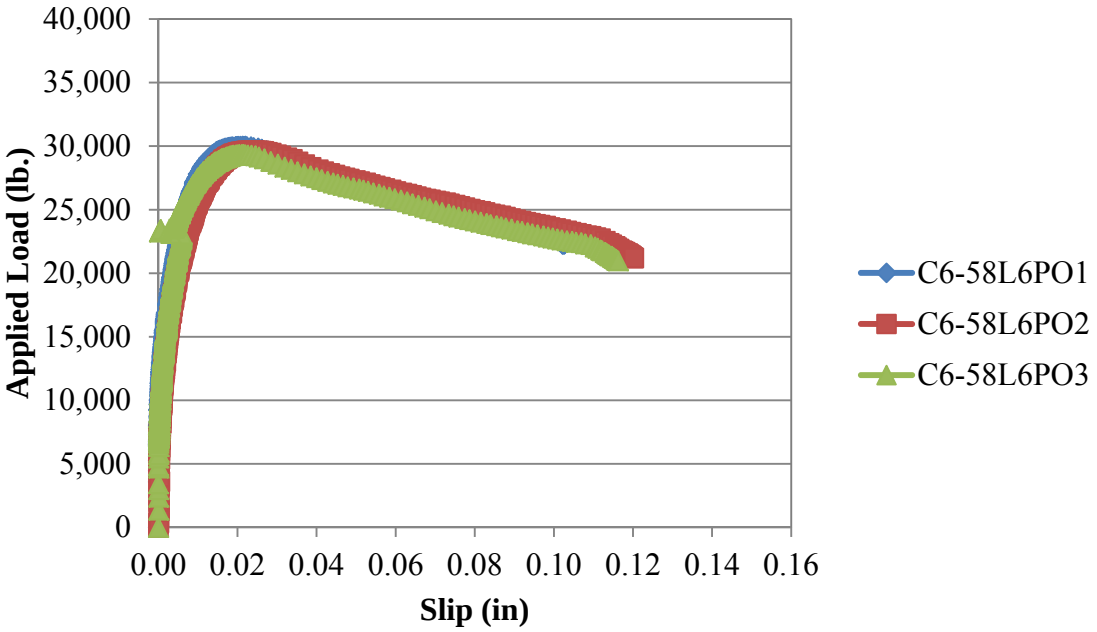

Figure B.7 – Applied load vs. slip plot for #6 (#19) C6-58L
Conversion: 1 in. = 25.4 mm
1 lb. = 4.45 N

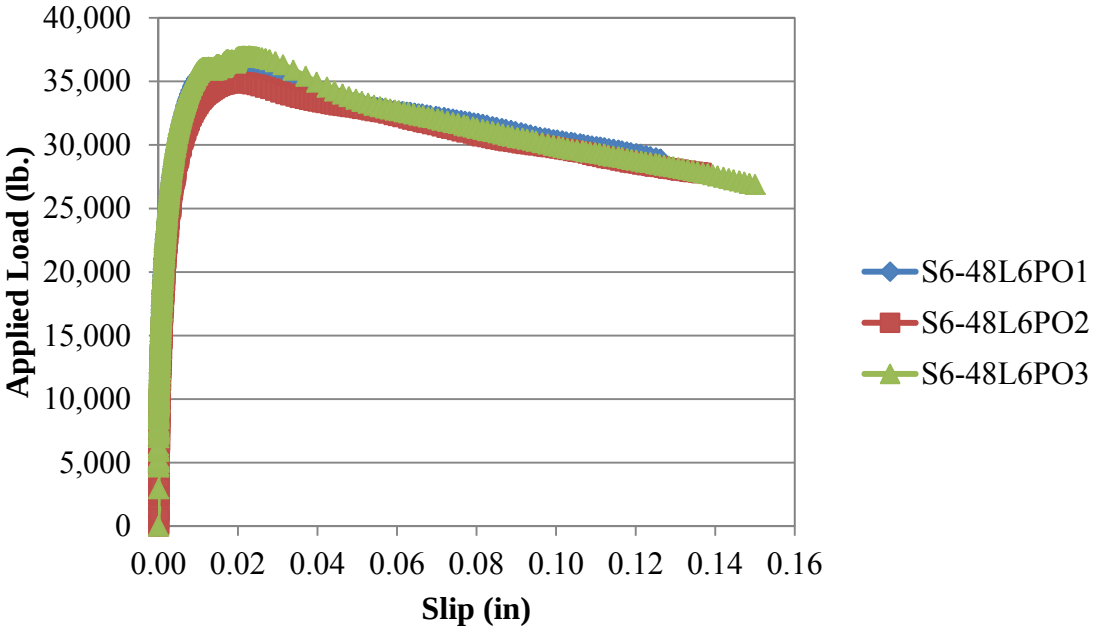

Figure B.8 – Applied load vs. slip plot for #6 (#19) S6-48L
Conversion: 1 in. = 25.4 mm
1 lb. = 4.45 N

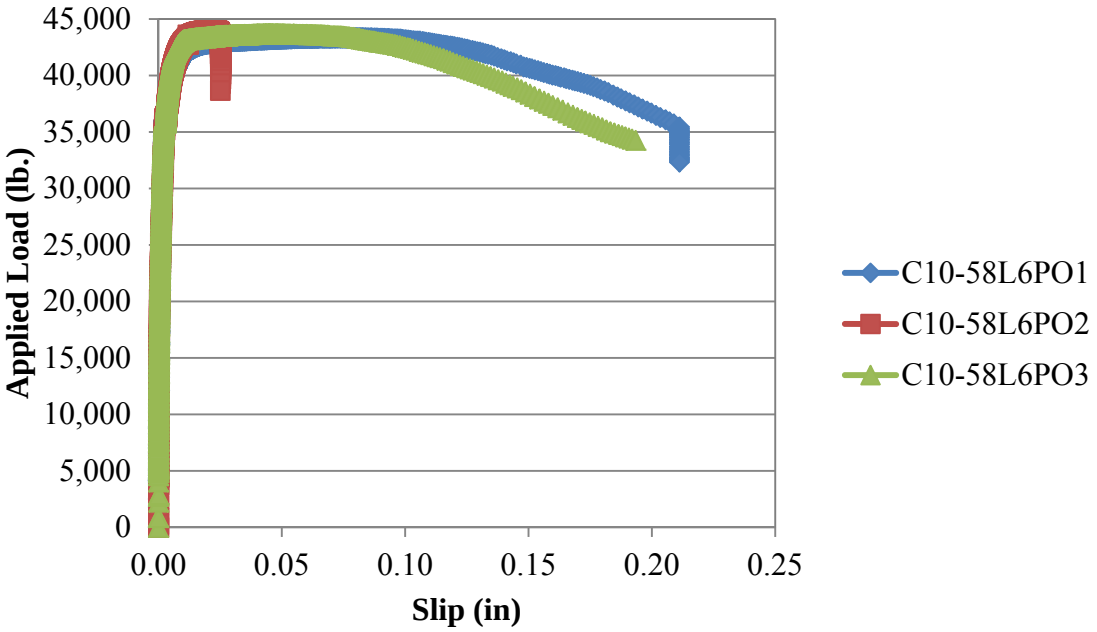

Figure B.9 – Applied load vs. slip plot for #6 (#19) C10-58L
Conversion: 1 in. = 25.4 mm
1 lb. = 4.45 N

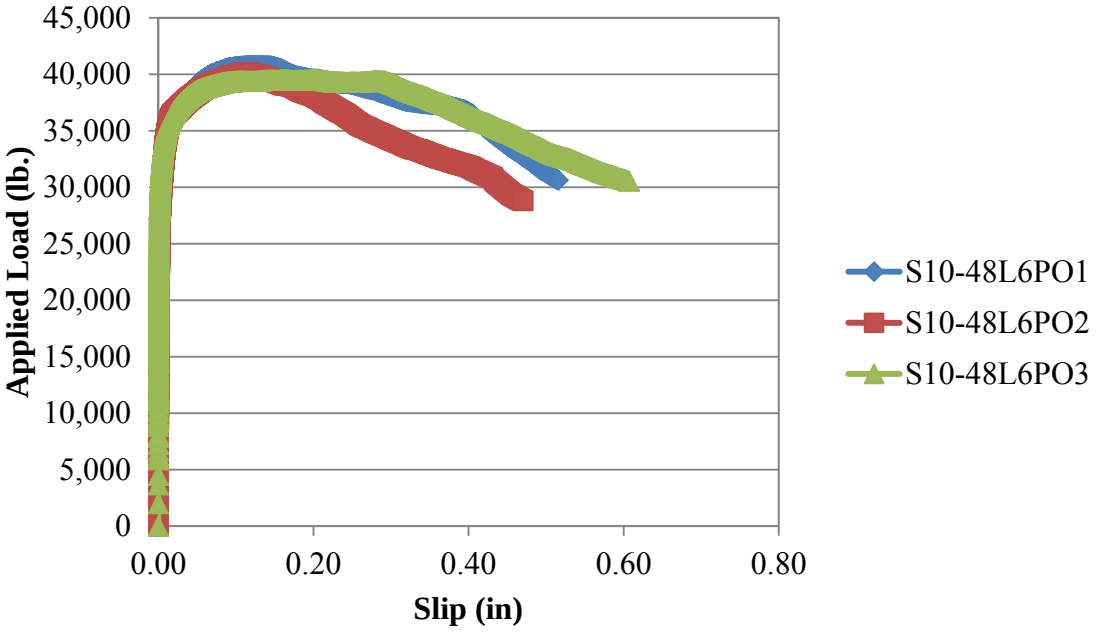

Figure B.10 – Applied load vs. slip plot for #6 (#19) S10-48L
Conversion: 1 in. = 25.4 mm
1 lb. = 4.45 N

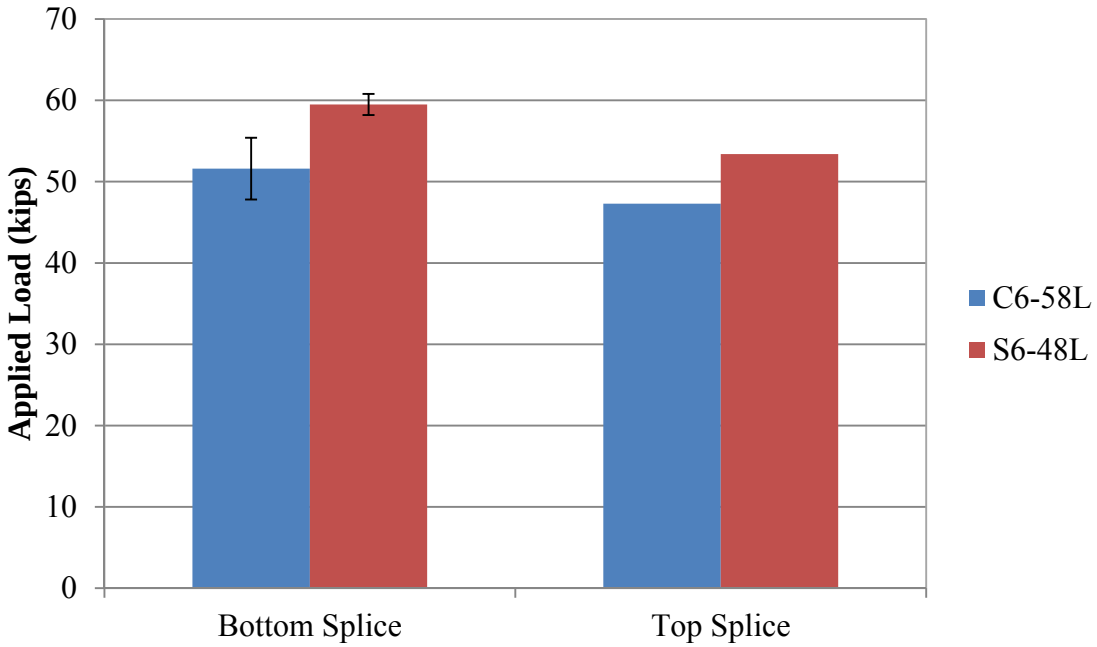

Figure B.11 – Normal strength beam splice applied load comparisons
Conversion: 1 kip = 4.45 kN

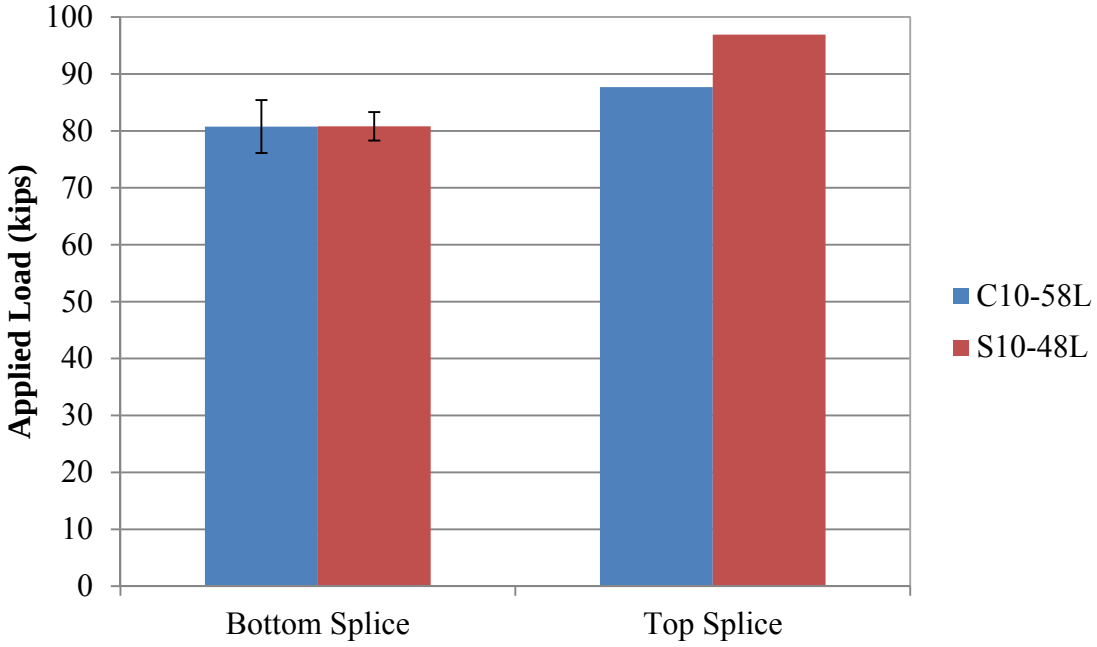

Figure B.12 – High strength beam splice applied load comparisons
Conversion: 1 kip = 4.45 kN

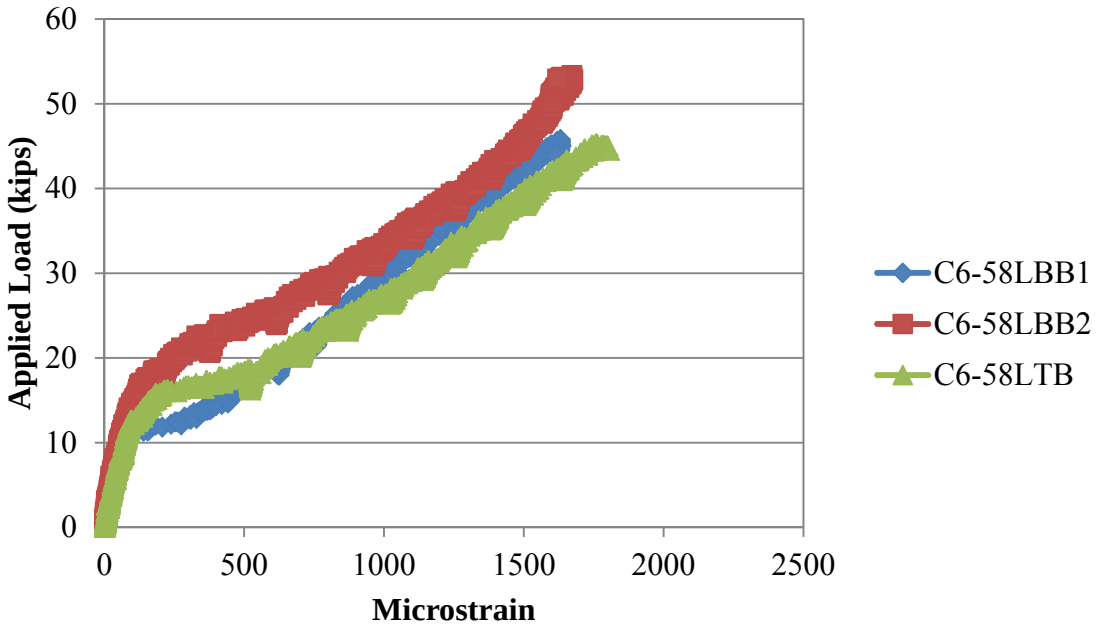

Figure B.13 – Applied load vs. strain (average of all gages per specimen) for C6-58L
Conversion: 1 kip = 4.45 kN

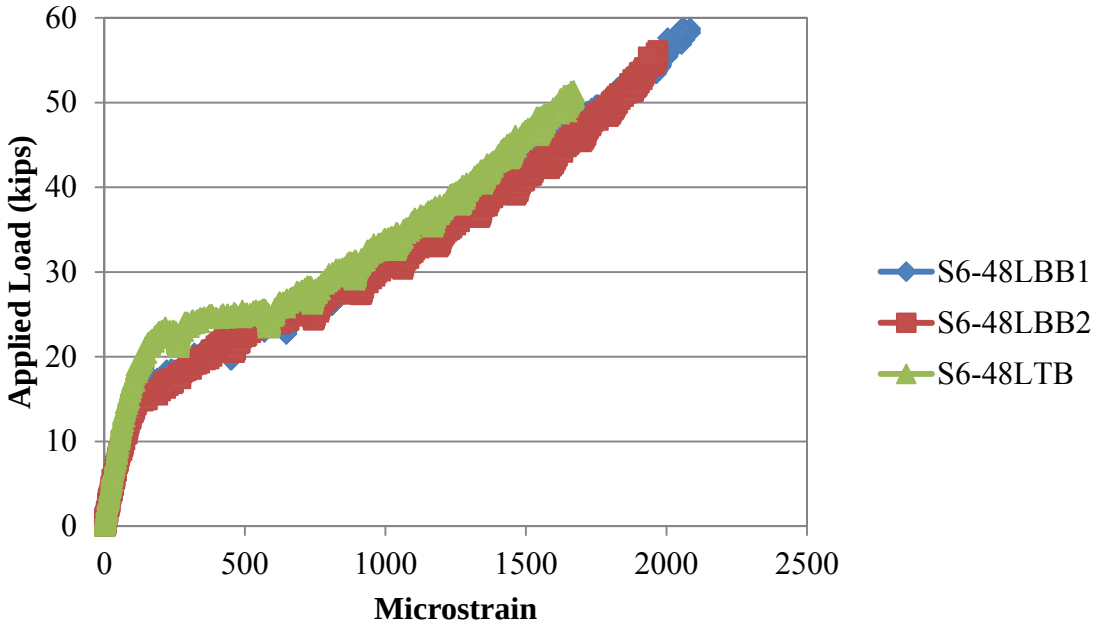

Figure B.14 – Applied load vs. strain (average of all gages per specimen) for S6-48L
Conversion: 1 kip = 4.45 kN

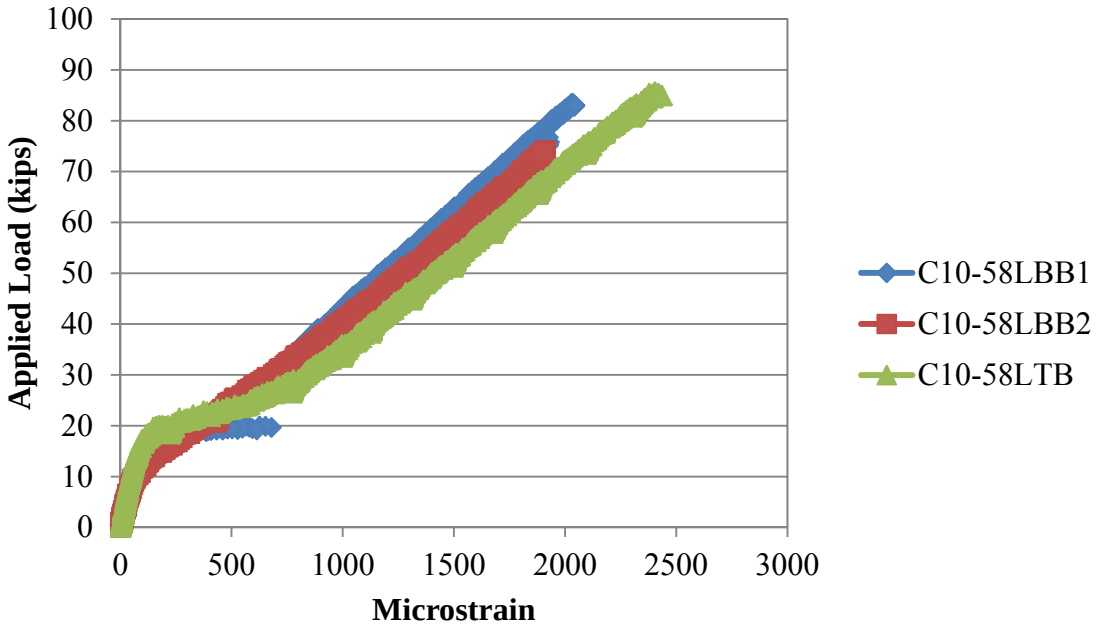

Figure B.15 – Applied load vs. strain (average of all gages per specimen) for C10-58L
Conversion: 1 kip = 4.45 kN

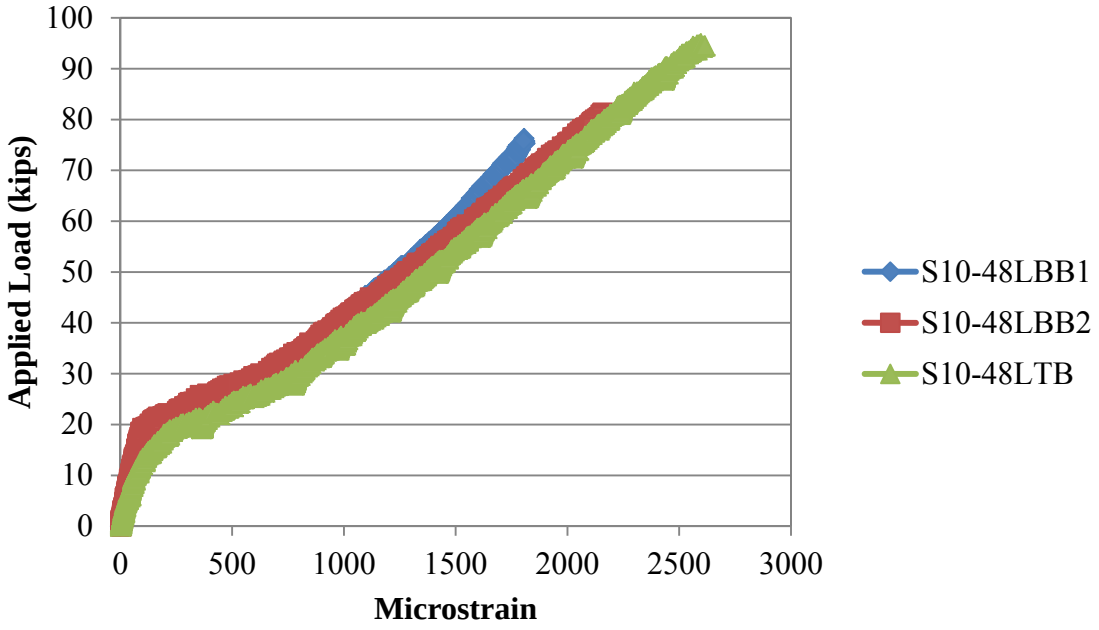

Figure B.16 – Applied load vs. strain (average of all gages per specimen) for S10-48L
Conversion: 1 kip = 4.45 kN

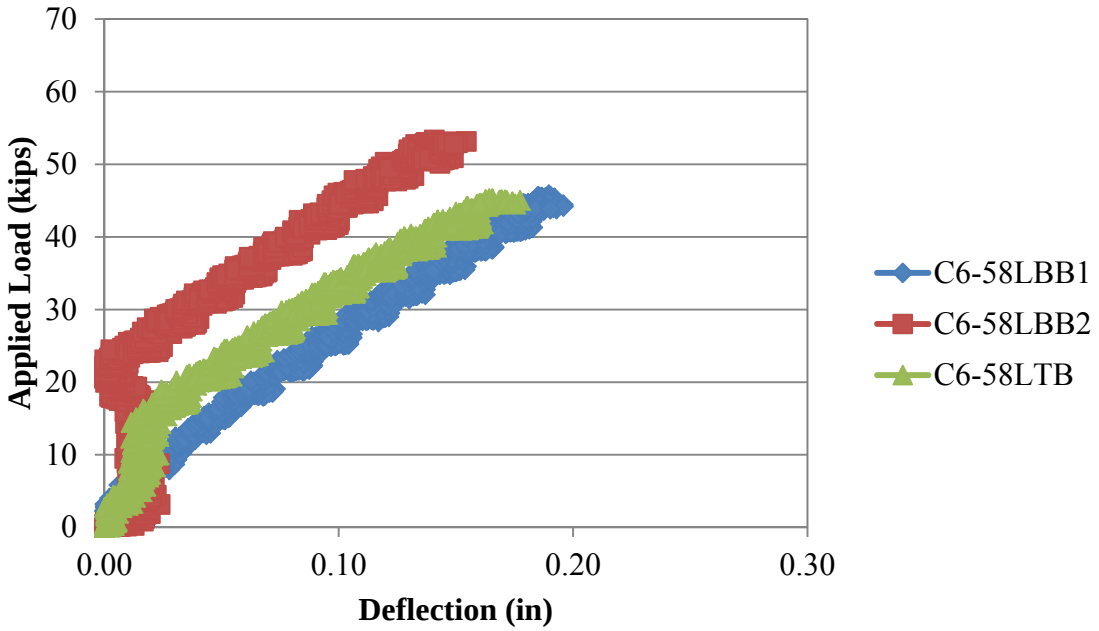

Figure B.17 – Applied load vs. displacement for C6-58L
Conversion: 1 in. = 25.4 mm
1 kip. = 4.45 kN

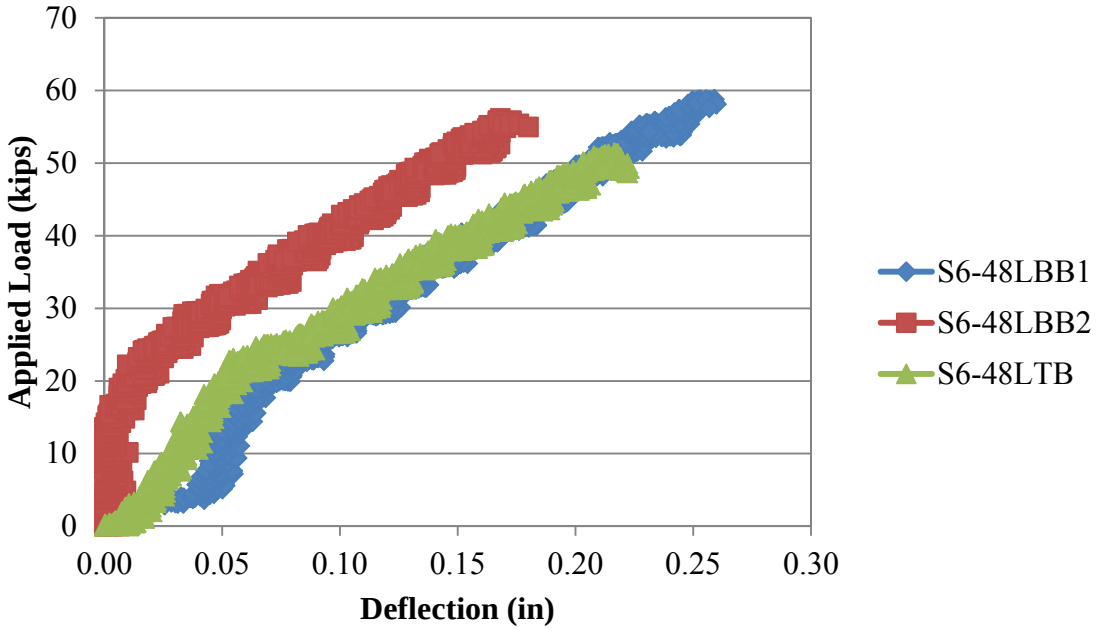

Figure B.18 – Applied load vs. displacement for S6-48L
Conversion: 1 in. = 25.4 mm
1 kip. = 4.45 kN

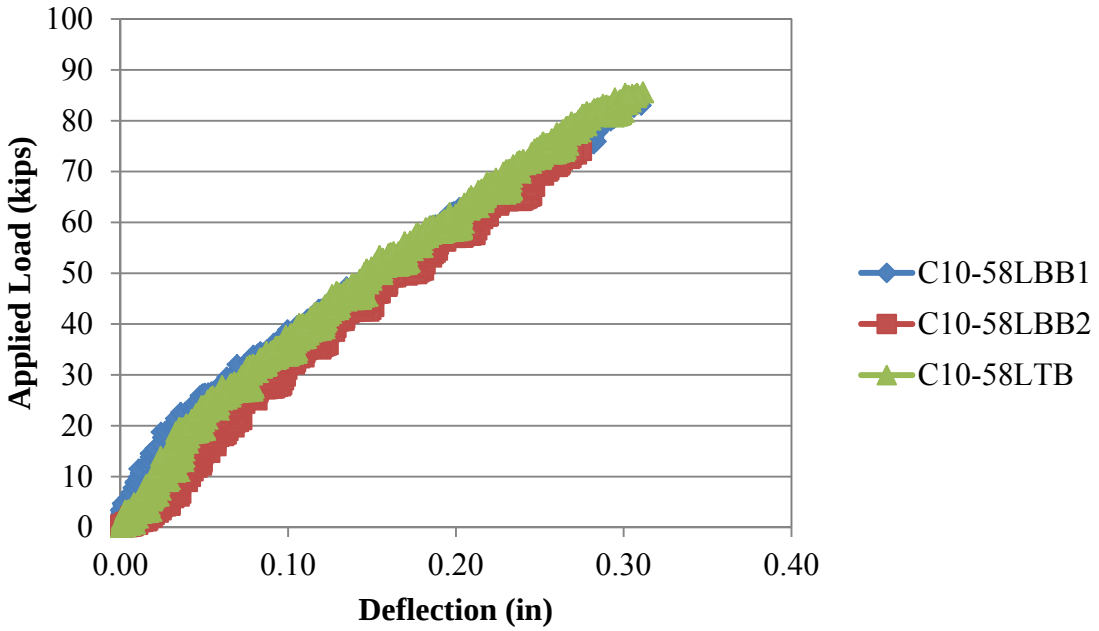

Figure B.19 – Applied load vs. displacement for C10-58L
Conversion: 1 in. = 25.4 mm
1 kip. = 4.45 kN

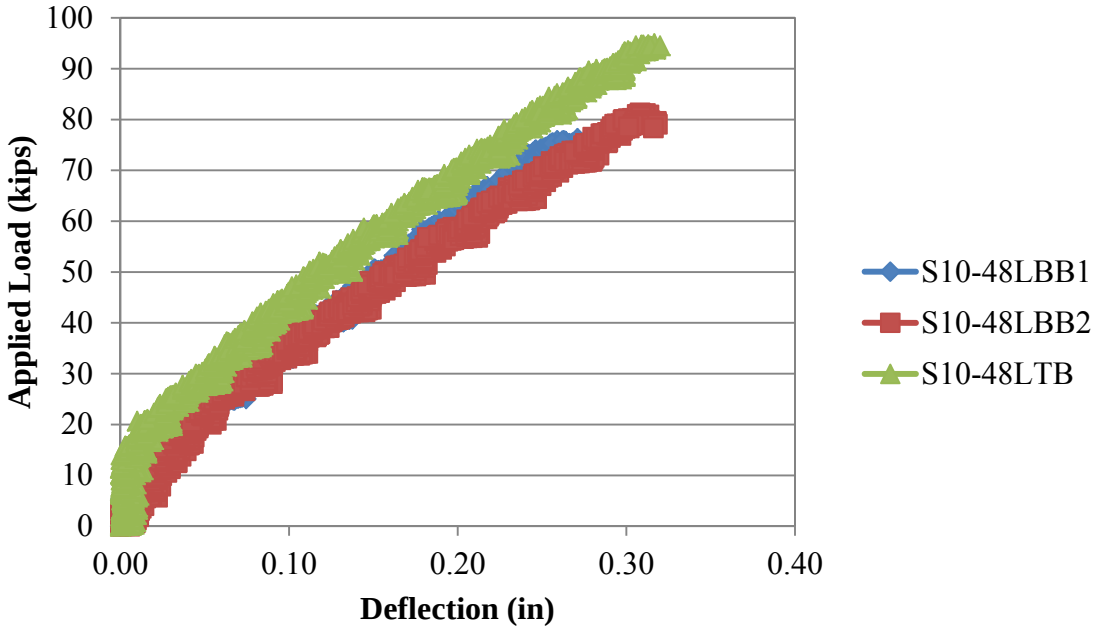

Figure B.20 – Applied load vs. displacement for S10-48L
Conversion: 1 in. = 25.4 mm
1 kip. = 4.45 Kn

APPENDIX C

SCC TEST PROGRAM STATISTICAL ANALYSIS

Table C.1 – t-test for #4 (#13) C6-58L and S6-48L direct pull-out specimen average comparison

	Variable 1	*Variable 2*
Mean	12299.77281	14170.70786
Variance	192306.7928	67409.77444
Observations	3	3
Pearson Correlation	0.999925572	
Hypothesized Mean Difference	0	
df	2	
	-	
t Stat	18.10958303	
P(T<=t) one-tail	0.001517652	
t Critical one-tail	2.91998558	
P(T<=t) two-tail	0.003035304	
t Critical two-tail	4.30265273	

Table C.2 – t-test for #4 (#13) C10-58L and S10-48L direct pull-out specimen average comparison

	Variable 1	*Variable 2*
Mean	19291.505	18116.022
Variance	996006.58	58255.052
Observations	3	3
Pearson Correlation	0.9461693	
Hypothesized Mean Difference	0	
df	2	
t Stat	2.631888	
P(T<=t) one-tail	0.0595581	
t Critical one-tail	2.9199856	
P(T<=t) two-tail	0.1191161	
t Critical two-tail	4.3026527	

Table C.3 – t-test for #6 (#19) C6-58L and S6-48L direct pull-out specimen average comparison

	Variable 1	*Variable 2*
Mean	30133.52917	33551.81008
Variance	111376.4402	923374.4939
Observations	3	3
Pearson Correlation	0.994319729	
Hypothesized Mean Difference	0	
df	2	
	-	
t Stat	9.396487376	
P(T<=t) one-tail	0.005568476	
t Critical one-tail	2.91998558	
P(T<=t) two-tail	0.011136952	
t Critical two-tail	4.30265273	

Table C.4 – t-test for #6 (#19) C10-58L and S10-48L direct pull-out specimen average comparison

	Variable 1	*Variable 2*
Mean	44524.47747	40530.32231
Variance	110031.5152	407511.2922
Observations	3	3
Pearson Correlation	0.994406672	
Hypothesized Mean Difference	0	
df	2	
t Stat	22.28085073	
P(T<=t) one-tail	0.001004146	
t Critical one-tail	2.91998558	
P(T<=t) two-tail	0.002008291	
t Critical two-tail	4.30265273	

Table C.5 – t-test for C6-58L and S6-48L beam splice average comparison

	Variable 1	*Variable 2*
Mean	52.49015377	53.88631511
Variance	7.720148065	36.49494056
Observations	3	3
Pearson Correlation	-0.999116478	
Hypothesized Mean Difference	0	
df	2	
t Stat	-0.274238986	
P(T<=t) one-tail	0.404815006	
t Critical one-tail	2.91998558	
P(T<=t) two-tail	0.809630013	
t Critical two-tail	4.30265273	

Table C.6 – t-test for C10-58L and S10-48L beam splice average comparison

	Variable 1	*Variable 2*
Mean	65.81842085	67.16694327
Variance	71.11065656	151.7248173
Observations	3	3
Pearson Correlation	-0.767542424	
Hypothesized Mean Difference	0	
df	2	
t Stat	-0.293378545	
P(T<=t) one-tail	0.398437399	
t Critical one-tail	2.91998558	
P(T<=t) two-tail	0.796874798	
t Critical two-tail	4.30265273	

BIBLIOGRAPHY

AASHTO (2007). AASHTO LRFD Bridge Design Specification. Fourth Edition, Washington, D.C.

ACI 318 (2008). Building Code Requirements for Structural Concrete (ACI 318-08) and Commentary. American Concrete Institute, Farminton Hills, MI.

ACI 408R (2003). Bond and Development of Straight Reinforcing Bars in Tension. American Concrete Institute, Farminton Hills, MI.

ASTM C 39 (2011). Standard Test Method for Compressive Strength of Cylindrical Concrete Specimens. *American Society for Testing and Materials*. West Conshohocken, PA.

ASTM C 78 (2010). Standard Test Method for Flexural Strength of Concrete (Using Simple Beam with Third-Point Loading). *American Society for Testing and Materials*. West Conshohocken, PA.

ASTM C 138 (2010). Standard Test Method for Density (Unit Weight), Yield, and Air Content (Gravimetric) of Concrete. *American Society for Testing and Materials*. West Conshohocken, PA.

ASTM C 143 (2010). Standard Test Methods for Slump of Hydraulic Cement Concrete. *American Society for Testing and Materials*. West Conshohocken, PA.

ASTM C 231 (2010). Standard Test Method for Air Content of Freshly Mixed Concrete by the Pressure Method. *American Society for Testing and Materials*. West Conshohocken, PA.

ASTM C 496 (2011). Standard Test Method for Splitting Tensile Strength of Cylindrical Concrete Specimens. *American Society for Testing and Materials*. West Conshohocken, PA.

ASTM C 1611 (2009). Standard Test Method for Slump Flow of Self-Consolidating Concrete. *American Society for Testing and Materials*. West Conshohocken, PA.

ASTM C 1621 (2009). Standard Test Method for Passing Ability of Self-Consolidating Concrete by J-Ring. *American Society for Testing and Materials*. West Conshohocken, PA.

ASTM E 8 (2009). Standard Test Methods for Tension Testing of Metallic Materials. *American Society for Testing and Materials*. West Conshohocken, PA.

Bentz, E., Collins, M. (2000). Response-2000 Reinforced Concrete Sectional Analysis. Version 1.0.5. Toronto, Canada.

Castel, A., Thierry, V., Kriengkai, V., Raoul, F. (2006). Effect of Reinforcing Bar Orientation and Location on Bond with Self-Consolidating Concrete. *ACI Structural Journal*, 100-S59.

Castel, A., Vidal, T., Francois, R. (2010). "Bond and Cracking Properties of Self-Consolidating Concrete." Université de Toulouse, France.

Chan, Y., Chen, Y., Liu, Y.(2003). Development of Bond Strength of Reinforcement Steel in Self-Consolidating Concrete. *ACI Structural Journal*, 100-S52.

Dehn, F., Holschemacher, K., Weibe, D. (2000). "Self-Compacting Concrete (SCC) Time Development of the Material Properties and the Bond Behavior." Universität Leipzig.

Foroughi-Asl, A., Dilmaghani, S., Famili, H. (2008). "Bond Strength of Reinforcement Steel in Self-Compacting Concrete." University of Tabriz, Iran.

Hassan,, A., Hossain, K., Lachemi, M. (2009). "Bond Strength of Deformed Bars in Large Reinforced Concrete Members Cast with Industrial Self-Consolidating Concrete Mixture." Ryerson University, Toronto, Canada.

RILEM 7-II-28. (1994). "Bond Test for Reinforcing Steel. 2. Pull-out test." E & FN Spon, London.

Turk, K., Benli, A., Calayir, Y. (2009). "Bond Strength of Tension Lap-Splices in Full Scale Self-Consolidating Concrete Beams." Harran University, Sanliurfa, Turkey.

Valcuende, M., Parra, C. (2008). "Bond Behavior of Reinforcement in Self-Compacting Concrte." Polytechnic University of Valencia, Spain.

Wight, J., MacGregor, J. (2009). "Reinforced Concrete Mechanics and Design." Fifth Edition. Upper Saddle River, NJ: Pearson Education, Inc., 360-406.

Wolfe, M. (2011). "Bond Strength of High-Volume Fly Ash Concrete." M.S. Thesis, Missouri University of Science and Technology, Rolla, MO.